Proofreading
The most efficient (and highly encouraged) way to correct the page proofs and return them to AMS is to electronically annotate the PDF file containing your proof **using the annotation tools** described below in Adobe Acrobat and **send it via e-mail to pdfproofs@ametsoc.org**. Instructions for the PDF annotation process appear on the following pages. If necessary, you may instead print out your page proofs, make your corrections on the pages, and fax or express mail them to AMS. The fax number and delivery address are located at the end of this document.

Proofread the proofs carefully, as this will be your only chance to see your article before publication. **Pay special attention to color figures (if any), and characters such as Greek letters and mathematical symbols**. Make sure that everything is typeset the way that you want it as the corrected proofs will not be returned to you.

Return of your e-proof to AMS signifies that you have thoroughly read and approve of the proof, and thereby authorize publication based on the proof (except where you have identified errors or indicated desired changes within the proof file, or clearly itemized these changes in the email to pdfproofs@ametsoc.org). Adjustments for AMS style may be made prior to publication.

Alterations
Answer author queries at the appropriate place in the text and correct any errors you find. **Authors are allowed up to 10 new textual edits at proof stage at no additional charge** (copy and technical editing errors are not charged to authors at any time)**. Additional edits will be charged at the rate of $4.50 per edit, and changes to figures are more expensive (~$20 per black and white figure and ~$30-$50 per color figure).**

The layout in the page proof is considered final unless changes are essential. Every effort should be made to balance text and figure alterations so that deletions are compensated by nearby additions, and figure substitutions should be of the same size and shape, if possible. Please also note that material changes to the *science* in the manuscript at this stage will require further peer review, substantially increasing the time to publication. **The editors reserve the right to accept or reject proposed alterations.**

Figures
The figures that appear in your page proofs are lower resolution than the final printed article. The primary AMS technical editor for your journal will receive photoprints and the original figures for the purposes of checking the figure quality. If you have specific concerns about any of your figures, especially if any color figures do not appear in color, please describe them in your return. Please verify that each figure properly corresponds with the figure captions and citations in the text. If there are corrections that need to be made, send a new electronic version in eps or tiff format of the corrected figure with your corrected proofs. Include your name, the figure number, and the manuscript number.

Reprints
For manuscripts accepted starting in January 2009, a PDF file of the final published paper will be sent to the corresponding author at no extra charge in lieu of hard-copy reprints. If you would still like to order hard-copy reprints, please use the reprint order form (available at http://www.ametsoc.org/PUBS/journals/reprintorder.pdf).

Page and Color Charges
Please note that when your paper was accepted you were sent a link to the Journals Page and Color Charge form (http://www.ametsoc.org/PUBS/pagecolorcharge.pdf). This form should have been returned to AMS at that time. If you have not completed and returned the form, please contact Christine Keane at AMS Headquarters *immediately* (617-227-2426, ext. 254 or ckeane@ametsoc.org) to ensure publication of your paper.

Thank you very much for your cooperation, and thank you for publishing with the AMS.

Gwendolyn Whittaker, Publications Coordinator
American Meteorological Society
45 Beacon St.
Boston, MA 02108-3693
Fax: (617) 973-0468

Annotating PDFs

ams_annotating_pdfs1.1; April 09, 2009; full release

1. Introduction

eProof files are self-contained PDF documents for viewing on-screen and for printing. They contain all appropriate formatting and fonts to ensure correct rendering on-screen and when printing hardcopy. DJS sends eProofs that can be viewed, annotated, and printed using the free version of Acrobat Reader 7 (or greater). These eProofs are “enabled” with commenting rights, therefore they can be modified by using special markup tools in Acrobat Reader that are not normally available unless using the Standard or Professional version.

The screen images in this document were captured on a PC running Adobe Acrobat Reader version 8.1.0. Though some of the images may differ in appearance from your platform/version, basic functionality remains similar. At the time of this writing, Acrobat Reader v9.1 is freely available and can be downloaded from: http://get.adobe.com/reader/

2. Comment & Markup toolbar functionality

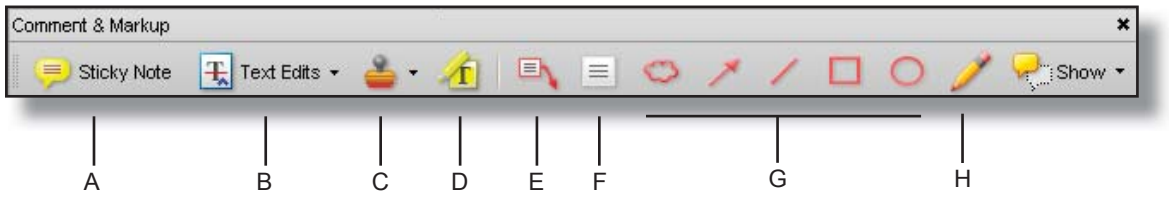

A. Sticky Note tool; B. Text Edits tool; C. Stamp tool; D. Highlight Text tool; E. Callout tool; F. Text Box tool; G. Various Object tools; H. Pencil tool

A. Show the Comment & Markup toolbar

The Comment & Markup toolbar doesn’t appear by default. Do one of the following:

- Select View > Toolbars > Comment & Markup.
- Select Tools > Comment & Markup > Show Comment & Markup Toolbar.
- Click the Review & Comment button in the Task toolbar, and choose Show Comment & Markup Toolbar.

To add or remove tools for this toolbar, right-click the toolbar and select the tool. Or, select Tools > Customize Toolbars.

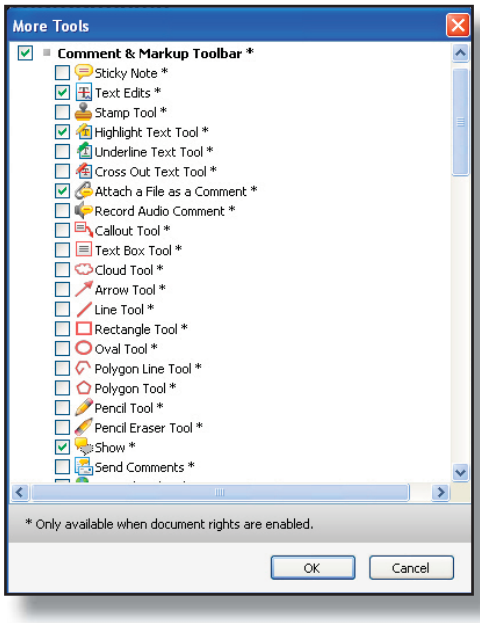

Choose Tools > Customize Toolbars to remove unnecessary items from the toolbar (see Section 7 for suggested toolbar layout)

B. Select a commenting or markup tool

Do one of the following:

- Select a tool from the Comment & Markup toolbar.
- Select Tools > Comment & Markup > [tool].

Note: After an initial comment is made, the tool changes back to the Select tool so that the comment can be moved, resized, or edited. (The Pencil, Highlight Text, and Line tools stay selected.)

C. Keep a commenting tool selected

Multiple comments can be added without reselecting the tool. Select the tool to use (but don’t use it yet).

- Select View > Toolbars > Properties Bar.
- Select Keep Tool Selected.

3. The Properties bar

The Properties bar can be used to format text and select options for individual tools.

To view the Properties bar, do one of the following:

- Choose View > Toolbars > Properties Bar.
- Right-click the toolbar area; choose Properties Bar.
- Select [Ctrl-E]

4. Using the comment and markup tools

To *insert*, *delete*, or *replace* text, use the **Text Edits** tool. Select the Text Edits tool, then select the text with the cursor (or simply position it) and begin typing. A pop-up note will appear based upon the modification (e.g., inserted text, replacement text, etc.). Use the Properties bar to format text in pop-up notes. A pop-up note can be minimized by selecting the ⊟ button inside it.

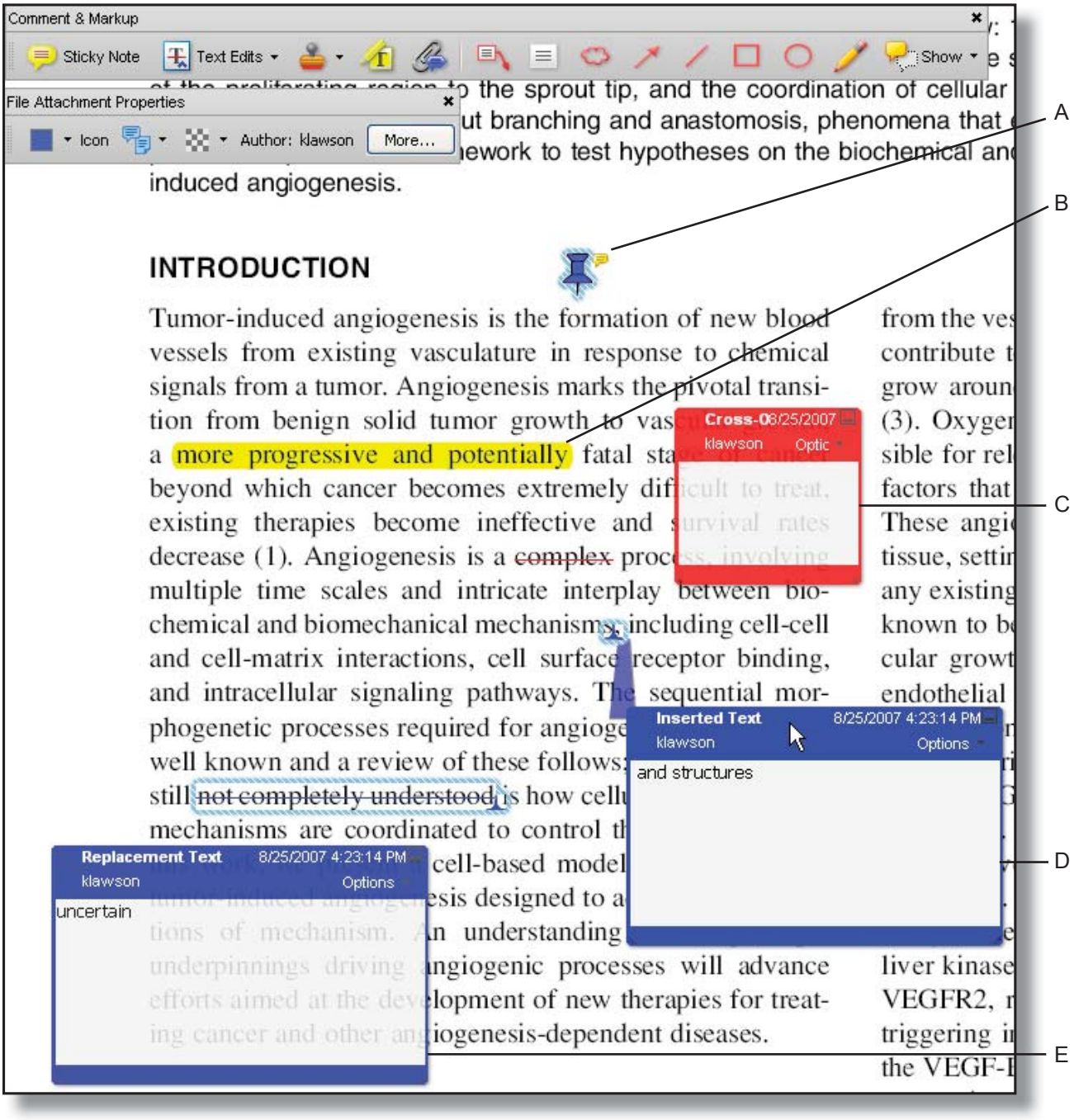

A. Attached file; B. Highlighted text; C. Crossed-out (strike-through) text; D. Inserted text; E. Replaced text

5. Inserting symbols or special characters

An 'insert symbol' feature is not available for annotations, and copying/pasting symbols or non-keyboard characters from Microsoft Word does not always work. Use angle brackets < > to indicate these special characters (e.g., <alpha>, <beta>).

6. Editing near watermarks and hyperlinked text

eProof documents often contain watermarks and/or hyperlinked text. Selecting characters near these items can be difficult using the mouse alone. To edit an eProof which contains text in these areas, do the following:

- Without selecting the watermark or hyperlink, place the cursor near the area for editing.
- Use the arrow keys to move the cursor beside the text to be edited.
- Hold down the shift key while simultaneously using arrow keys to select the block of text, if necessary.
- Insert, replace, or delete text, as needed.

7. Summary of main functions

Suggested toolbar layout

Insert text - Use Text Edits tool (position cursor and begin typing)
Replace text - Use Text Edits tool (select text and begin typing)
Delete text - Use Text Edits tool (select text and press delete key)
Highlight text - Use Highlight Text tool (select text)
Attach a file - Use the Attach a File with Comment tool (select tool, position cursor and click mouse, select file)

8. Reviewing changes

To review all changes, do the following:

- Select the Show button on the Comment & Markup toolbar.
- Select Show Comments List.

Note: *Selecting a correction in the list will highlight the corresponding item in the document, and vice versa.*

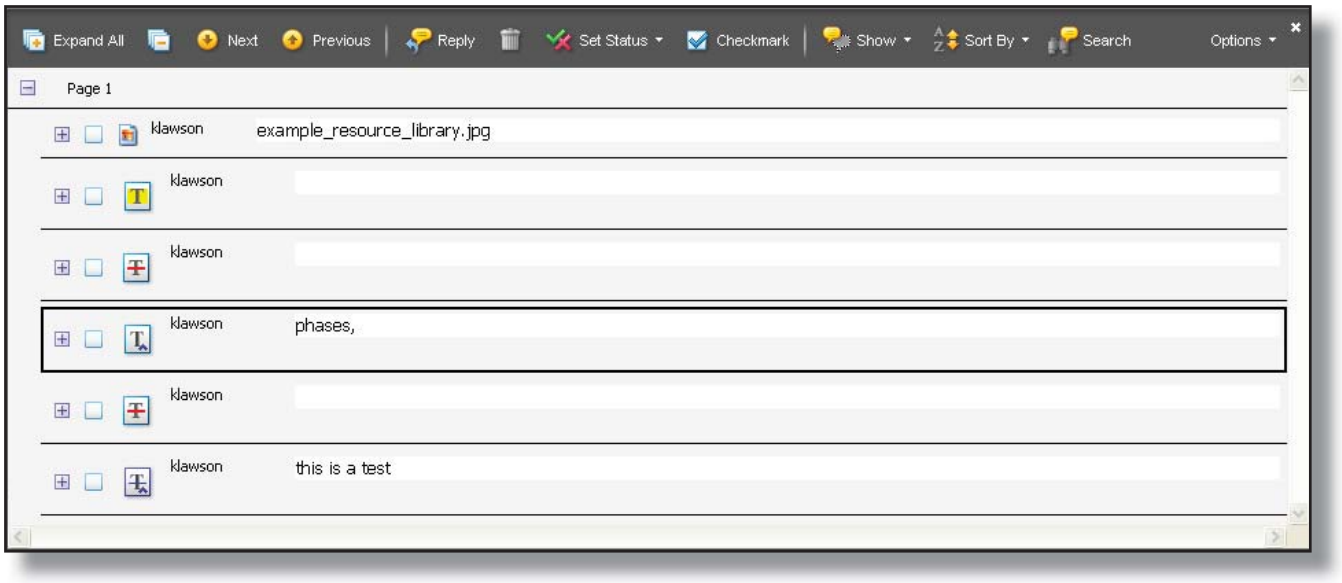

Use the Comments list to review all changes

NUMBER 1 OF 1

AUTHOR QUERIES

DATE 2/15/2010
JOB NAME WAF
JOB NUMBER 0

ARTICLE waf2222297
QUERIES FOR AUTHORS CORFIDI ET AL.

PLEASE ANSWER THE AUTHOR QUERIES WHERE THEY APPEAR IN THE TEXT.

AU1: The first two sentences are nearly identical to the first two sentences of the abstract. Consider rewriting.
AU2: Change to Kalnay et al. (1996), to match the reference list, best? Or should a new reference be added?
AU3: Consider rewording the phrase "grazing illumination" with a better word choice.
AU4: Change to Kalnay et al. (1996), to match the reference list, best? Or should a new reference be added?
AU5: For Fujita (1975) is there a document ID number for this map? How may a reader of your paper obtain this map?
AU6: For NOAA (1974) please provide the issue number(s) and page count(s) for the month(s) being referenced.

JOBNAME: WAF 0#00 PAGE: 1 SESS: 8 OUTPUT: Mon Feb 15 23:56:26 2010 Total No. of Pages: 45
/ams/waf/0/waf2222297

Revisiting the 3–4 April 1974 Super Outbreak of Tornadoes

STEPHEN F. CORFIDI AND STEVEN J. WEISS

NOAA/NWS/NCEP/Storm Prediction Center, Norman, Oklahoma

JOHN S. KAIN

~~Cooperative Institute for Mesoscale Meteorological Studies, University of Oklahoma,~~ ~~and~~ NOAA/National Severe Storms Laboratory, Norman, Oklahoma

SARAH J. CORFIDI

Cooperative Institute for Mesoscale Meteorological Studies, University of Oklahoma, Norman, Oklahoma

ROBERT M. RABIN

Cooperative Institute for Mesoscale Meteorological Studies, University of Oklahoma, and NOAA/National Severe Storms Laboratory, Norman, Oklahoma

JASON J. LEVIT

NOAA/NWS/NCEP/Storm Prediction Center, Norman, Oklahoma

(Manuscript received 27 April 2009, in final form 22 October 2009)

ABSTRACT

The Super Outbreak of tornadoes over the central and eastern United States on 3–4 April 1974 remains the most outstanding severe convective weather episode on record in the continental United States. ~~By nearly every metric imaginable,~~ the outbreak far surpassed previous and succeeding events in severity, longevity, and extent. In this paper, surface, upper-air, radar, and satellite data are used to provide an updated synoptic and subsynoptic overview of the event. Emphasis is placed on identifying the major factors that contributed to the development of the three main convective bands associated with the outbreak, and on identifying the conditions that may have contributed to the outstanding number of intense and long-lasting tornadoes. Selected output from a 29-km, 50-layer version of the Eta forecast model, a version similar to that available operationally in the mid-1990s, also is presented to help depict the evolution of thermodynamic stability during the event.

1. Introduction

AU1 The Super Outbreak of tornadoes of 3–4 April 1974 remains the most outstanding severe convective weather F1 episode on record in the continental United States (Fig. 1). By nearly every metric imaginable, the outbreak far surpassed previous and succeeding events in severity, longevity, and extent. A sampling of statistics only partially conveys its enormity: 148 tornadoes, of which 95 were F2 or stronger and 30 were F4 or F5; 48 killer tornadoes resulting in 335 deaths and more than 6000 injured; pathlengths up to 145 km (90 mi), with a total pathlength >4000 km (2500 mi); F2s or greater present for each three hour period between 1200 UTC 3 April and 1500 UTC 4 April; 15 tornadoes in progress simultaneously at the height of the event; and 10 states declared federal disaster areas. Further appreciation for the phenomenal nature of the Super Outbreak may be gleaned from Fig. 2, which depicts the maximum, week-long running total of F2 or greater tornadoes from 1915 through 2008. Entire *years* noted for their prominent tornado counts (e.g., 1947, 1953, and 2003) pale in comparison to the 18-h period that began around midday on Wednesday, 3 April 1974. Twenty-five F3 or greater long-track [>40 km (25 mi)] tornadoes occurred during the same F2

Corresponding author address: Stephen F. Corfidi, Storm Prediction Center, 120 David L. Boren Blvd., Ste. 2300, Norman, OK 73072.
E-mail: stephen.corfidi@noaa.gov

DOI: 10.1175/2009WAF2222297.1

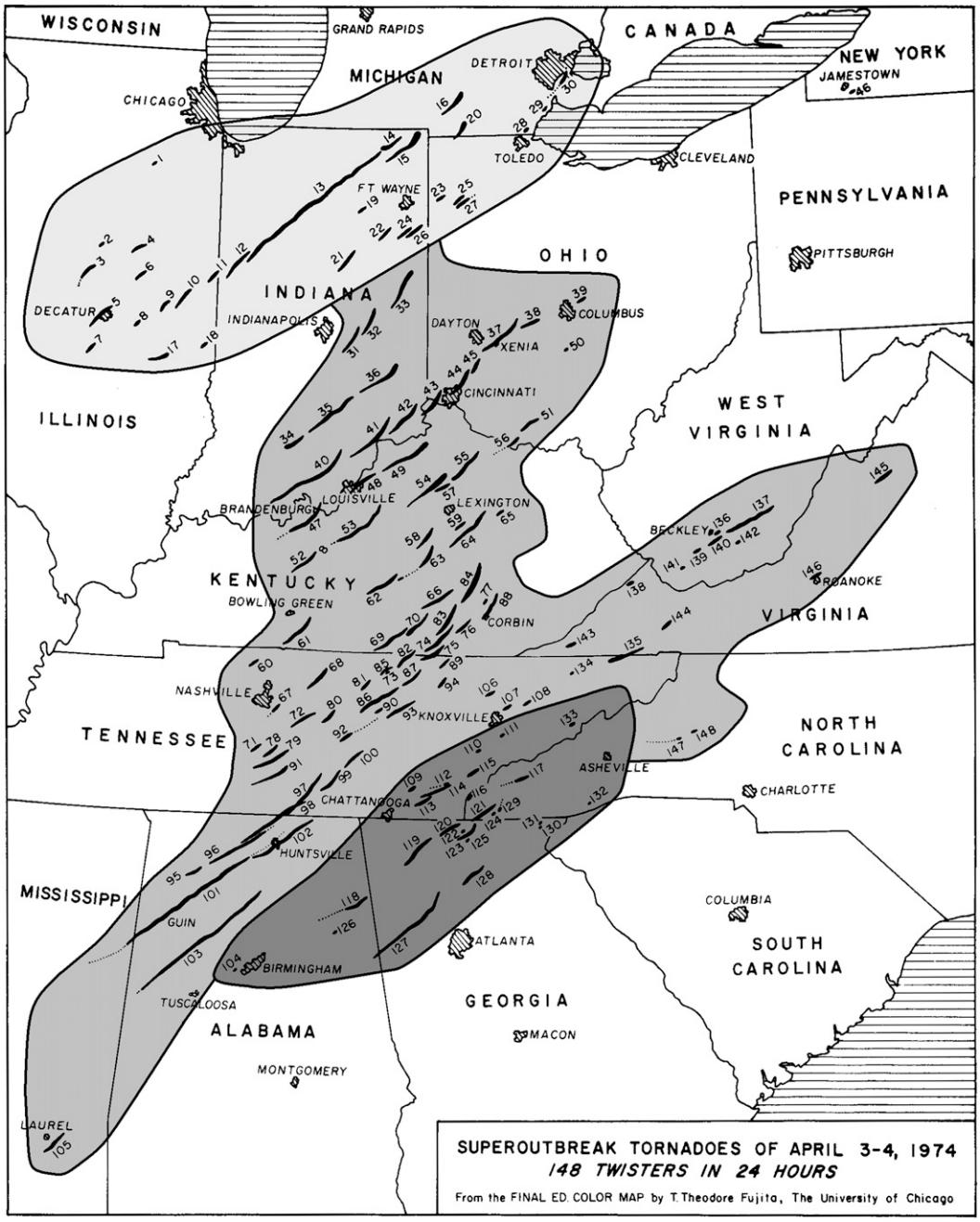

FIG. 1. Tracks of the 148 Super Outbreak tornadoes documented by Fujita (1975). Areas affected by tornadic supercells composing convective bands one, two, and three are depicted in dark, medium, and light gray shading, respectively. (See section 3 for discussion of convective bands one, two, and three.) The tornado in southwestern NY was an isolated event loosely associated with band two.

period, more than triple the annual average of such events since 1880 (Broyles and Crosbie 2004).

More than a third of a century has passed since the Super Outbreak inflicted its toll on the Midwest and the Ohio and Tennessee Valleys. Despite its breadth and intensity, little has been written about lessons that the forecast and research communities might learn from the event. From this perspective, it is important to ask what characteristics of the synoptic- and mesoscale environments might have made the April 1974 outbreak so extraordinary, and how this analysis might be used to anticipate such a rare event in the future. In particular, it is incumbent upon severe weather forecasters to attempt to understand why so many significant, long-lasting tornadic storms occurred.

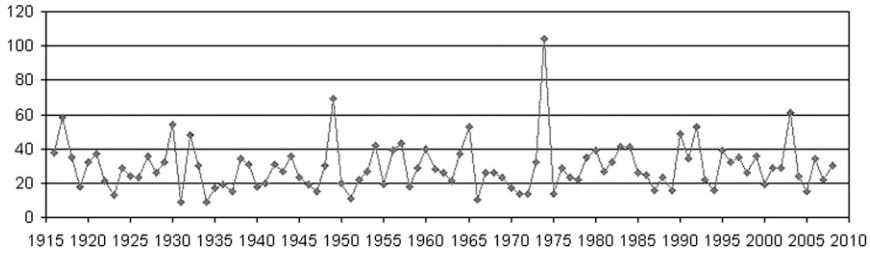

FIG. 2. Maximum, week-long running total of F2 or stronger tornadoes per year since 1915. Data from Grazulis (1993). (Graphic courtesy of H. Brooks, NOAA/National Severe Storms Laboratory.)

In the present paper, surface and upper-air analyses as well as radar and satellite data are used to provide an updated synoptic- and subsynoptic-scale overview of the 1974 Super Outbreak. Emphasis is placed on 1) identifying the major factors involved in the development of the four convective bands associated with the event and 2) identifying the conditions that may have contributed to the outstanding number of intense and long-lasting tornadoes. Given the paucity of radar and satellite data relative to that routinely available today, discussion necessarily focuses on mesoalpha- and mesobeta-scale aspects, with only limited mention of storm-scale processes.

2. Data

Plots of twice-daily (0000 and 1200 UTC) mandatory-level rawinsonde observations over the United States and adjacent parts of Canada and Mexico for 2 April–4 April 1974 were hand analyzed in a conventional manner; the analyses for the period 1200 UTC 2 April–1200 UTC 4 April are provided in Fig. 3. The decision to perform a hand analysis reflected 1) a desire to minimize the effects of smoothing inherent in objective analysis schemes and 2) the belief that hand analysis can serve to further one's familiarization with and understanding of meteorological events.

Plots of hourly surface observations over the central and eastern United States also were manually analyzed for the period 1200 UTC 2 April–1200 UTC 4 April 1974. A selection of these analyses is presented in Fig. 4. Although their inclusion substantially lengthens this presentation, examination of the long-term evolution of surface (and upper level) features is essential to understanding this event. The observed data (station plots) appear in each analysis. The data are too small for clear display on the printed page, but are legible when viewed with magnification on a computer monitor. The data density is sufficient to enable the reader to critique the analyses.

Emphasis during the surface analysis process was placed on identifying subsynoptic-scale wind and thermodynamic discontinuities believed to be important to thunderstorm initiation, and on tracking these features consistently over space and time. Most of the discontinuities were characterized conventionally as cold fronts, warm fronts, drylines, and outflow boundaries, etc. Wind shift lines, short-lived troughs, and other features that appeared to be of lesser significance or of unknown origin were denoted by dashed lines. One discontinuity had characteristics of both a cold front and a dryline; this feature is discussed in section 3. The 3-hourly analyses presented in Hoxit and Chappell (1975) provided a valuable first guess for the period from 1200 UTC 3 April through 0300 UTC 4 April. Large-scale, hourly, manually digitized radar composite charts from the Storm Prediction Center (formerly the National Severe Storms Forecast Center) archive assisted in the identification of thunderstorm outflow boundaries, as did radar data presented in Forbes (1975), and plotted storm reports contained within the Storm Prediction Center database.[1] Because the Super Outbreak occurred just prior to the launch of the first geosynchronous weather satellite in May 1974, the temporal and spatial resolutions of the satellite data covering the event are quite limited relative to those routinely available today. The analyses did, however, benefit from 29 hard-copy, national-scale Applications Technology Satellite-III visible data images for the period from 1342 to 2324 UTC 3 April; a few of these images appear in Fig. 4.

To depict the spatial evolution of thermodynamic stability during the outbreak, selected output fields from a 29-km, 50-layer version of the Eta forecast model (hereafter "Eta29"), are presented. The model, similar to that used operationally by the National Weather Service (NWS) in the mid-1990s (Black 1994), was initialized with data valid at 0000 UTC 3 April. It uses a modified Betts–Miller cumulus parameterization scheme (Betts 1986,

[1] Because severe weather report gathering efforts in 1974 were very limited relative to those of today, it should be recognized that the number of nontornadic severe events for the Super Outbreak likely far exceeds that indicated by the Storm Prediction Center database.

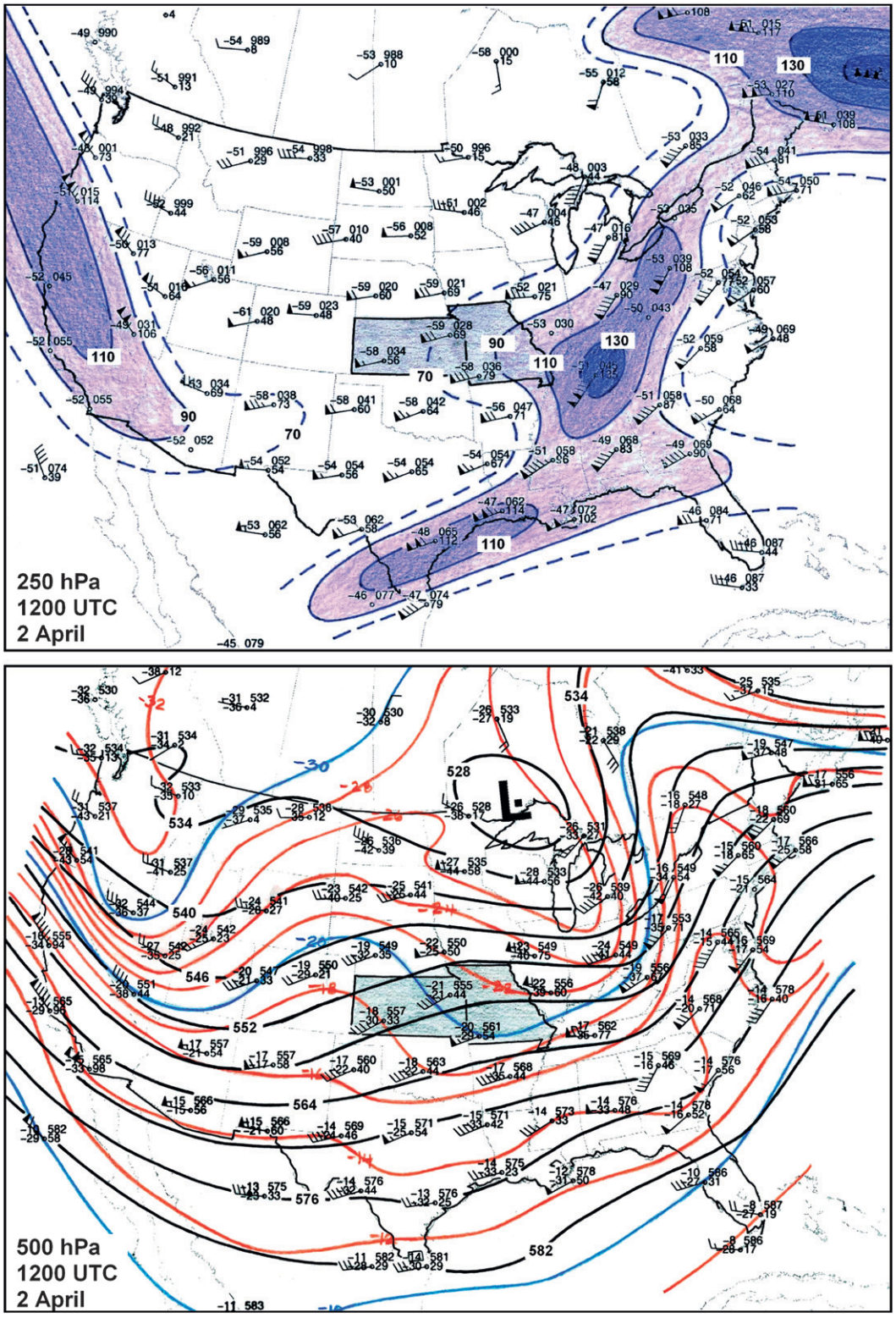

FIG. 3. Sequence of 250-, 500-, 700-, and 850-hPa manual upper-air analyses for (a) 1200 UTC 2 Apr, (b) 0000 UTC 3 Apr, (c) 1200 UTC 3 Apr, (d) 0000 UTC 4 Apr, and (e) 1200 UTC 4 Apr 1974 over the continental United States. Conventional data plots using metric units, except wind speed, which is in knots (1 kt = 0.51 m s^{-1}). Wind speeds equal to or greater than 35 m s^{-1} (70 kt) are shaded purple at 250 hPa; dewpoints greater than or equal to 4°C are shaded green at 850 hPa. Troughs are depicted by dashed black lines at 700 hPa. The states of Kansas and Missouri are shaded for reference.

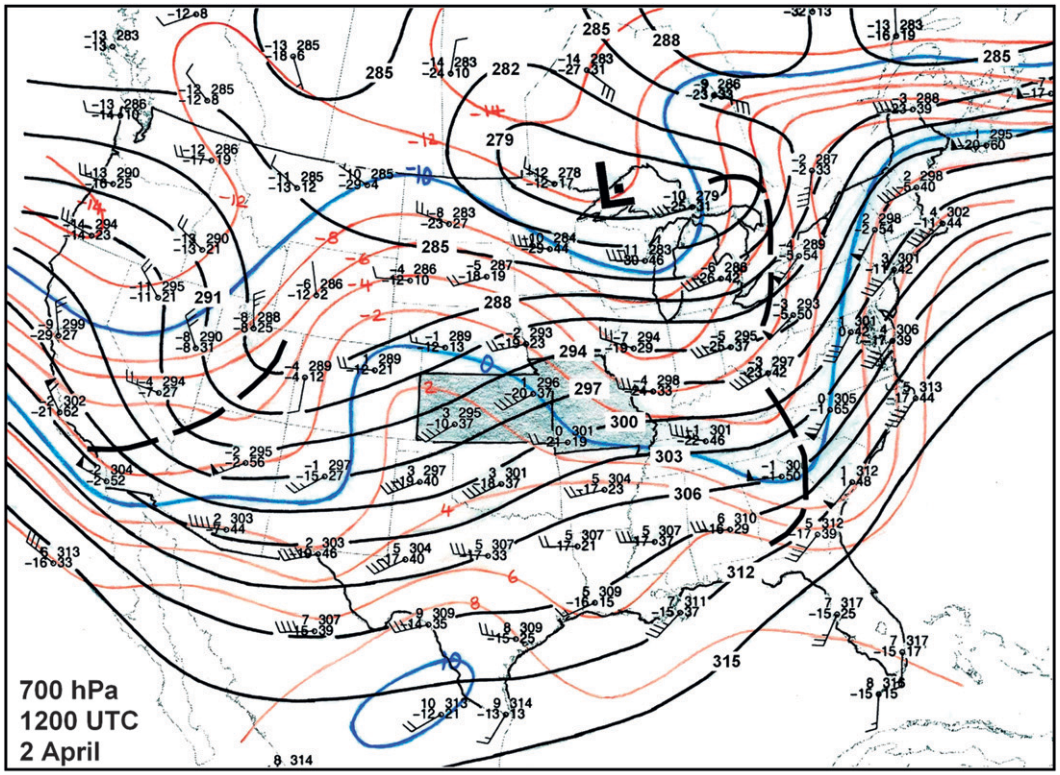

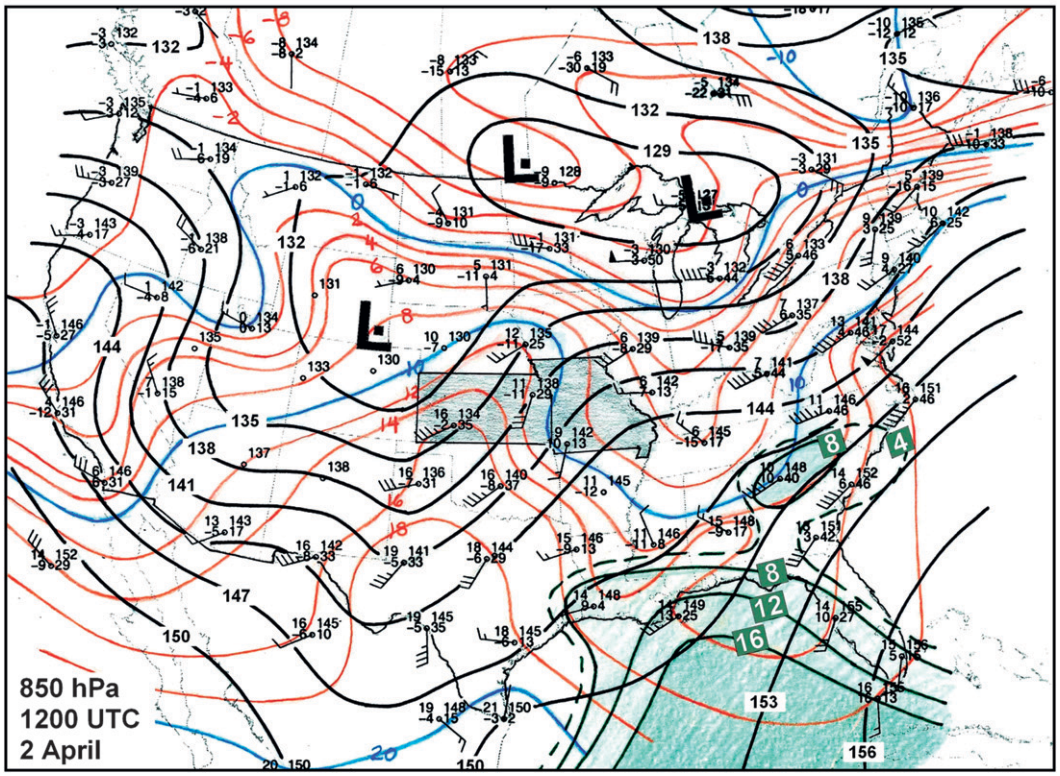

FIG. 3. (*Continued*)

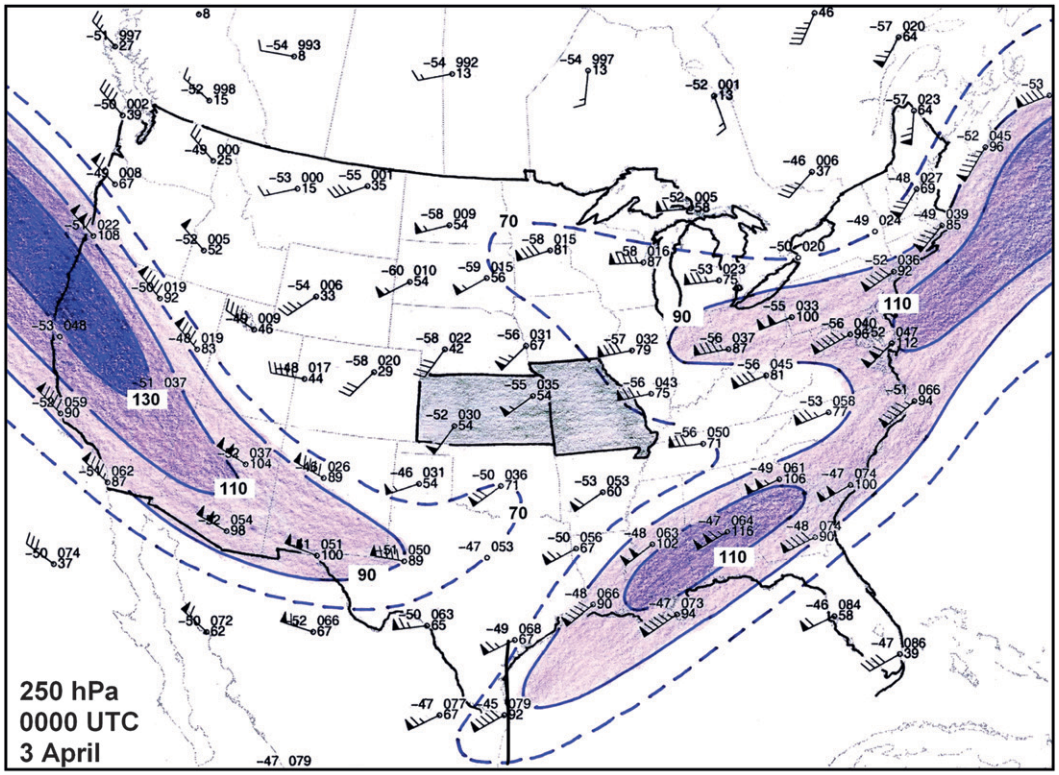

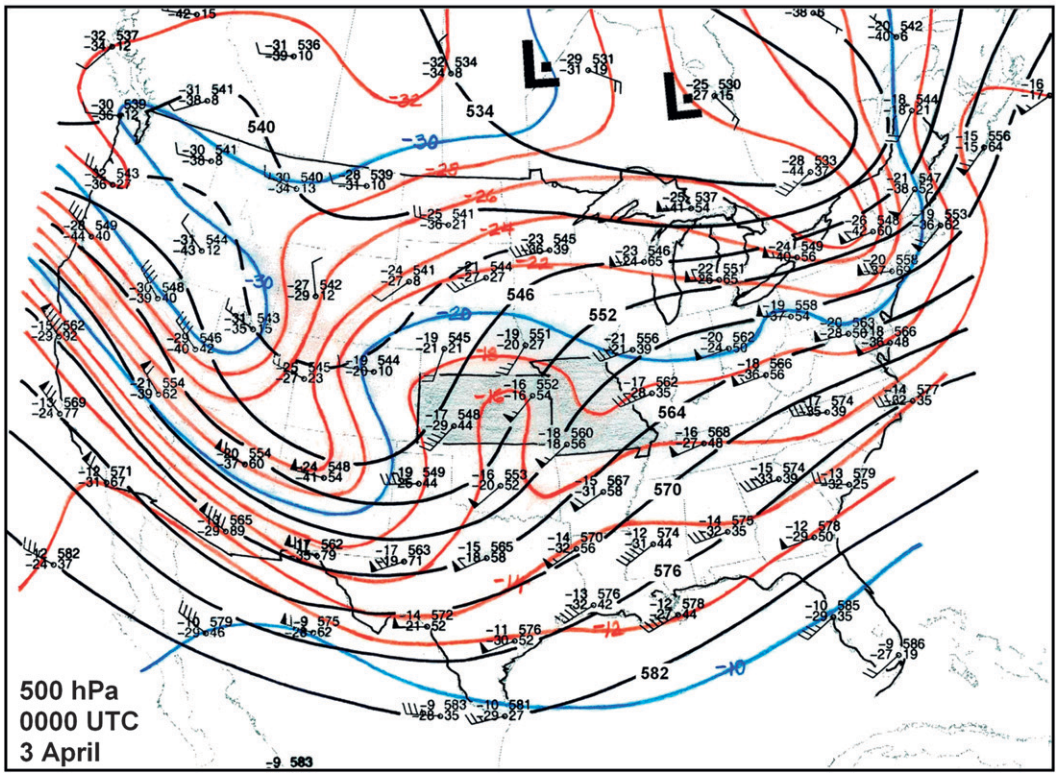

FIG. 3. (*Continued*)

JOBNAME: WAF 0#00 PAGE: 7 SESS: 8 OUTPUT: Mon Feb 15 23:59:04 2010 Total No. of Pages: 45
/ams/waf/0/waf2222297

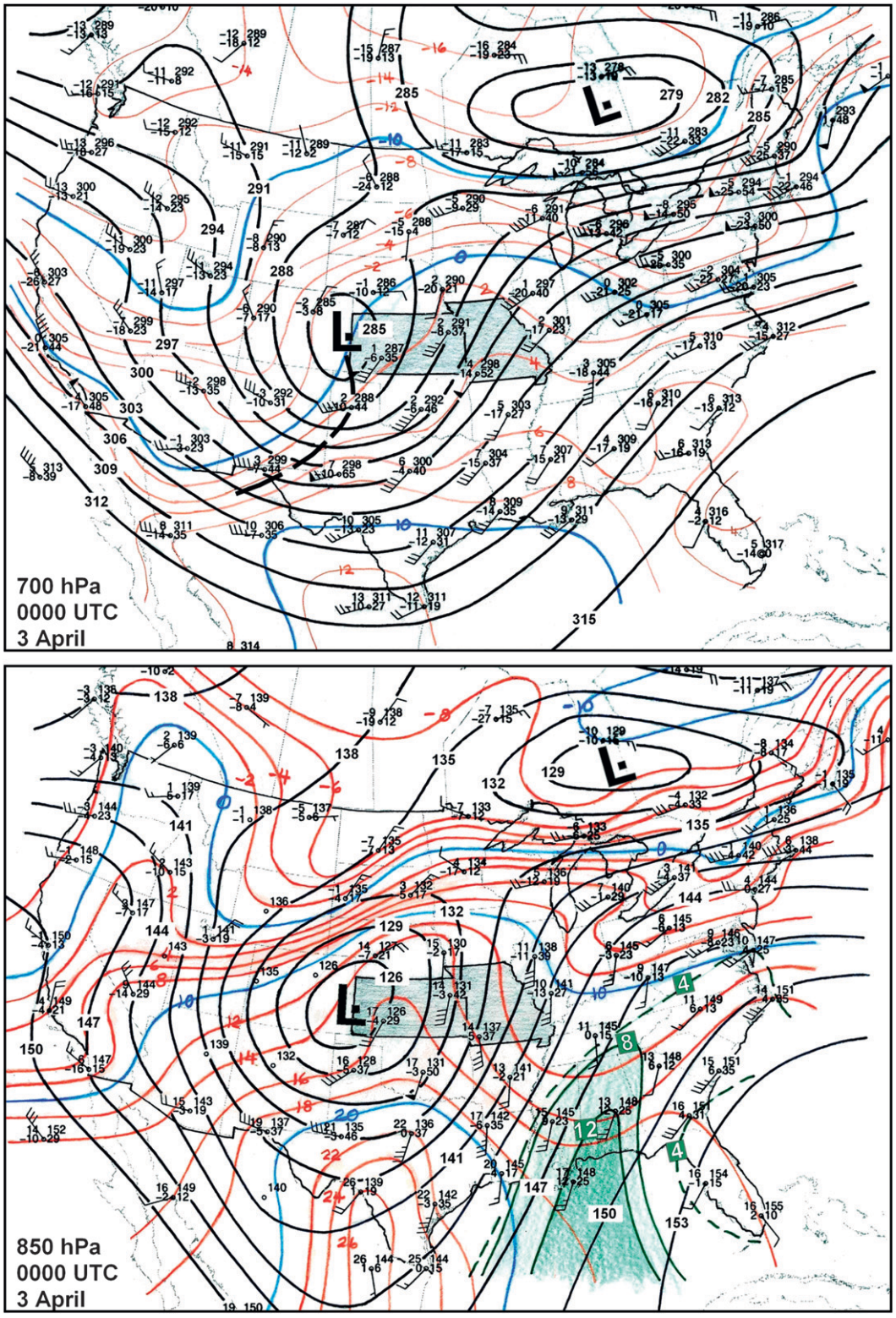

FIG. 3. (*Continued*)

JOBNAME: WAF 0#00 PAGE: 8 SESS: 8 OUTPUT: Mon Feb 15 23:59:57 2010 Total No. of Pages: 45
/ams/waf/0/waf2222297

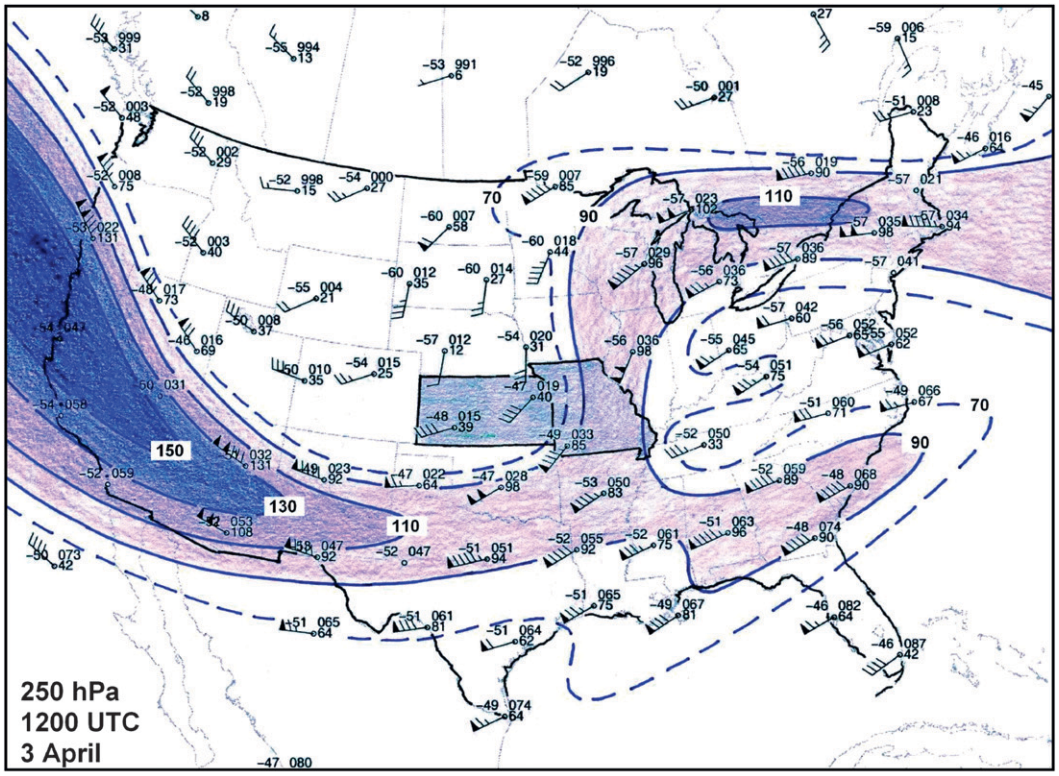

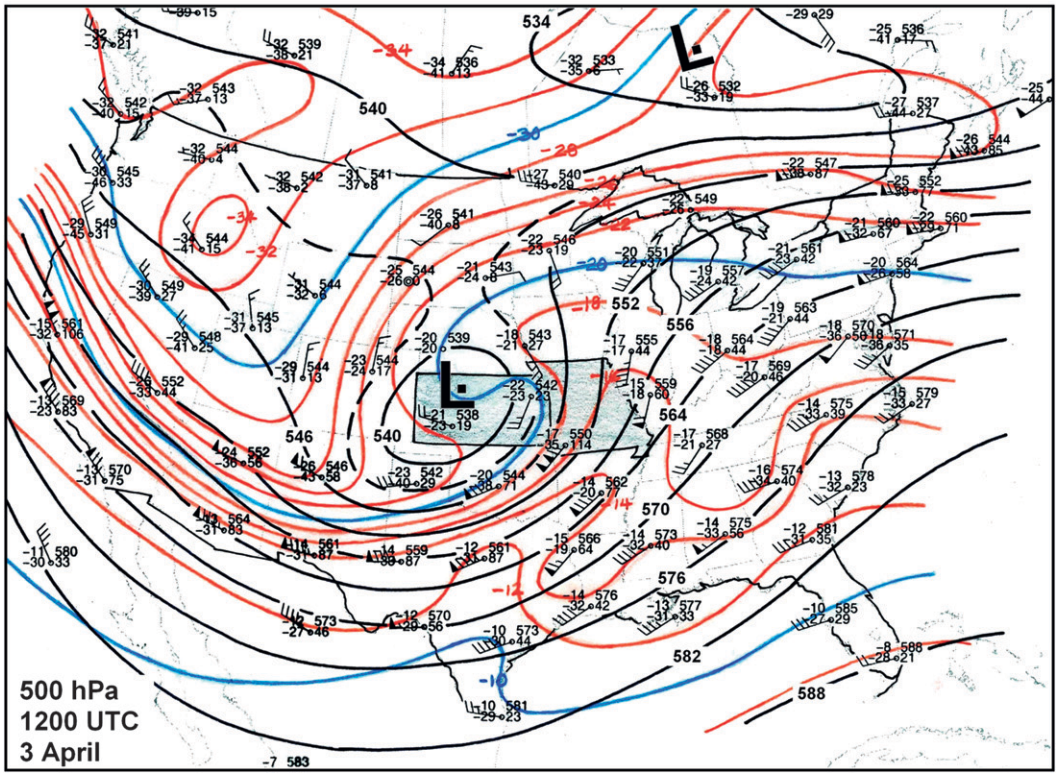

FIG. 3. (*Continued*)

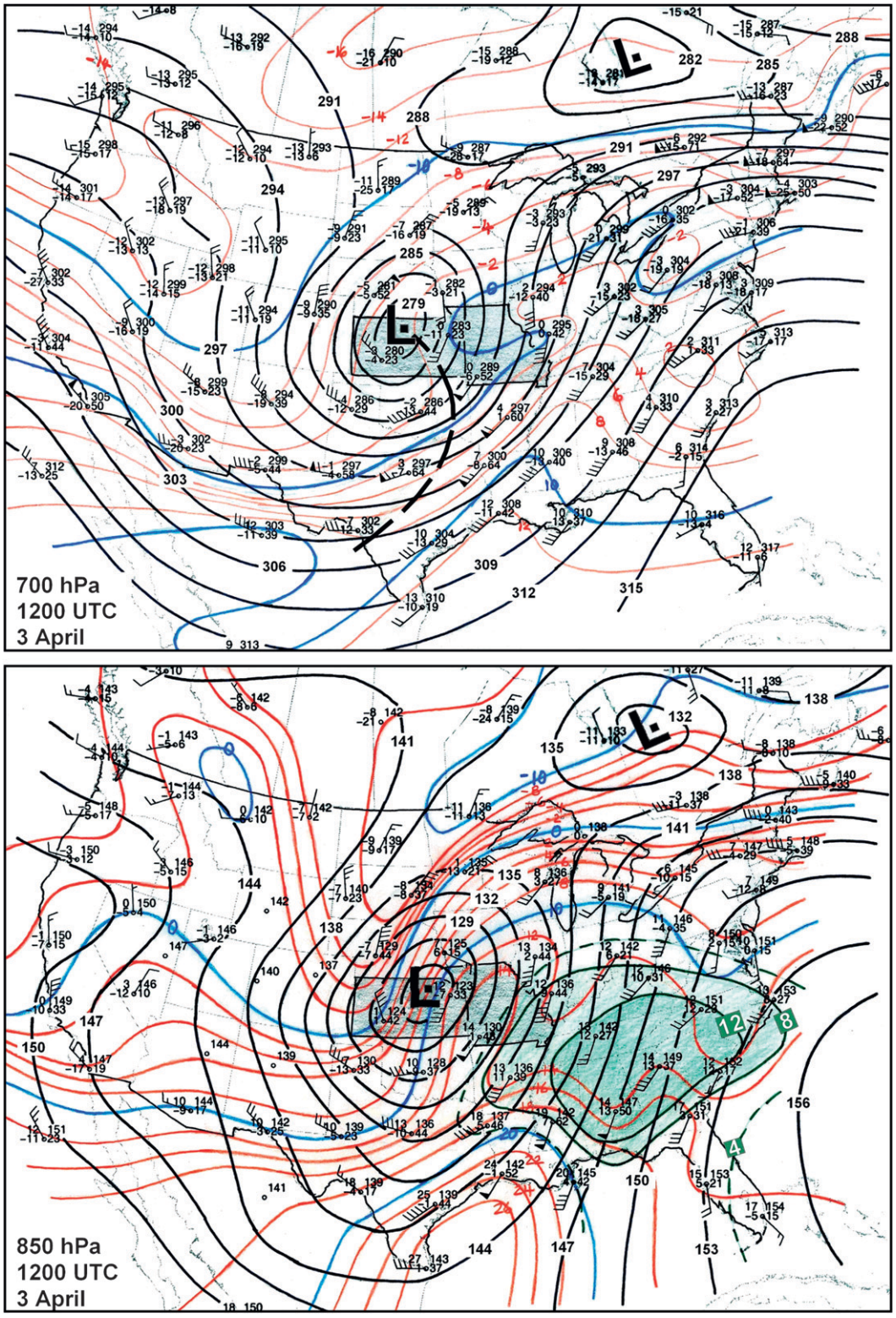

FIG. 3. (*Continued*)

JOBNAME: WAF 0#00 PAGE: 10 SESS: 8 OUTPUT: Tue Feb 16 00:03:16 2010 Total No. of Pages: 45
/ams/waf/0/waf2222297

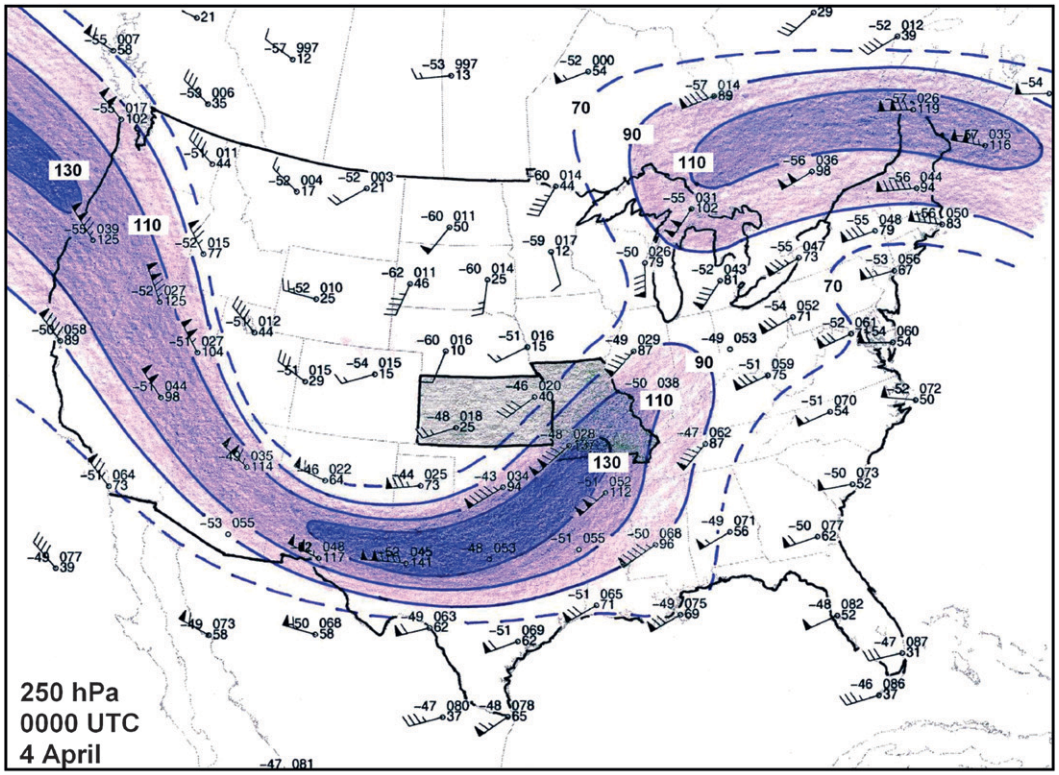

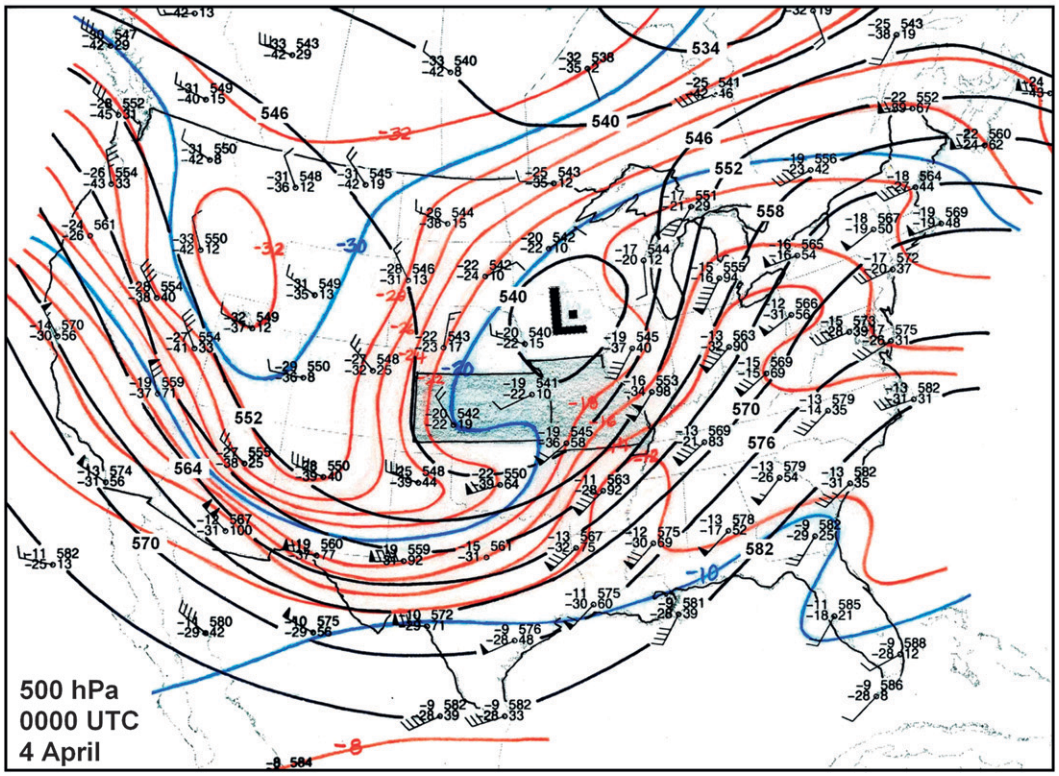

FIG. 3. (*Continued*)

JOBNAME: WAF 0#00 PAGE: 11 SESS: 8 OUTPUT: Tue Feb 16 00:05:36 2010 Total No. of Pages: 45
/ams/waf/0/waf2222297

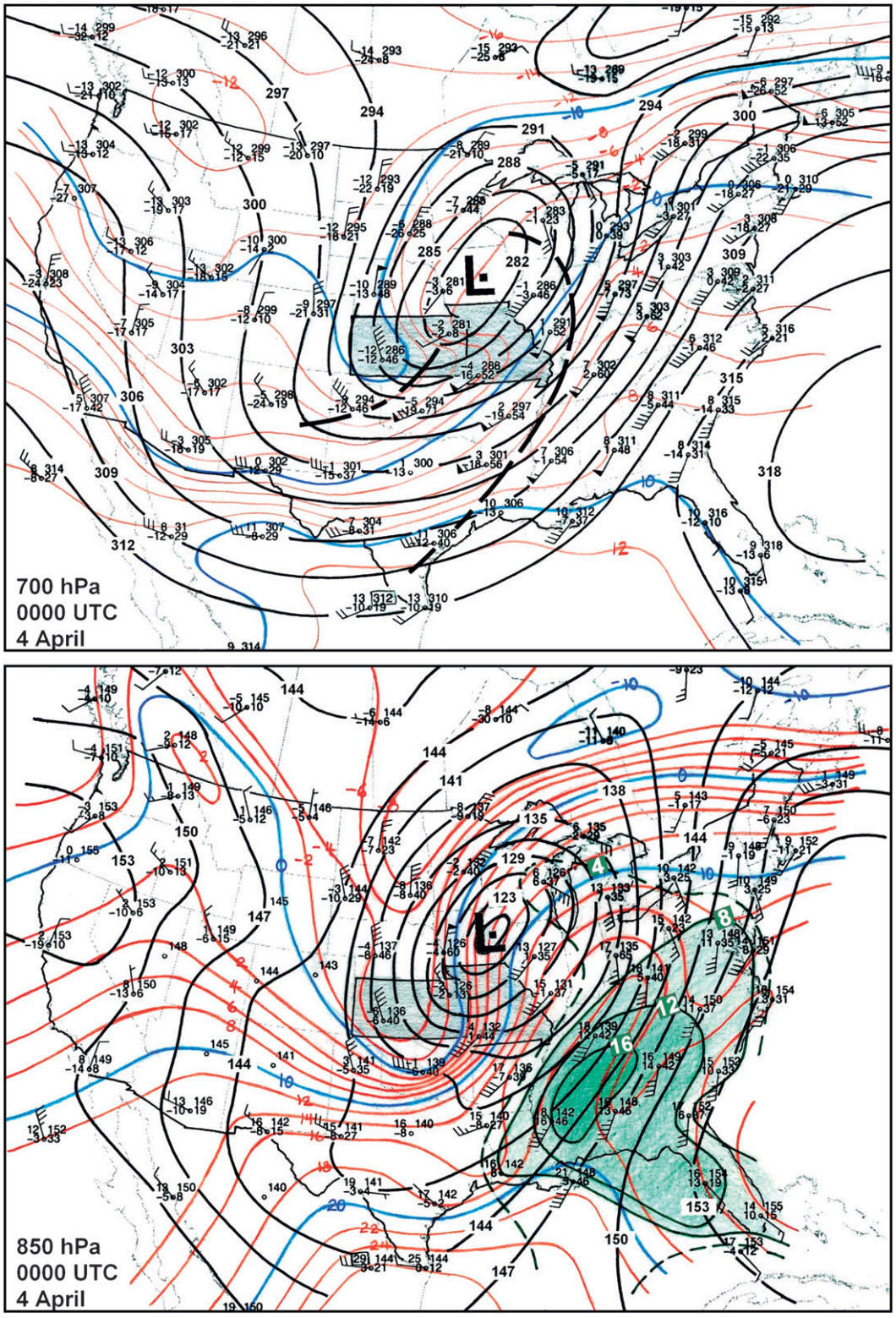

FIG. 3. (*Continued*)

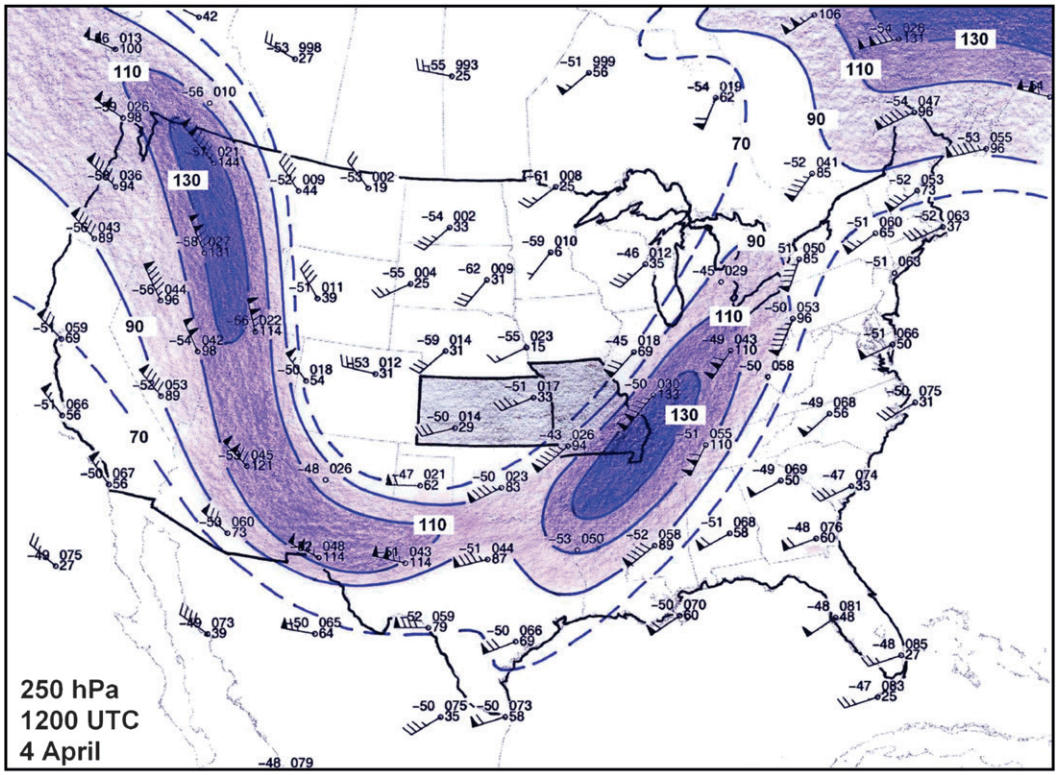

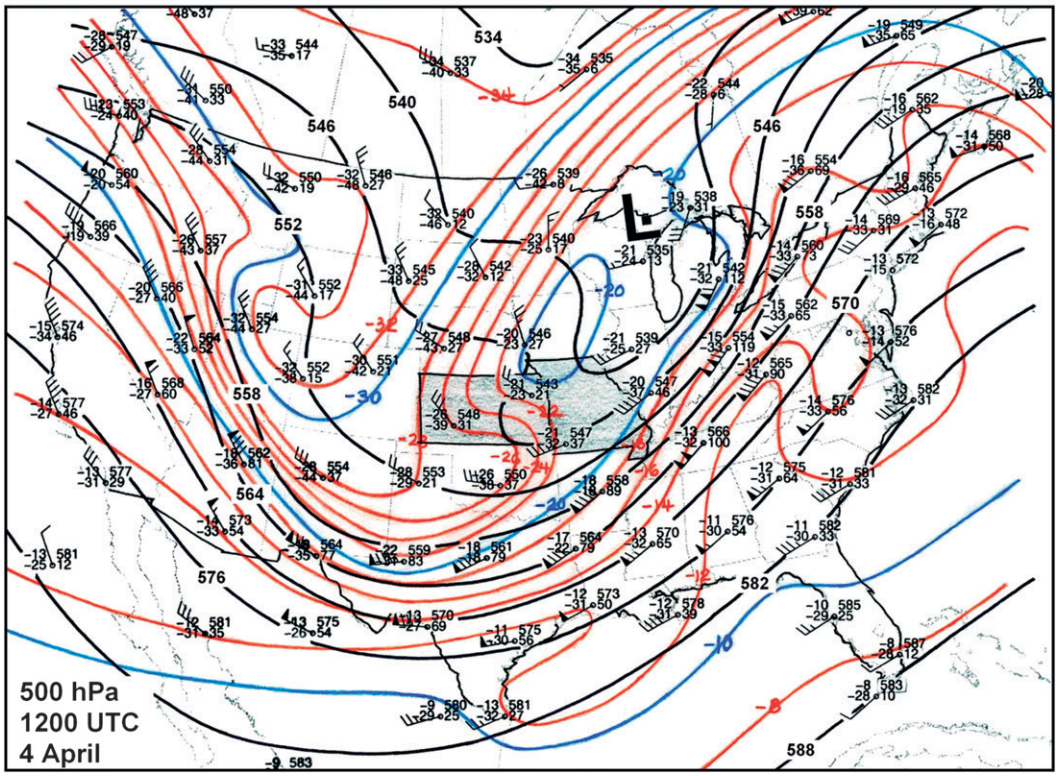

FIG. 3. (*Continued*)

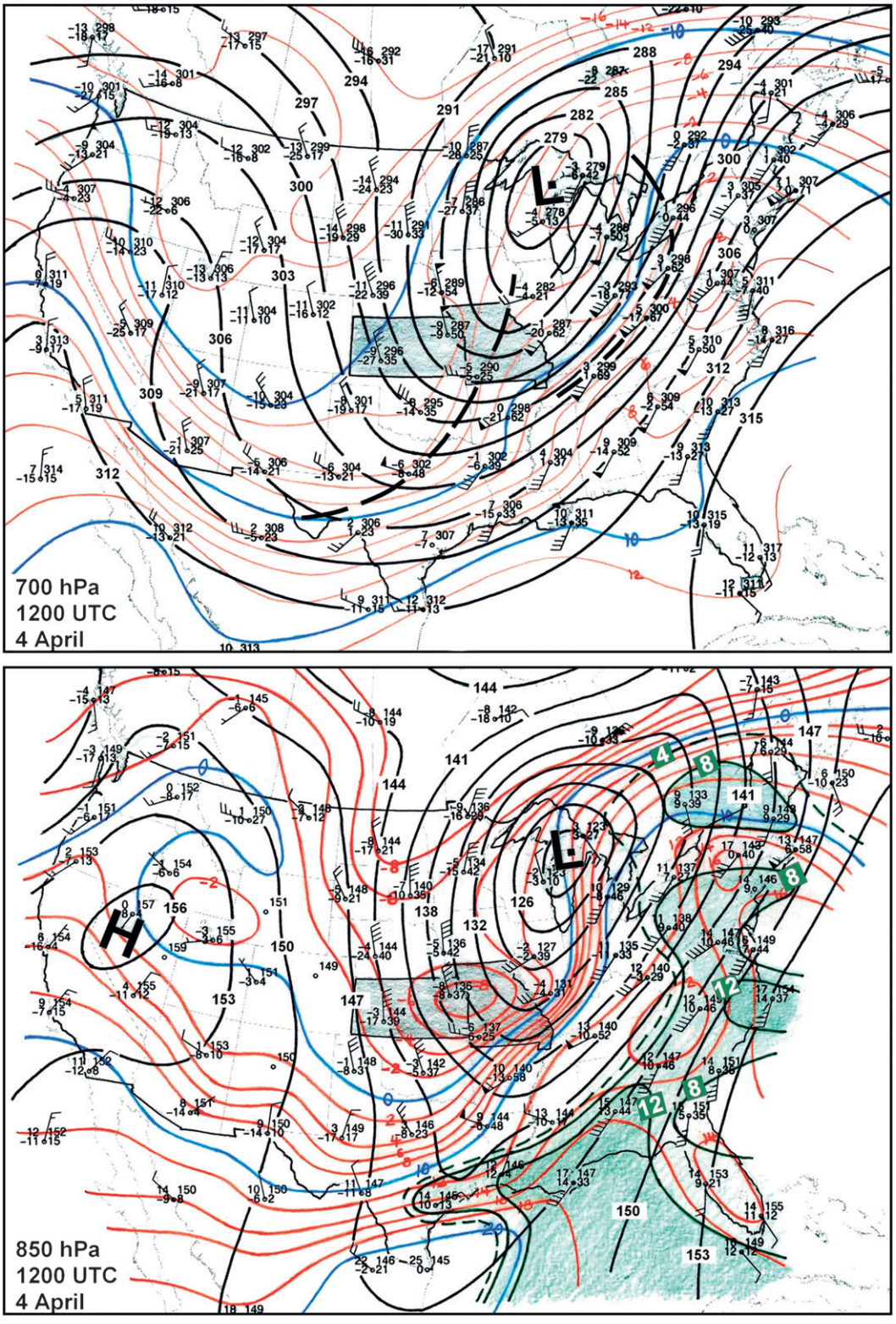

FIG. 3. (*Continued*)

Janjić 1994), with initial and boundary conditions provided by the National Centers for Environmental Prediction–National Center for Atmospheric Research (NCEP–NCAR) global reanalysis dataset (Kalnay et al. 1996). The reanalysis dataset is on a 2.5° × 2.5° grid with 17 levels.

Model forecast fields, rather than reanalysis data, were chosen to depict the spatial stability because of the coarse nature of the reanalysis data, and to provide a 3-hourly regional evolution of the thermodynamic environment between the routine 0000 and 1200 UTC rawinsonde observation times. Use of the Eta29 primarily reflected that model's availability at the time the preliminary work was being conducted on this project in spring 2004. Because the present paper focuses on the synoptic- and mesoalpha-scale aspects of the Super Outbreak, little benefit would be derived from presenting thermodynamic or kinematic fields from a higher-resolution model, especially considering that such a model would be initialized with the same low-resolution (global reanalysis) data.

Subjective evaluation of model mass fields revealed that the Eta29 provided excellent forecasts of major synoptic-scale features, including the position and intensity of the lee cyclone and accompanying midlevel jet streak associated with the event. Development of widespread convective precipitation in the model appeared to impact the Eta29's thermodynamic fields after 2100 UTC. Prior to that time, however, the model's stability fields are believed to be reasonably representative of the actual thermodynamic environment over the central and eastern United States.

3. Chronological overview of the event

In this section, surface and upper-air analyses, as well as radar and satellite data, are used to provide an updated synoptic- and subsynoptic-scale overview of the 1974 Super Outbreak. To date, no such overview has appeared in the refereed literature. Given the limited amount of radar and satellite data available relative to that routinely collected today, our discussion necessarily focuses on mesoalpha- and mesobeta-scale features.

a. Morning through afternoon, Tuesday, 2 April

The morning of Tuesday, 2 April 1974, was characterized by a broad, low-amplitude mid- and upper-level trough over the continental United States (Fig. 3a). Embedded in the trough were two moderately strong short-wave disturbances that were apparent at both 700 and 500 hPa. One of these extended from the upper Ohio Valley into the southern Appalachians, while the other was over the Great Basin. The latter impulse was accompanied by 500-hPa wind speeds of 50 m s^{-1} (100 kt) across southern California, while downstream speeds were less than 25 m s^{-1} (50 kt) over the southern plains. The eastern short wave was deamplifying at this time and was associated with a weakening surface and 850-hPa low over northern Lake Huron (Figs. 3a and 4a).

Trailing generally south from the surface low, a cold front extended along the western slopes of the Appalachians into the northwestern Gulf of Mexico. Thunderstorms that formed along and ahead of the front on the

→

FIG. 4. Sequence of hand-analyzed surface charts for the central and eastern United States for (a) 1200 UTC 2 Apr, (b) 1800 UTC 2 Apr, (c) 0000 UTC 3 Apr, (d) 0300 UTC 3 Apr, (e) 0600 UTC 3 Apr, (f) 0900 UTC 3 Apr, (g) 1200 UTC 3 Apr, (h) 1500 UTC 3 Apr, (i) 1800 UTC 3 Apr, (j) 2100 UTC 3 Apr, (k) 0000 UTC 4 Apr, (l) 0300 UTC 4 Apr, (m) 0600 UTC 4 Apr, (n) 0900 UTC 4 Apr, and (o) 1200 UTC 4 Apr 1974. Conventional data plots using English units, with wind speed in knots, and data believed to be erroneous enclosed in rectangles. Green lines depict the 56°, 62°, and 68°F (13.3°, 16.6°, and 20.0°C) isodrosotherms; green shading indicates areas with dewpoints ≥ those values. (Note that in a few instances, isodrosotherms are drawn slightly awry to minimize data obscuration.) Frontal symbols are conventional, with outflow boundaries depicted using small pips. Wind shifts lines, short-lived troughs, and lesser features of uncertain origin are denoted by dashed lines. Axes of relatively concentrated convection (per composite radar data, satellite data, and/or surface imagery) are shown by solid lines without pips. Convective bands one, two, three, and four are indicated by large black numerals. Mesohighs ("bubble highs") are denoted by scripted Bs. Visible Applications Technology Satellite III satellite imagery, and National Weather Service composite radar data (adapted from Hoxit and Chappell 1975), are included in (g)–(k); the exact times of these products are given in the lower-left corner of each view. The composite radar images depict echo tops in thousands of feet (last two digits omitted), echo motions (arrows with speed in knots). Scalloping denotes subjectively determined areas of scattered (circle with a single line) and broken (circle with a double line) echo coverage. IP, S, RW, and TRW denote, respectively, ice pellets, snow, rainshowers, and thunder showers, based subjectively on radar reflectivity data. Isolated is indicated by ISOLD. Severe weather reports (as contained in the Storm Prediction Center database) for the 3-h period beginning at the surface analysis time included in (g)–(o). Tornadoes and/or tornado tracks are in red, accompanied by the highest F-scale rating for the event. Hail ≥ 1.9 cm (0.75 in.) is depicted by green dots, damaging wind and/ or observed wind gusts ≥25 m s^{-1} (50 kts) by blue crosses, and combined wind and hail events by purple dots. (Note that severe weather report gathering efforts in 1974 were very limited relative to those of today; the number of nontornadic reports for this event likely far exceeds that indicated by the figures.)

JOBNAME: WAF 0#00 PAGE: 15 SESS: 8 OUTPUT: Tue Feb 16 00:08:15 2010 Total No. of Pages: 45
/ams/waf/0/waf2222297

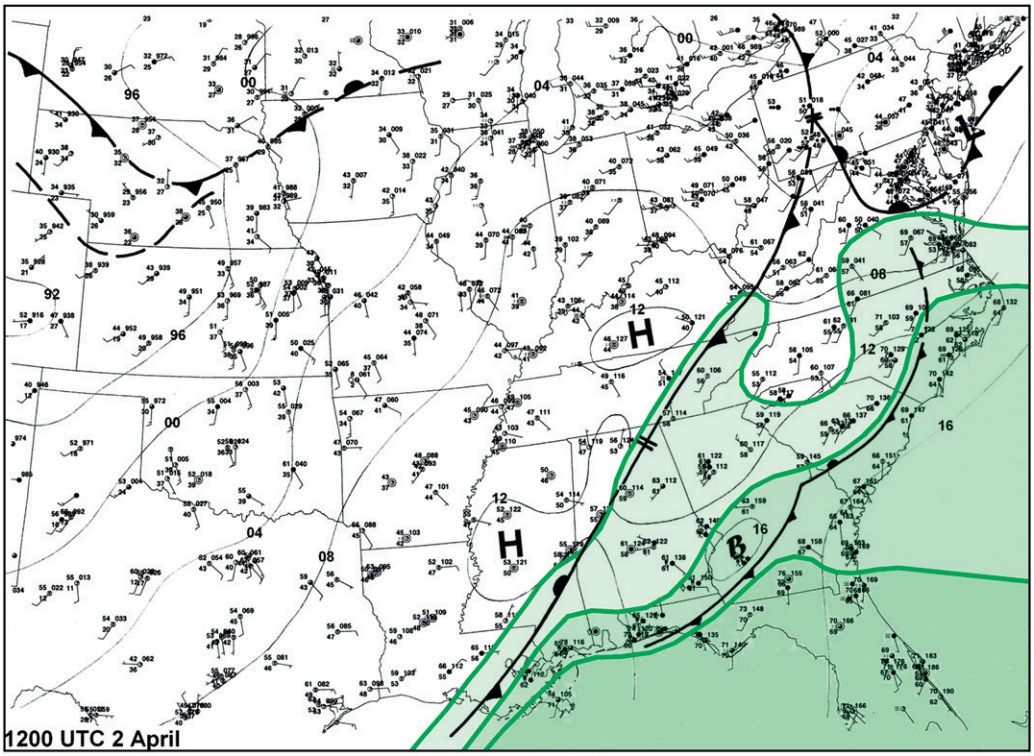

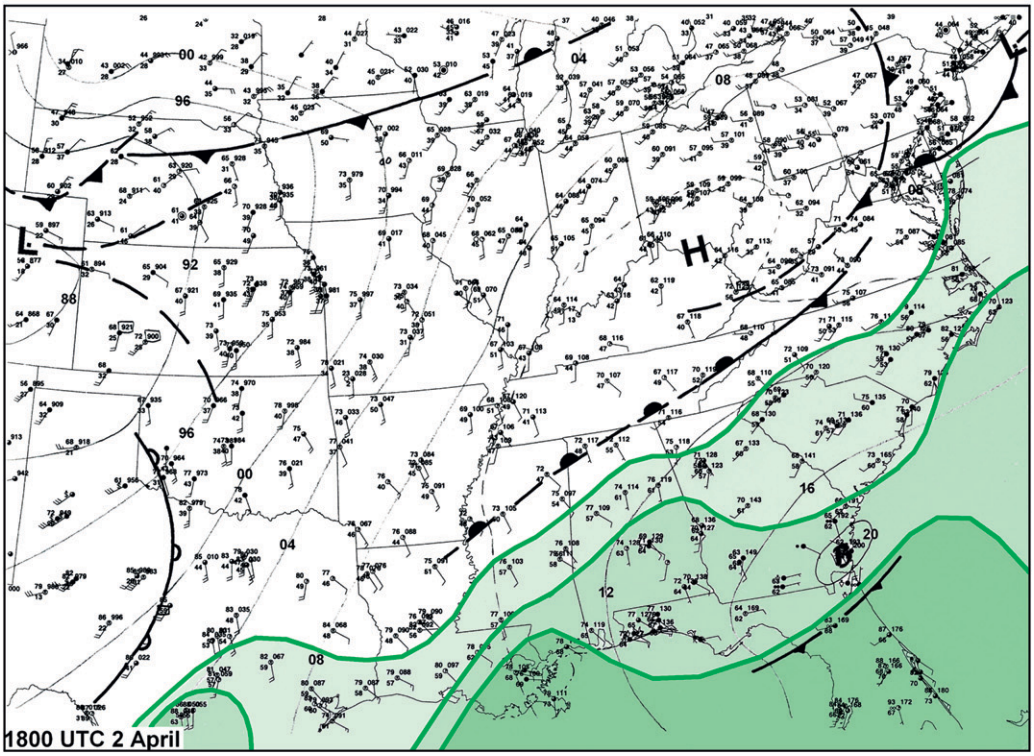

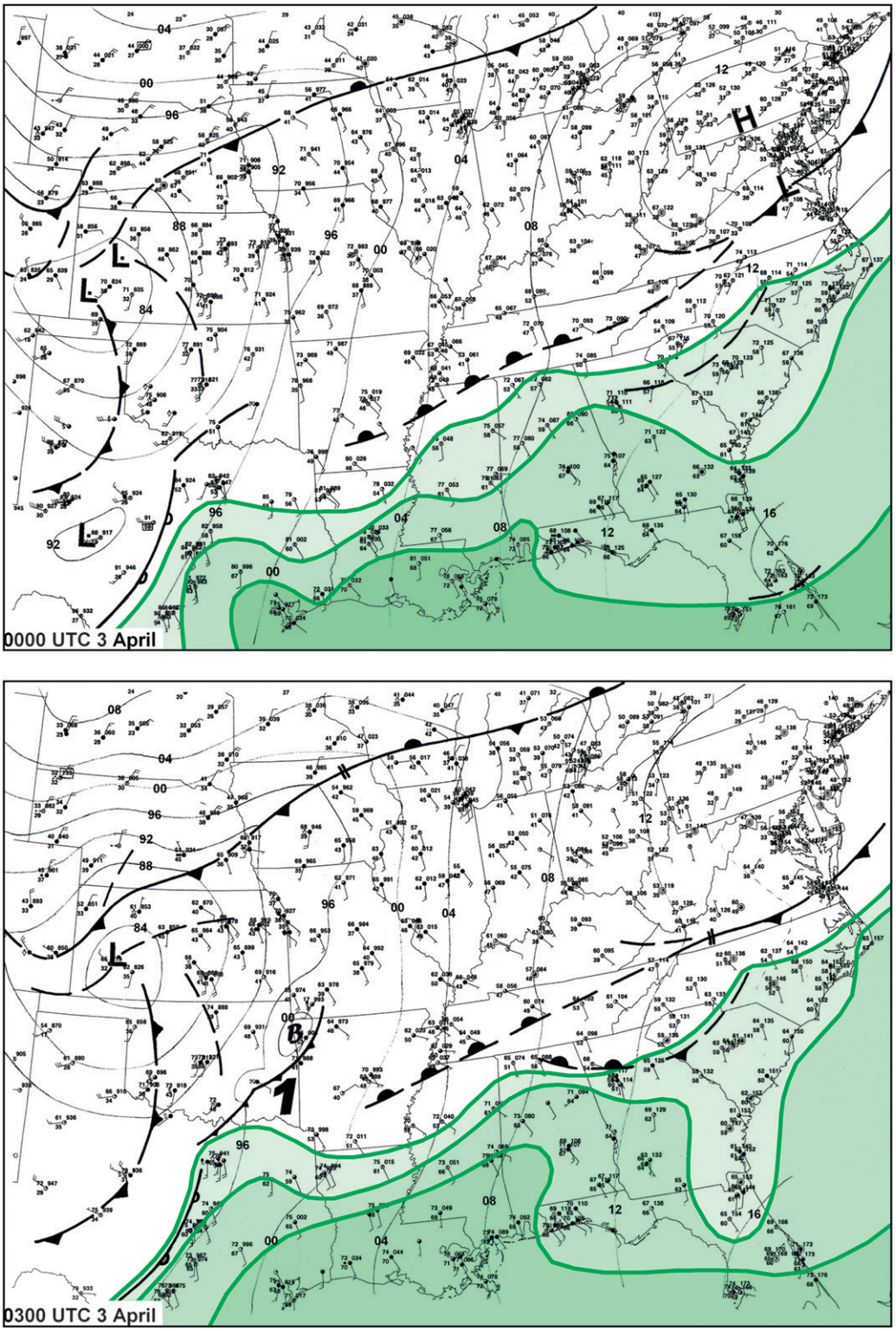

FIG. 4. (*Continued*)

JOBNAME: WAF 0#00 PAGE: 17 SESS: 8 OUTPUT: Tue Feb 16 00:09:57 2010 Total No. of Pages: 45
/ams/waf/0/waf2222297

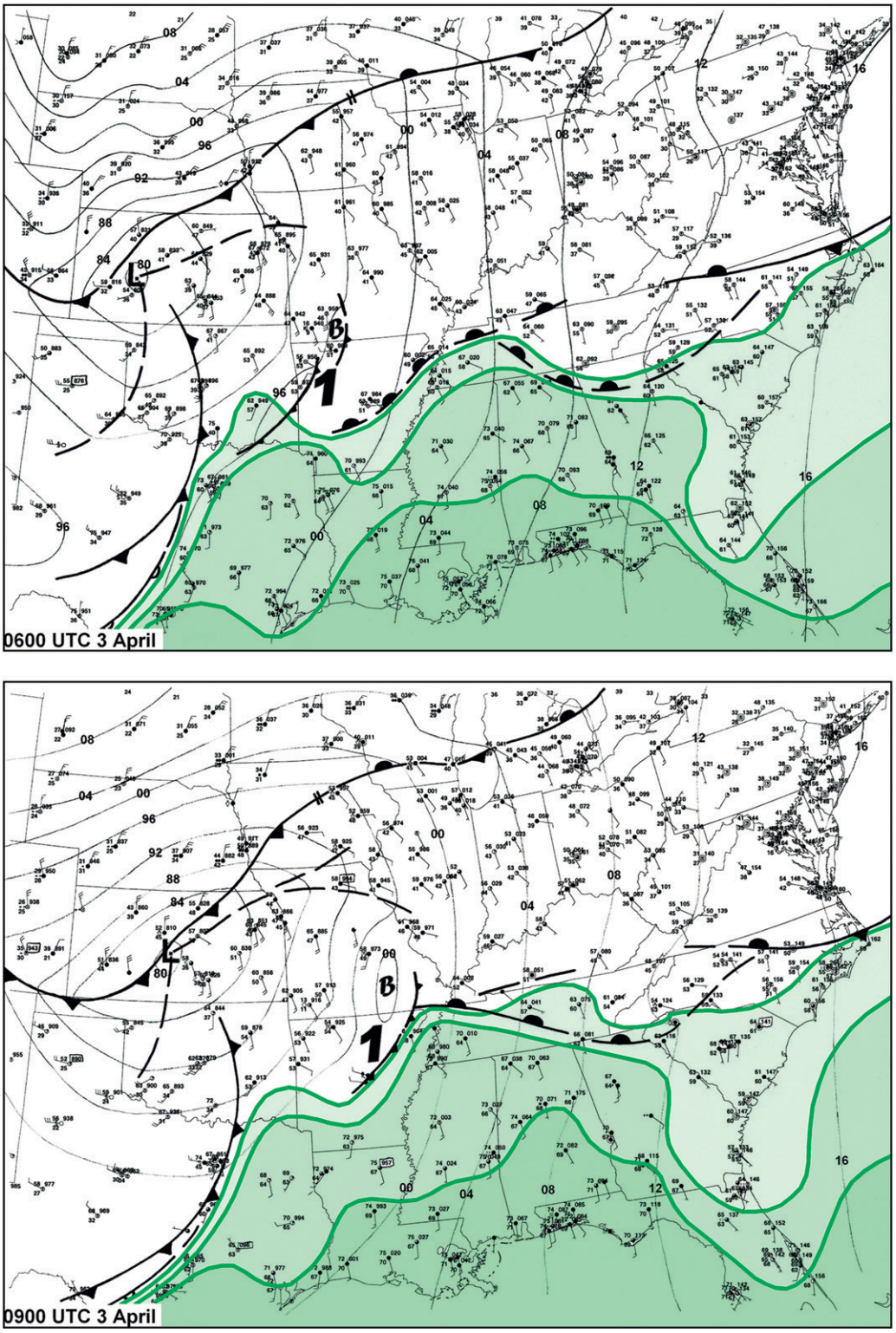

FIG. 4. (*Continued*)

JOBNAME: WAF 0#00 PAGE: 18 SESS: 8 OUTPUT: Tue Feb 16 00:10:46 2010 Total No. of Pages: 45
/ams/waf/0/waf2222297

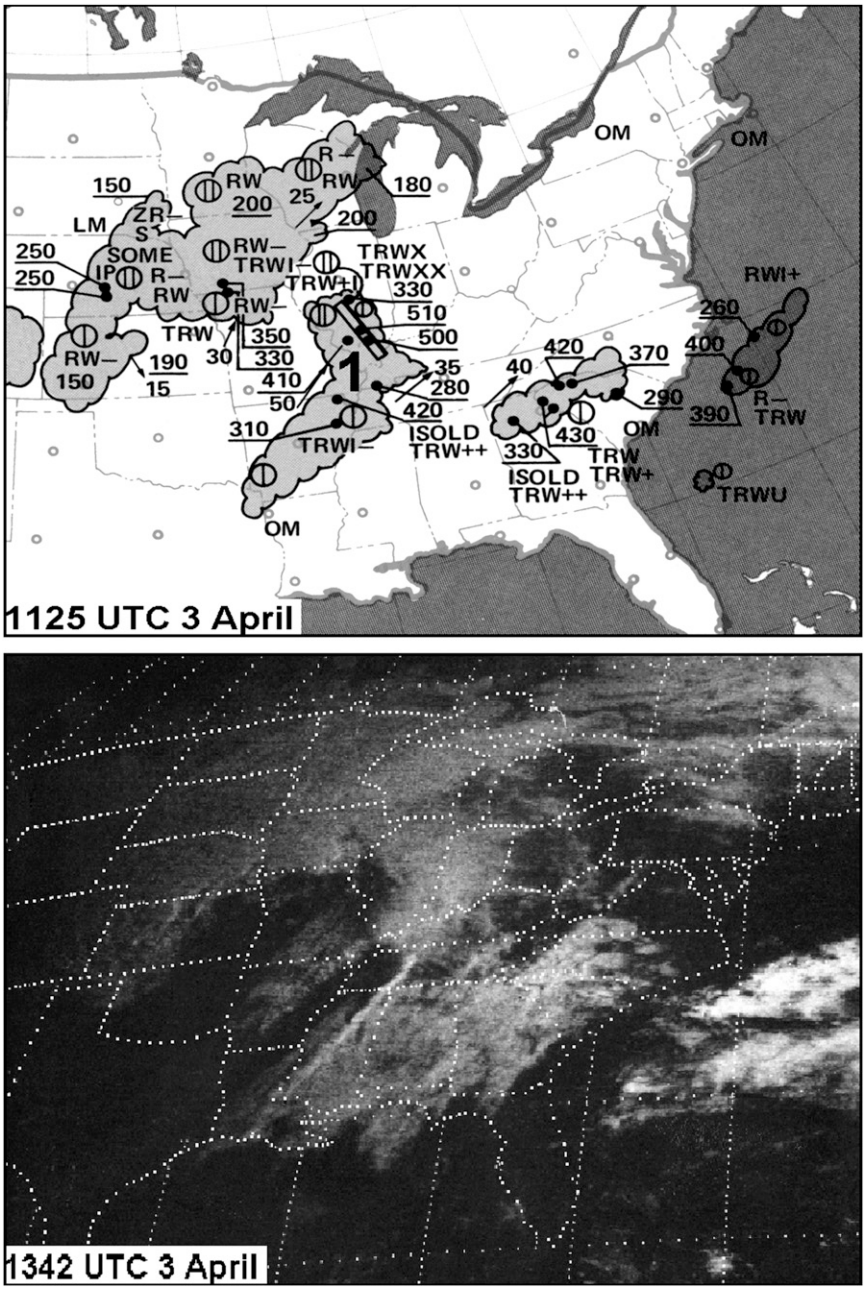

FIG. 4. (*Continued*)

afternoon and evening of 1 April produced a substantial outbreak of severe weather over the Ohio, Tennessee, and lower Mississippi Valleys. The region affected was nearly identical to that which would subsequently experience the Super Outbreak and included three F3 tornadoes, four fatalities, and numerous injuries. The storms continued through the night over the Southeast, generating copious low-level outflow. This allowed the convection to propagate well ahead of the front. By sunrise the storms and composite outflow boundary extended from eastern North Carolina to southwest Georgia (Fig. 4a). The thunderstorms finally weakened over the Gulf of Mexico and north Florida during the afternoon.

b. Evening, Tuesday, 2 April

By late in the day on Tuesday, 2 April (0000 UTC 3 April), the Lake Huron low had moved into Quebec as

JOBNAME: WAF 0#00 PAGE: 19 SESS: 8 OUTPUT: Tue Feb 16 00:10:55 2010 Total No. of Pages: 45
/ams/waf/0/waf2222297

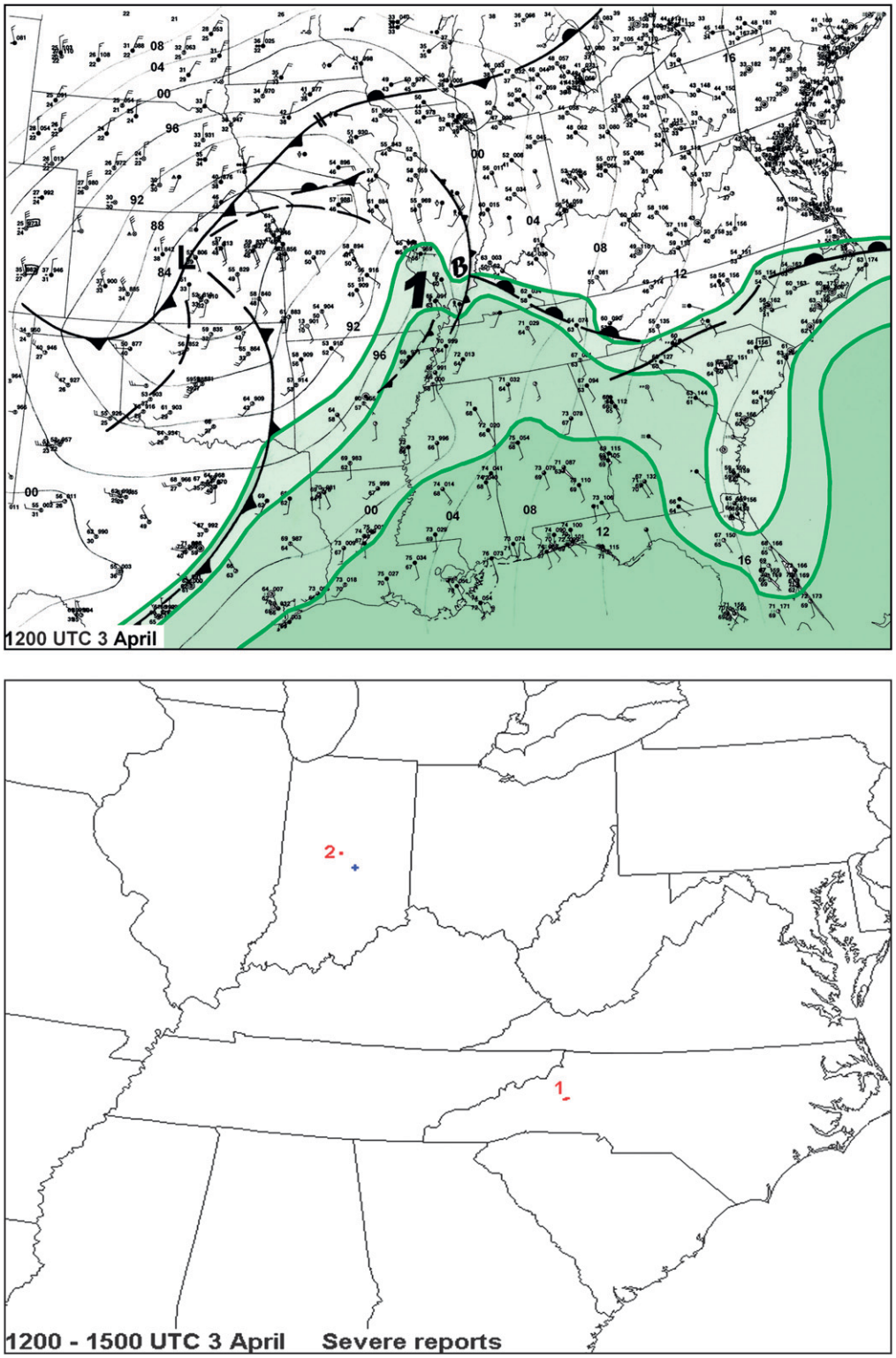

FIG. 4. (*Continued*)

JOBNAME: WAF 0#00 PAGE: 20 SESS: 8 OUTPUT: Tue Feb 16 00:11:52 2010 Total No. of Pages: 45
/ams/waf/0/waf2222297

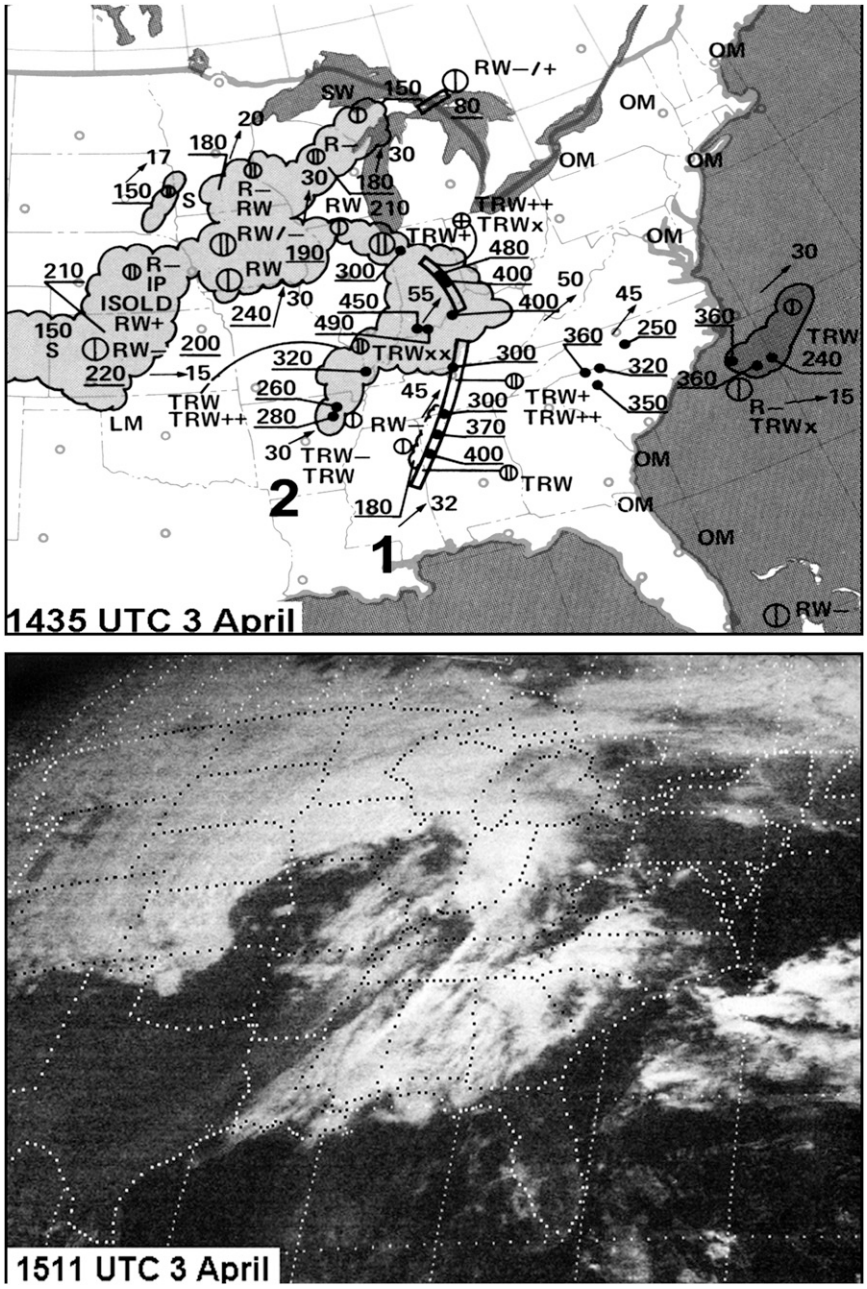

FIG. 4. (*Continued*)

the upper impulse continued northeastward into Canada (Fig. 3b). The trailing cold front extended through a low off the New England coast into southern Virginia and the southern Appalachians (Fig. 4b). Surface dewpoints south of the boundary were moist for the time of the year, ranging from around 16°C (low 60s °F) in north Florida to 21°C (low 70s °F) over coastal Louisiana. The western part of the front had begun to advance northward as a diffuse warm front through the Tennessee and lower Mississippi Valleys in response to strong lee cyclogenesis in eastern Colorado (Fig. 4b). Development of the low reflected increasing westerly flow aloft and the eastward advance of the Great Basin upper impulse. Cyclogenesis also was fostered by strong, along-stream variation of the upper-level flow (Uccellini and Johnson 1979); 250-hPa speeds at this time ranged from nearly 70 m s^{-1} (140 kt) in southern Nevada to less than 40 m s^{-1} (80 kt) in Oklahoma and north Texas.

JOBNAME: WAF 0#00 PAGE: 21 SESS: 8 OUTPUT: Tue Feb 16 00:12:01 2010 Total No. of Pages: 45
/ams/waf/0/waf2222297

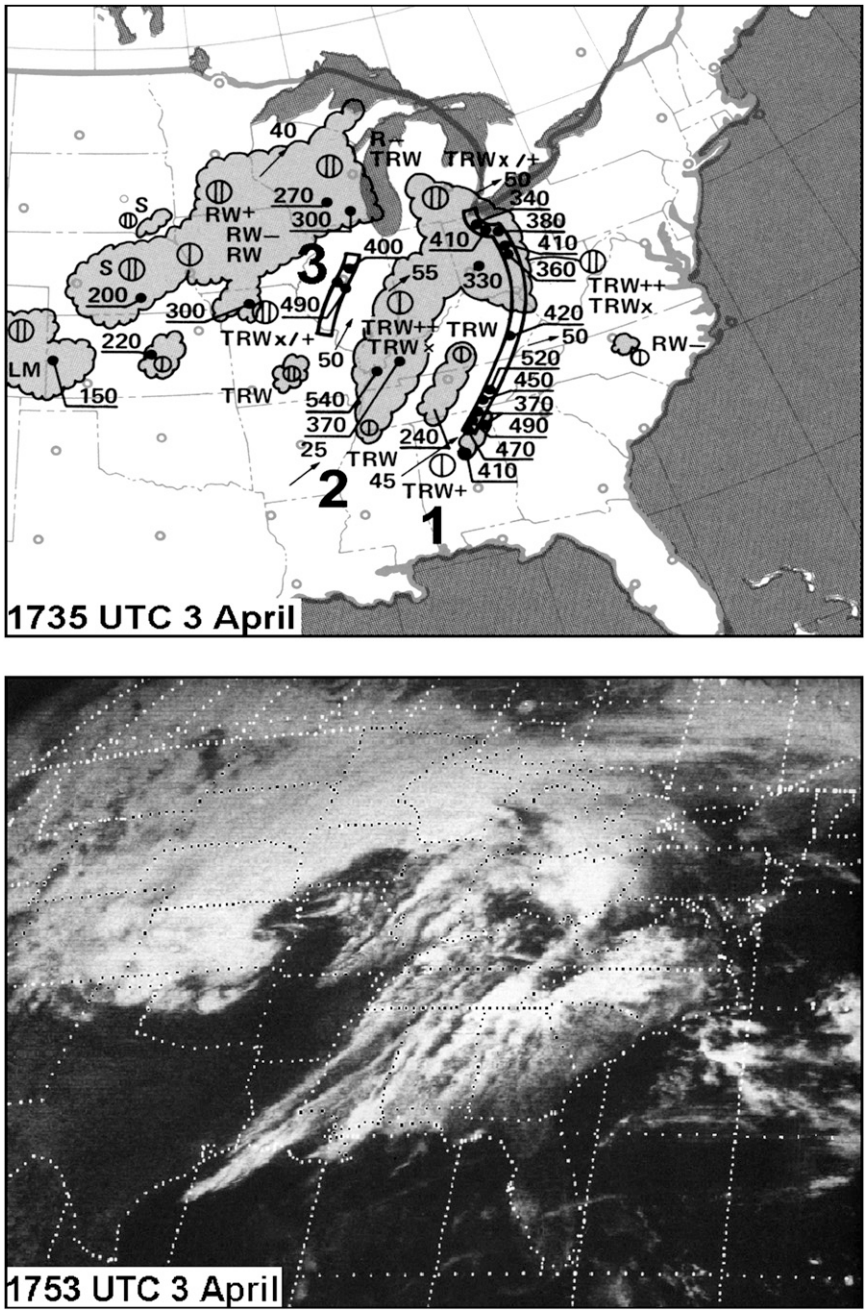

FIG. 4. (*Continued*)

The jet maximum associated with the Great Basin short-wave trough continued to move east- southeast Tuesday evening as a weak lead disturbance (most apparent in the temperature fields at 700 and 500 hPa) reached central Oklahoma (Fig. 3b). At the same time, the lee cyclone deepened to less than 984 hPa and edged eastward into Kansas (Fig. 4c). Frontogenesis downstream from the low led to the development of a stationary front that extended east-northeast into southern Michigan. Scattered high-based thunderstorms developed across north Texas and southern Oklahoma early in the evening; these are depicted schematically by the solid line near the Red River in Fig. 4c and by the dash–dot line in Fig. 5a. The storms formed in the vicinity of a dryline that F5
trailed southward from the Kansas low and likely reflected the presence of increasing large-scale ascent with the lead upper impulse. The storms grew more numerous later in the evening upon encountering the northwestern fringe of

JOBNAME: WAF 0#00 PAGE: 22 SESS: 8 OUTPUT: Tue Feb 16 00:12:09 2010 Total No. of Pages: 45
/ams/waf/0/waf2222297

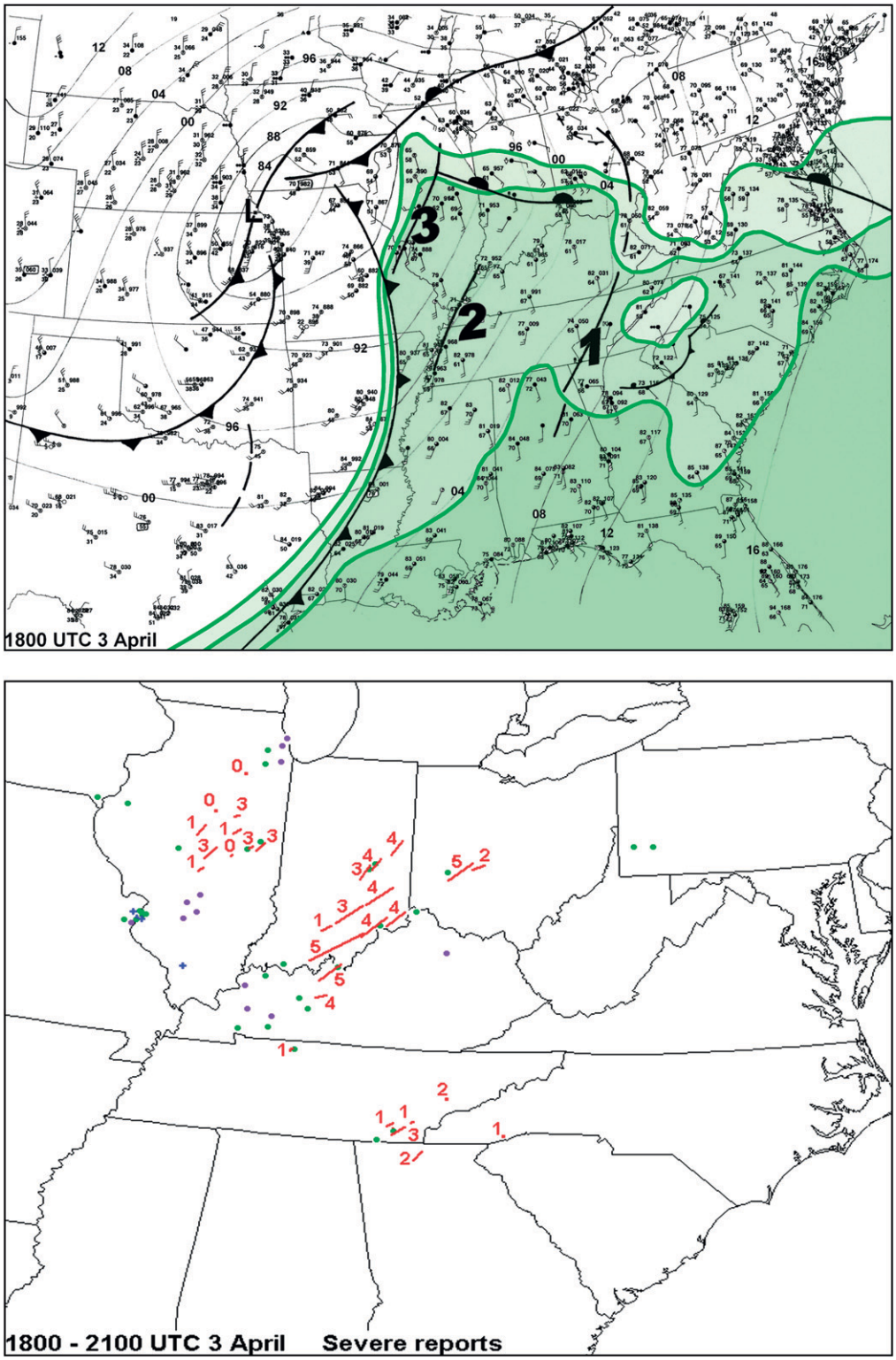

FIG. 4. (*Continued*)

JOBNAME: WAF 0#00 PAGE: 23 SESS: 8 OUTPUT: Tue Feb 16 00:12:58 2010 Total No. of Pages: 45
/ams/waf/0/waf2222297

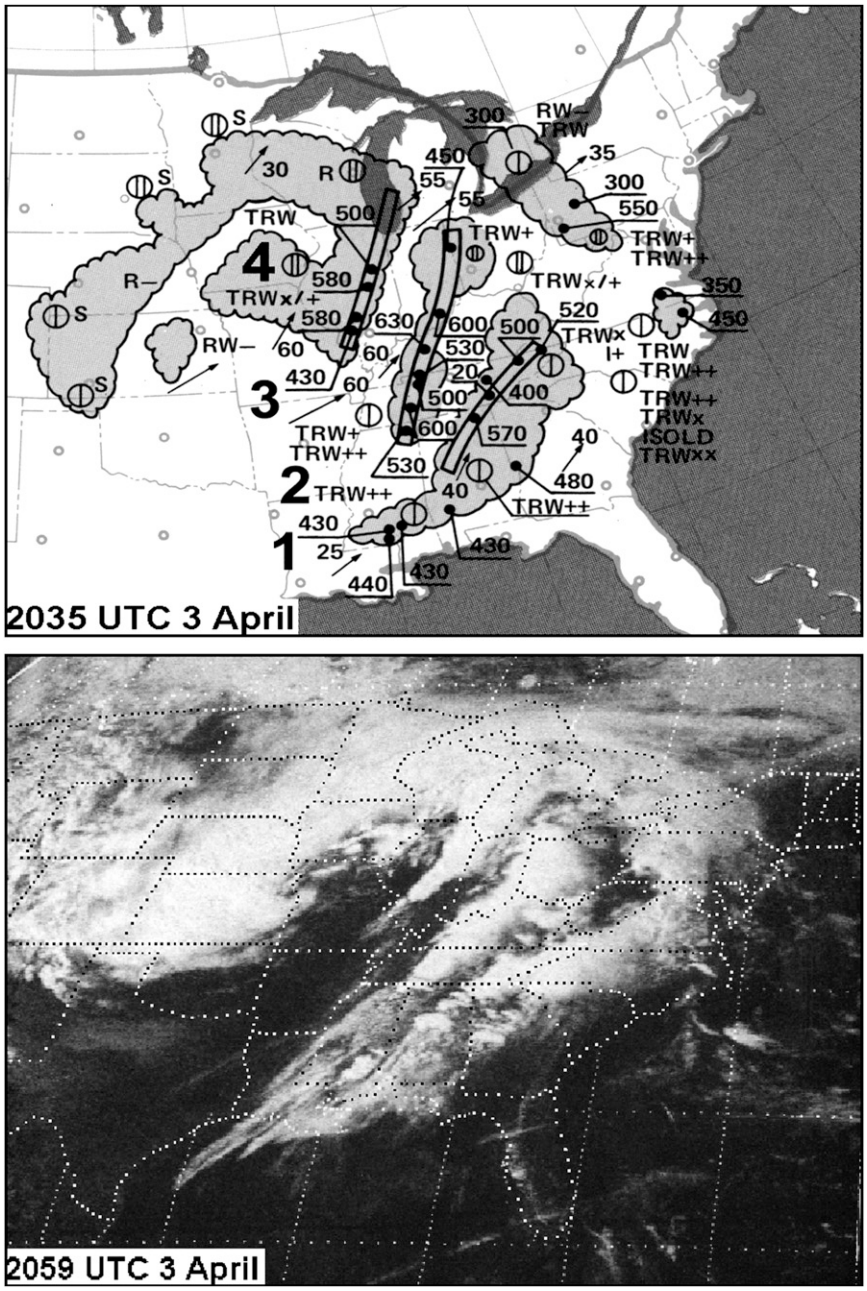

FIG. 4. (*Continued*)

returning Gulf moisture over northeast Texas and southeast Oklahoma. The resulting convective system continued east-northeast into Arkansas and southern Missouri early on Wednesday, 3 April, producing isolated severe hail and wind gusts in the Red River Valley.

The thermodynamic environment across the central and eastern United States late on Tuesday (0000 UTC 3 April) was dominated by a broad swath of steep low- to midtropospheric lapse rates that extended from the southern and central Rockies into the mid- and lower Mississippi Valley (Fig. 6a). Lapse rates were nearly dry F6
adiabatic in the deeply mixed boundary layer over western Texas, western Oklahoma, and southwest Kansas. Farther east, this air mass was present above the boundary layer as an elevated mixed layer (EML) over the Ohio and Tennessee Valleys. While EMLs originating over the high plateau of the southwestern United States and Mexico commonly are observed in soundings

JOBNAME: WAF 0#00 PAGE: 24 SESS: 8 OUTPUT: Tue Feb 16 00:13:06 2010 Total No. of Pages: 45
/ams/waf/0/waf2222297

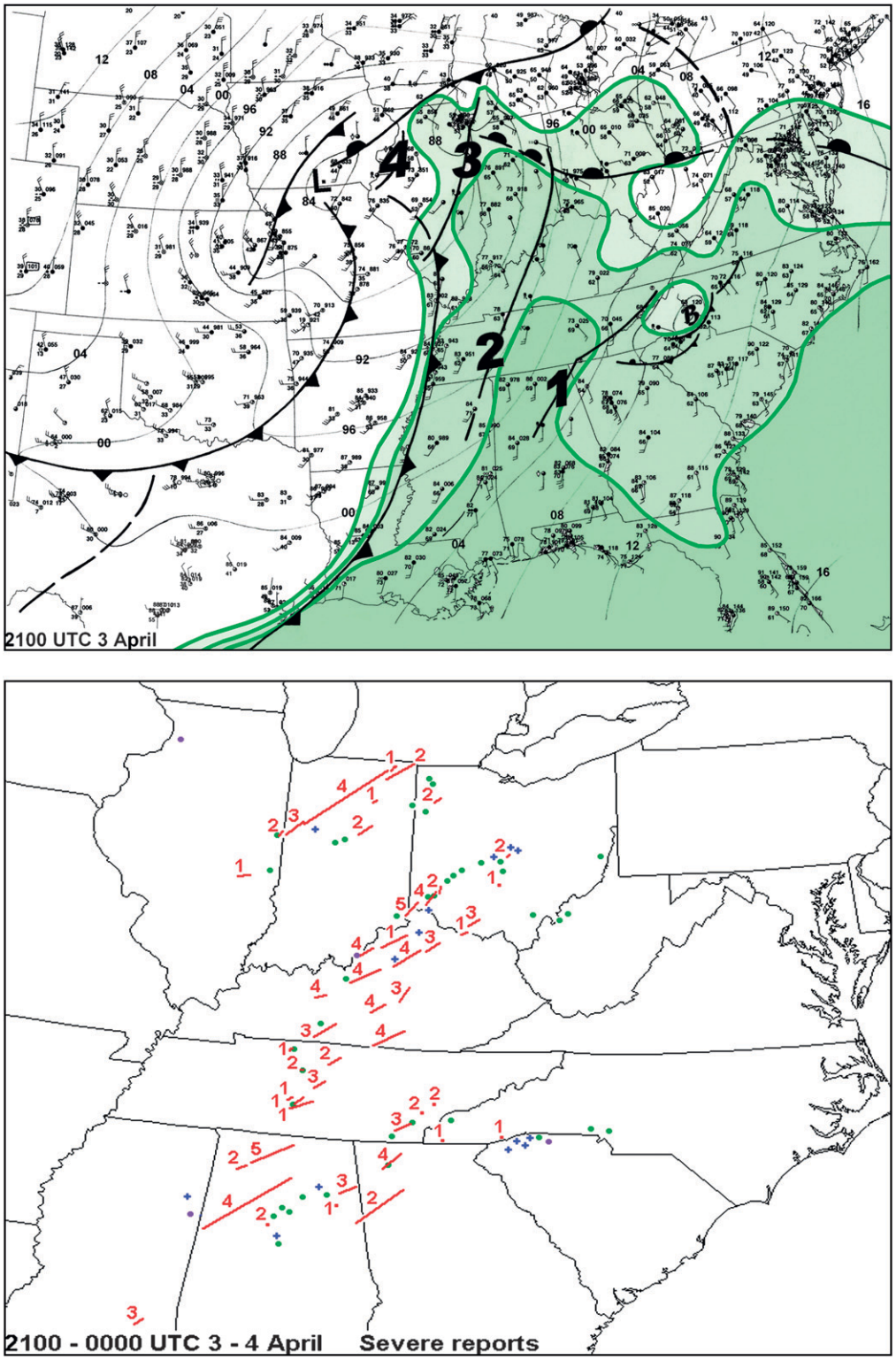

FIG. 4. (*Continued*)

JOBNAME: WAF 0#00 PAGE: 25 SESS: 8 OUTPUT: Tue Feb 16 00:13:54 2010 Total No. of Pages: 45
/ams/waf/0/waf2222297

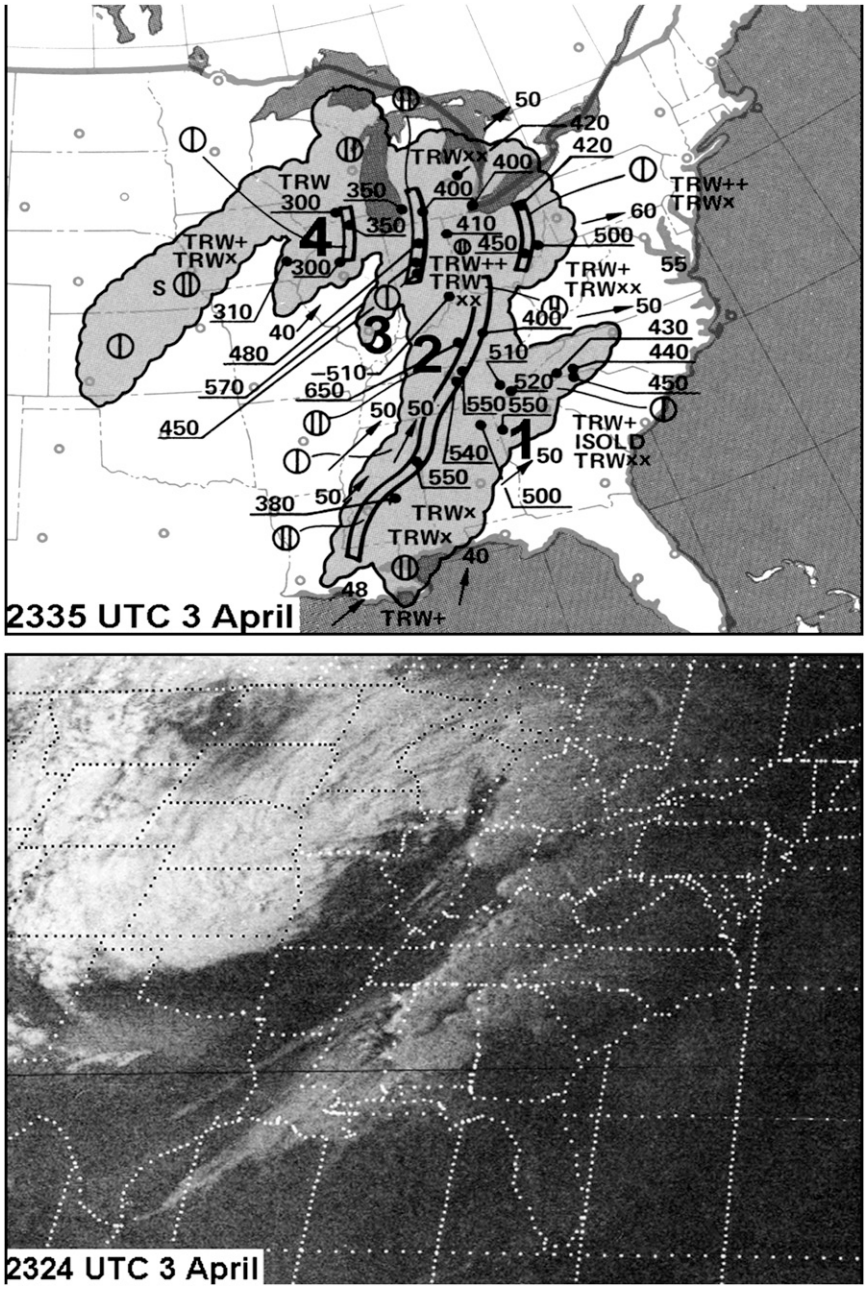

FIG. 4. (*Continued*)

taken over the plains and Mississippi Valley prior to spring tornado outbreaks, the areal extent of the EML in this case (and its potential to yield a broad region of potential instability) is notable. Nevertheless, because of the absence of substantial boundary layer moisture, significant surface-based convective available potential energy (CAPE) at this time was confined to the region along and south of the warm front over Louisiana and Mississippi (Fig. 7a). F7

c. *Early morning, Wednesday, 3 April*

The combination of potent dynamic forcing and favorably timed diurnal factors promoted substantial strengthening and broadening of the south-southwesterly low-level jet over the lower Mississippi Valley during the early morning (0600–1200 UTC) of Wednesday, 3 April. During the predawn hours, 850-hPa wind speeds increased to more than 25 m s^{-1} (50 kt) (Fig. 3c) across Louisiana,

JOBNAME: WAF 0#00 PAGE: 26 SESS: 8 OUTPUT: Tue Feb 16 00:14:02 2010 Total No. of Pages: 45
/ams/waf/0/waf2222297

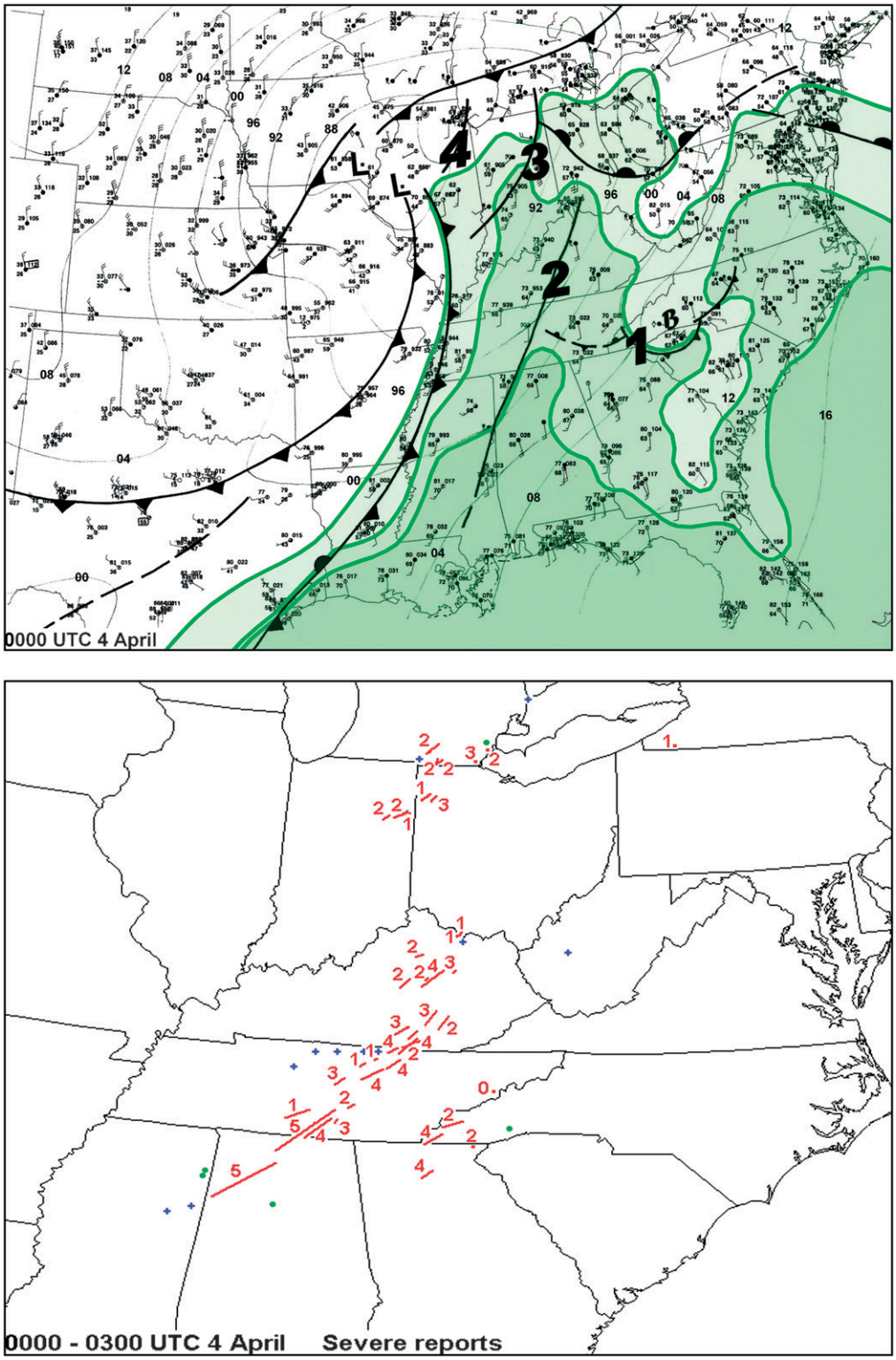

FIG. 4. (*Continued*)

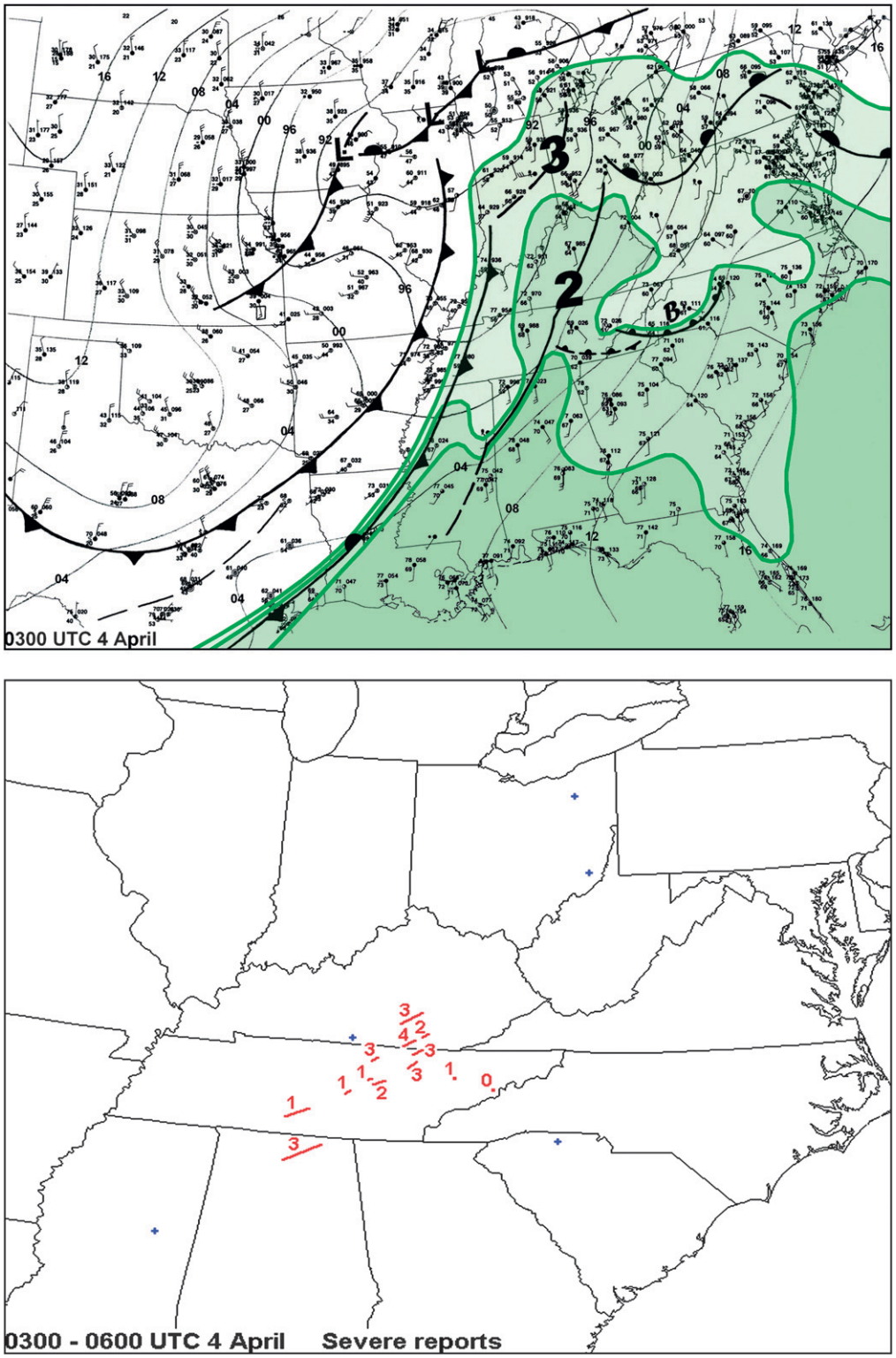

FIG. 4. (*Continued*)

JOBNAME: WAF 0#00 PAGE: 28 SESS: 8 OUTPUT: Tue Feb 16 00:15:40 2010 Total No. of Pages: 45
/ams/waf/0/waf2222297

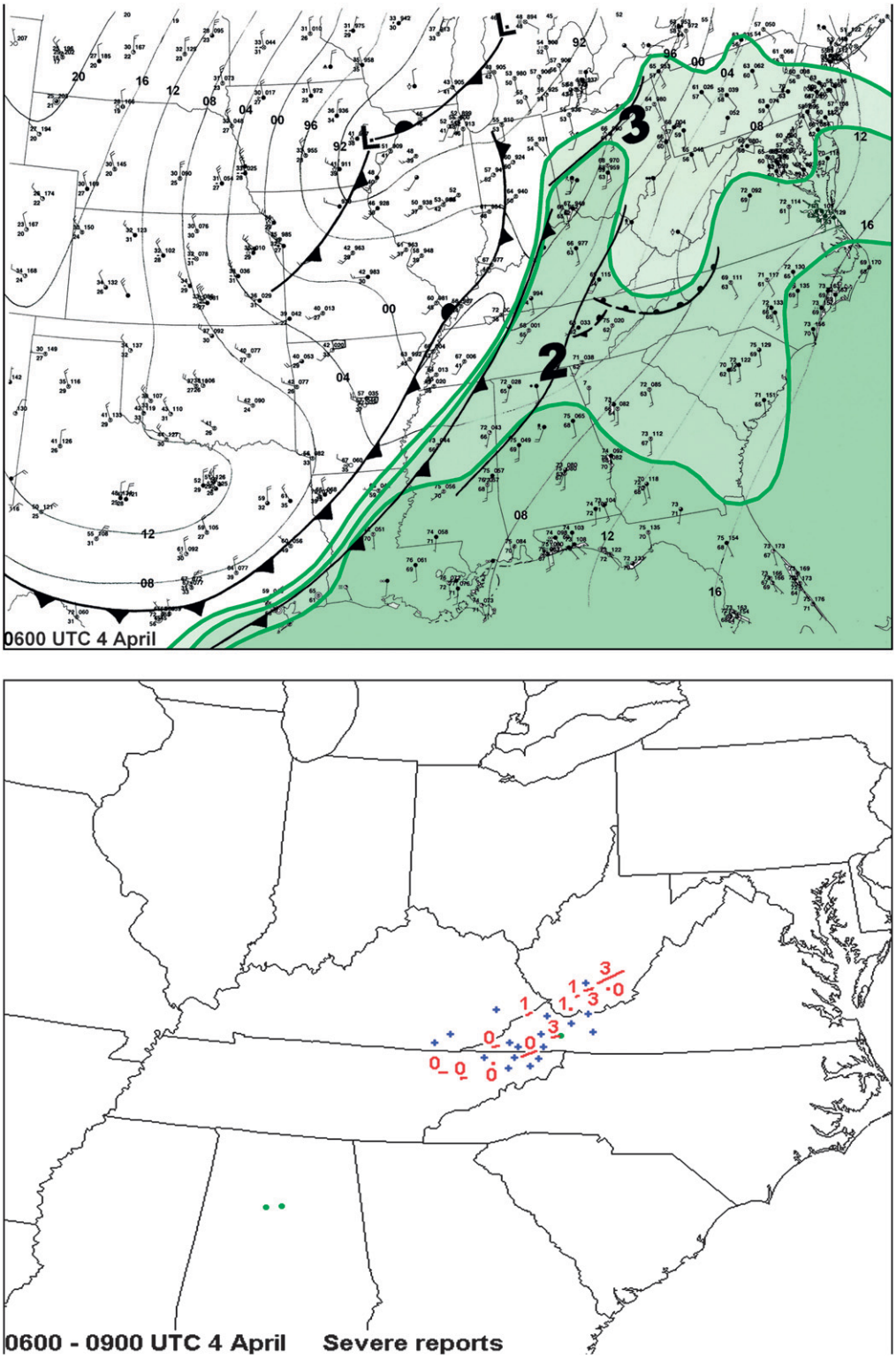

FIG. 4. (*Continued*)

JOBNAME: WAF 0#00 PAGE: 29 SESS: 8 OUTPUT: Tue Feb 16 00:16:26 2010 Total No. of Pages: 45
/ams/waf/0/waf2222297

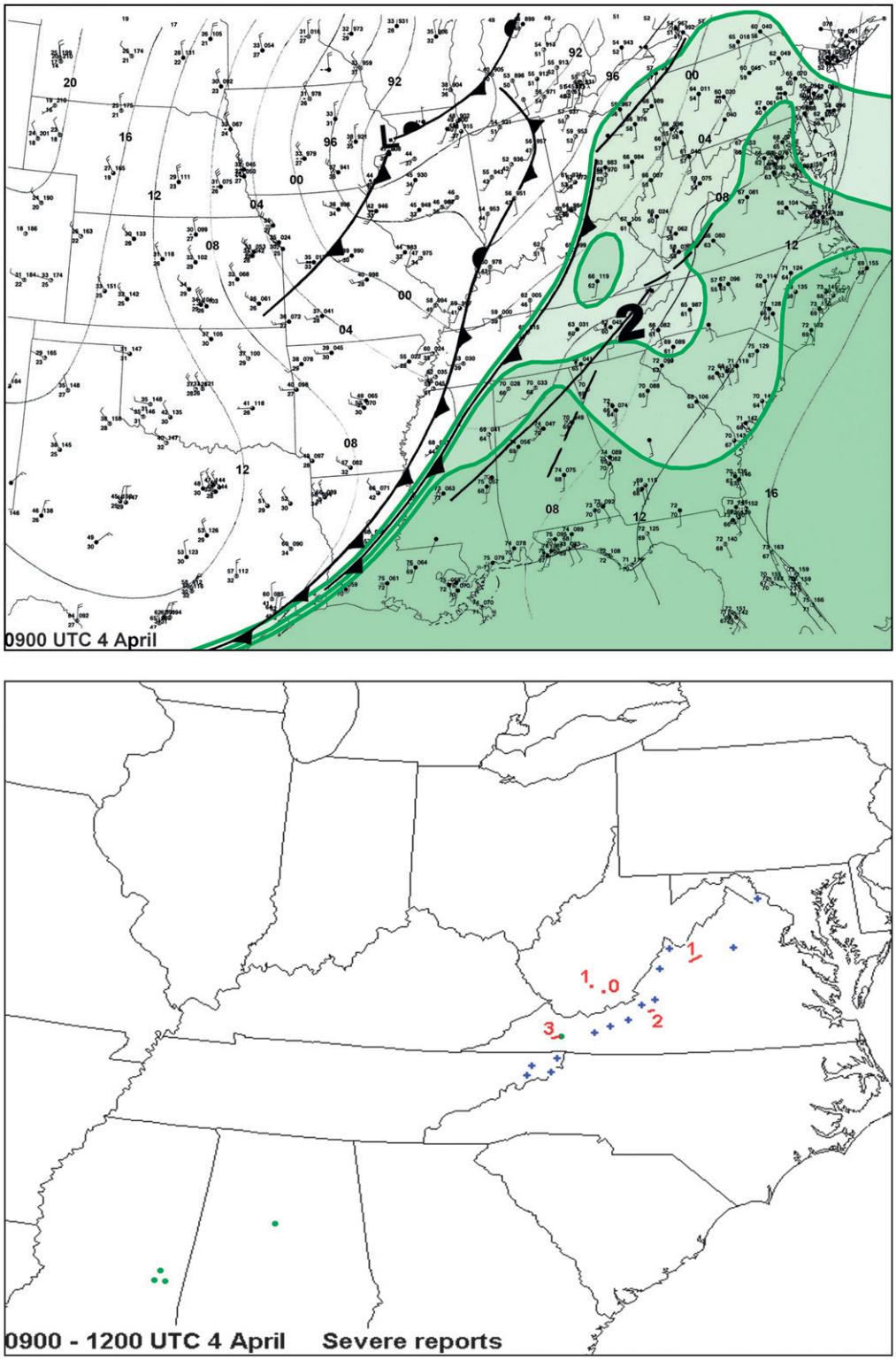

FIG. 4. (*Continued*)

JOBNAME: WAF 0#00 PAGE: 30 SESS: 8 OUTPUT: Tue Feb 16 00:17:23 2010 Total No. of Pages: 45
/ams/waf/0/waf2222297

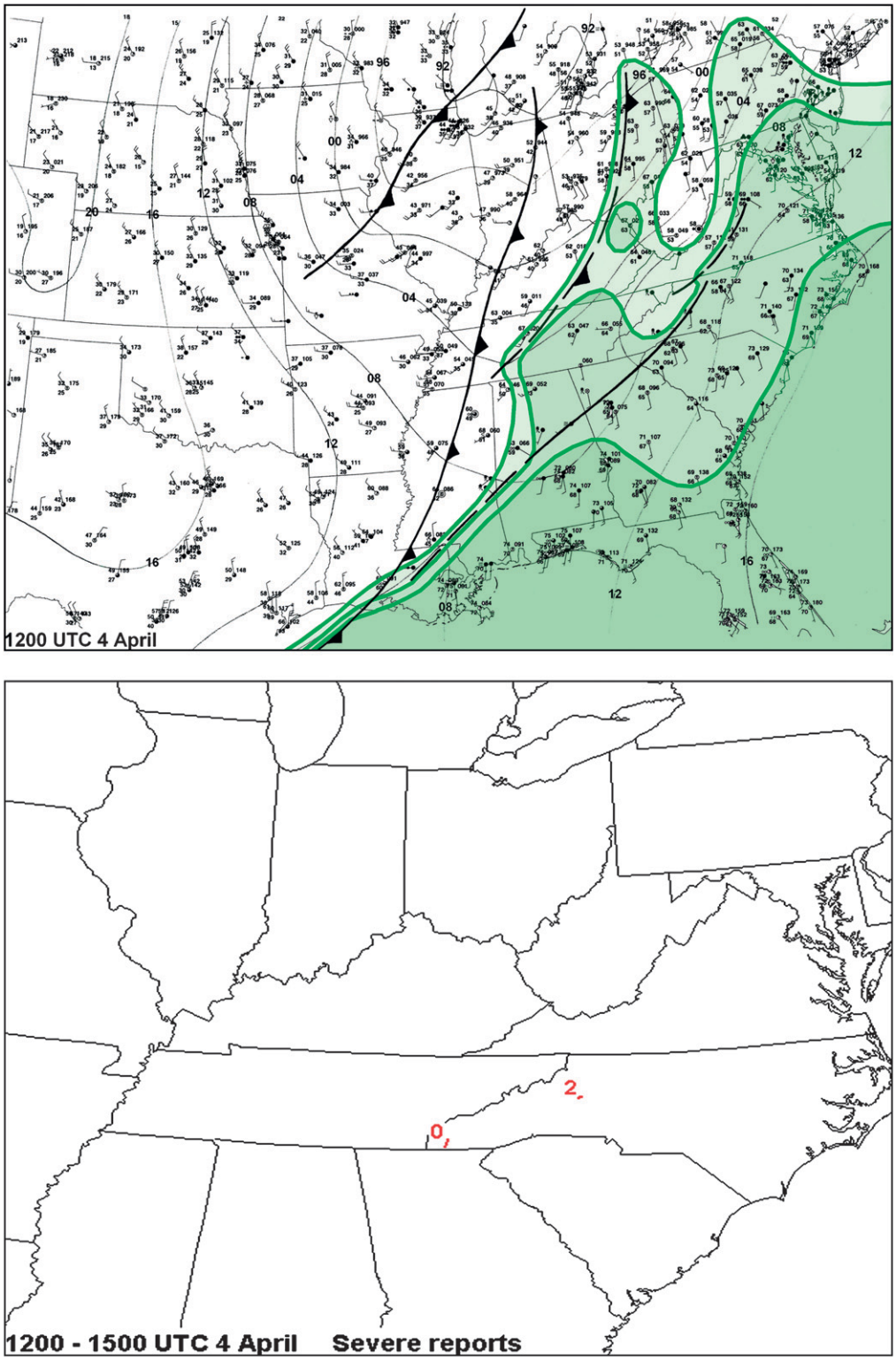

FIG. 4. (*Continued*)

JOBNAME: WAF 0#00 PAGE: 31 SESS: 8 OUTPUT: Tue Feb 16 00:18:14 2010 Total No. of Pages: 45
/ams/waf/0/waf2222297

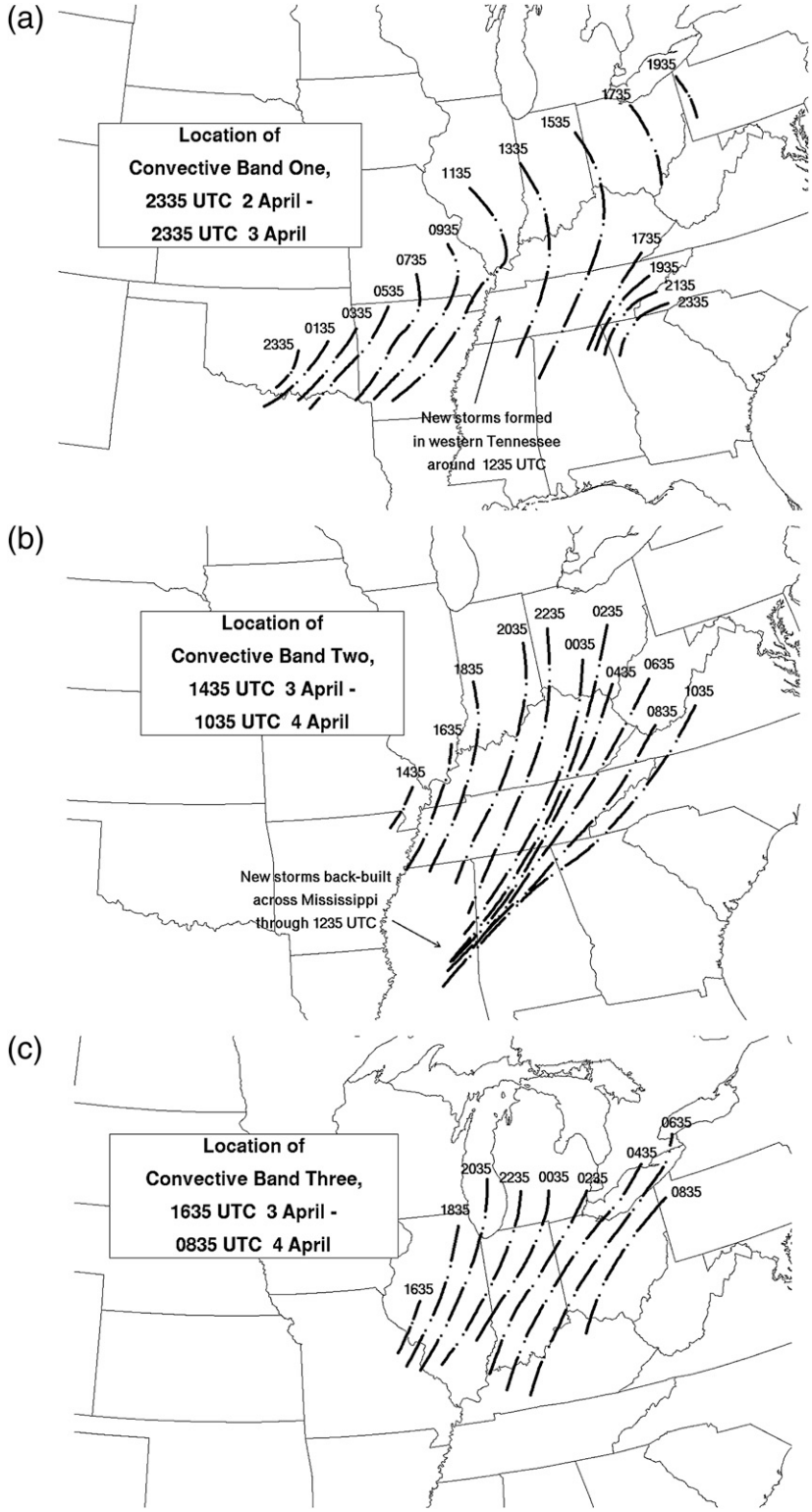

FIG. 5. Schematic diagrams showing approximate locations, for the times indicated, of convective bands (a) one, (b) two, and (c) three. Locations are based on NWS composite radar data, visible satellite imagery, and surface observations.

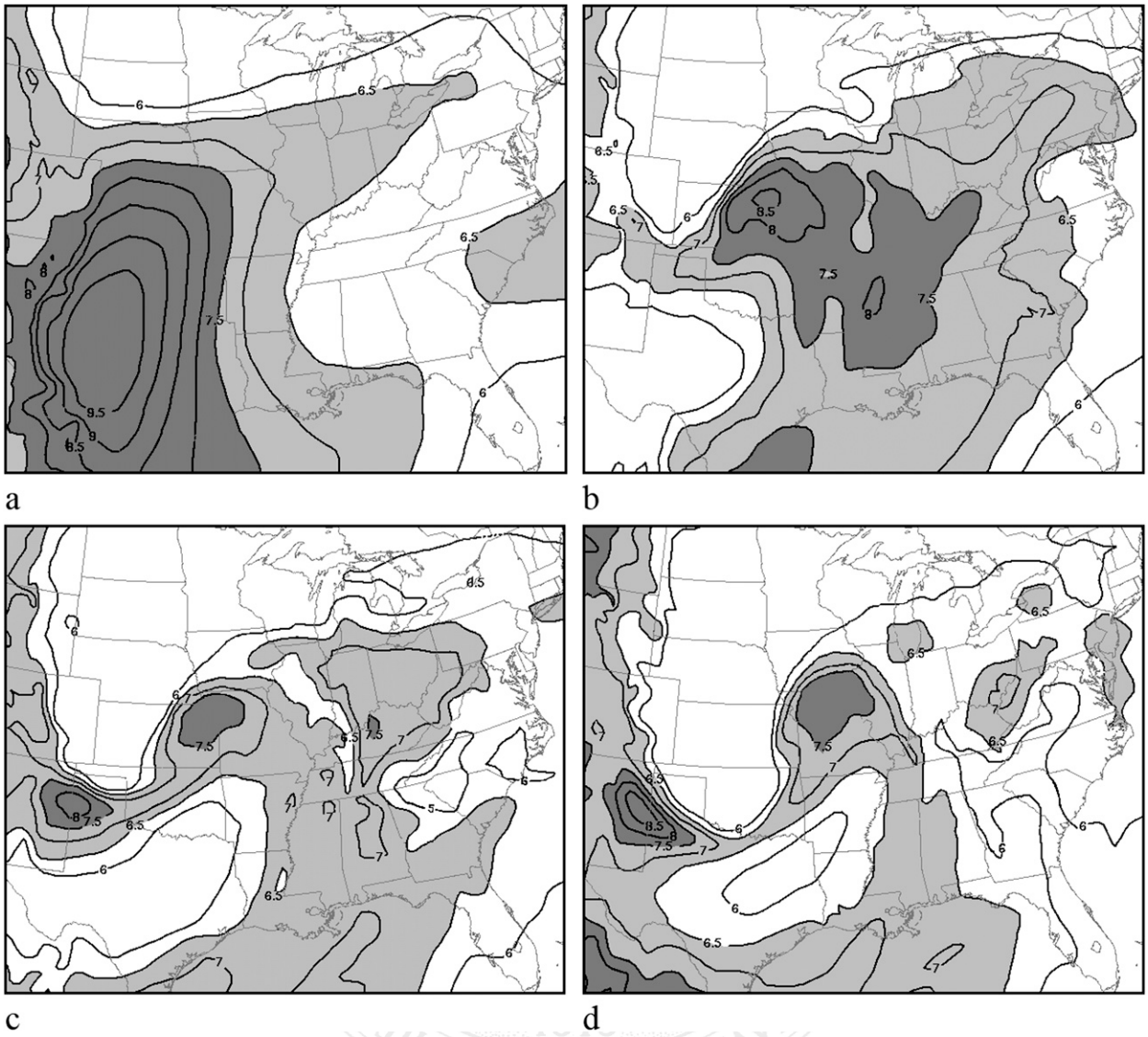

FIG. 6. Sequence of 29-km Eta 850–500-hPa lapse rates valid for (a) 0000 UTC 3 Apr, (b) 1200 UTC 3 Apr, (c) 1800 UTC 3 Apr, and (d) 0000 UTC 4 Apr 1974. Lapse rate contour interval is 0.5°C km^{-1}; lapse rates greater than 6.5 and 7.5°C km^{-1} are shaded orange and red, respectively. Model initialized at 0000 UTC 3 Apr.

Mississippi, and Alabama as the Kansas low deepened to 980 hPa (Fig. 4g) and the main upper impulse continued east-northeastward into eastern Kansas and Oklahoma. The associated northward transport of moisture resulted in rapid warm sector destabilization from the Gulf coast to the Tennessee Valley. By 1200 UTC, surface-based CAPE of 1000 J kg^{-1} was present as far north as the Ohio River (Fig. 7b), as the Tennessee–lower Mississippi Valley warm front redeveloped north into western Kentucky and extreme southern Illinois (Figs. 4e–g). However, because of the presence of the EML (implied by the steep 850–500-hPa lapse rates shown in Fig. 6b), most of the high CAPE area was ''capped'' to unassisted, deep, convective development.

Although the EML prohibited the development of surface-based thunderstorms over most of the warm sector early in the day, steep lapse rates within the EML and the presence of increasingly rich moisture just beneath it were favorable for the production of cold convective downdrafts from existing storms. This thermodynamic setup, in conjunction with the presence of fast, largely unidirectional cloud-layer flow, fostered continued overnight intensification and organization of the Arkansas and Missouri thunderstorms. By dawn (approximately 1200 UTC), composite radar data show that the storms

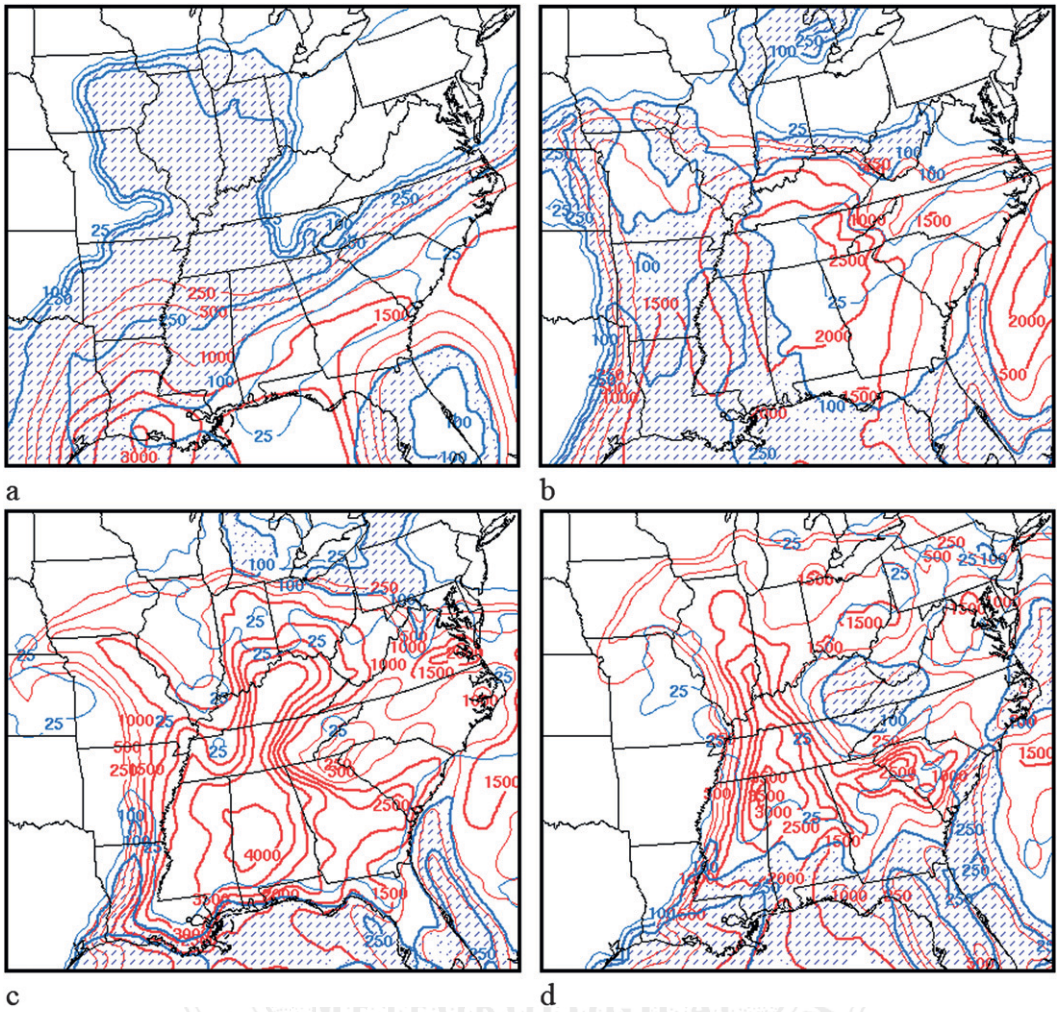

FIG. 7. Sequence of 29-km Eta surface-based CAPE (red), and CIN (blue), valid at (a) 0000 UTC 3 Apr, (b) 1200 UTC 3 Apr, (c) 1800 UTC 3 Apr, and (d) 0000 UTC 4 Apr 1974. CAPE is contoured at intervals of 500 J kg^{-1}. CIN is contoured at 25, 100, and 250 J kg^{-1}. CIN greater than 100 J kg^{-1} is stippled blue. The model is initialized at 0000 UTC 3 Apr.

had evolved into a strong, forward-propagating convective system that extended in a broken band from southern Illinois across far western Kentucky into central Arkansas (Figs. 4g and 5a). The surface data in Figs. 4d–g suggest that the convective complex likely was at least partly elevated, with storms fed by the strengthening and increasingly moist low-level jet atop what had become a fairly well-defined mesohigh [depicted by the ''B'' (for ''bubble'') in Figs. 4d–g]. Storm tops in Illinois, well north of the surface warm front, exceeded 15 km (50 000 ft), indicative of the quality of the returning Gulf moisture above the still-stable boundary layer. The convective system, and subsequent storms that evolved from its remnants later in the day, constituted the first of the three bands of severe storms that ultimately composed the Super Outbreak. Hereafter, this convective system will be referred to as convective band one.[2]

Convective band one moved east-northeastward at a modest pace during the night, averaging between 13 and 18 m s^{-1} (25–35 kt) in Arkansas and southern Missouri (Fig. 5a). Toward sunrise, however, the northern part accelerated east-northeastward. The system continued moving rapidly east-northeastward across the lower Ohio Valley through early afternoon, with a forward speed of nearly 30 m s^{-1} (60 kt). The southern part of band one also underwent acceleration, although somewhat later

[2] In this paper, the term convective band is favored over ''squall line'' to emphasize that the predominant convective mode remained quasi-cellular rather than linear throughout the Super Outbreak.

(around 1400 UTC), with the leading edge reaching northwest Alabama by 1535 UTC (Fig. 5a). Radar data (Fig. 4h) suggest that this occurred largely as a result of the development of new storms in western Tennessee, well ahead of existing activity in northeast Arkansas.

1) Origin of convective band one

Evidence exists that convective band one in some manner may have been associated with a solitary gravity wave or undular bore (Simpson 1997, p. 5; Locatelli et al. 1998) that moved eastward into the Tennessee and Ohio Valleys during the late morning and early afternoon of 3 April, more or less in tandem with the convection. Miller and Sanders (1980), for example, describe a persistent, small-scale pressure perturbation that moved from western Arkansas to the western slopes of the Appalachians in conjunction with the convective band. Supporting this notion, satellite data show an arc of what appear to be midlevel clouds that moved rapidly eastward across the lower Mississippi and Tennessee Valleys between sunrise and midday (Figs. 4g–i; the cloud band in question extends from west-central Tennessee through central Mississippi in Fig. 4g; an animated version of the satellite data is available online at http://www.spc.noaa.gov/publications/corfidi/74outbreak_slides/74loop.gif). The images suggest that the arc emanated from near the accelerating mesoscale convective system (MCS), and was oriented parallel to it. The cloud arc, however, extended southward to near the Gulf coast, well beyond the southernmost radar echo (Fig. 4g) in northern Mississippi. As the arc moved east, the northern part of the original convective band remained active northeastward into Pennsylvania, while the southern part developed south into Tennessee, Mississippi, and Alabama, more or less coincidental with passage of the arc.[3]

Further bolstering the idea that convective band one may have been related to a solitary wave or undular bore, Locatelli et al. (2002) present output from a mesoscale model simulation of the Super Outbreak showing a structure in the vicinity of the model's depiction of band one that has characteristics of a bore. In their simulation, the feature moved east across the Ohio and Tennessee Valleys in unison with the Arkansas MCS. They propose that the borelike structure formed when the lead ("Pacific") cold front associated with the Kansas surface low encountered the stably stratified, "loaded gun" type of thermodynamic environment over the southern plains. This seems plausible, as the feature was oriented roughly parallel to the model cold front and remained so through its lifetime. However, the model bore moved more slowly than the satellite-observed cloud arc. In addition, because satellite imagery is not available prior to 1342 UTC, knowledge of the arc's origin relative to the Arkansas MCS is open to speculation. Thus, the nature of the arc cloud and its possible association with a solitary wave or bore remain somewhat of a mystery. What is certain, however, is that the storms that ultimately evolved into convective band one formed during the previous evening in Oklahoma and Texas in an environment that was becoming increasingly favorable for forward-propagating, quasi-linear convection (e.g., Corfidi 2003). The storms had grown into an organized convective system well before the borelike structure became apparent in the Mississippi Valley. Although the bore may have indeed assisted the convective development over the Tennessee and Ohio Valley region after sunrise on 3 April, it is not apparent that the bore itself was *responsible* for the development of convective band one, as Locatelli et al. (2002, p. 1644) conclude. In fact, it appears that the bore itself may have originated from the mesohigh associated with Arkansas–Missouri complex.

2) Cold front–dryline discontinuity in the Ozarks

West of convective band one, a boundary that exhibited characteristics of both a cold front and a dryline reached southwest Missouri, western Arkansas, and northwest Louisiana around 1500 UTC Wednesday (Fig. 4h; depicted after 0900 UTC as a cold front).[4] This discontinuity appears to have evolved from two separate features: a cold front that was associated with the aforementioned lead upper-level impulse (evident in the 700- and 500-hPa thermal fields shown in Fig. 3b) and a dryline that had become discernible over western Oklahoma and central Texas early Tuesday afternoon (Fig. 4b). Overnight, the cold front overtook the dryline in Texas, while the Oklahoma part of the dryline became obscured by outflow from the evolving convective cluster near the Red River. With the onset of diurnal heating and increased boundary layer mixing on Wednesday morning, the cold front–dryline accelerated northeast across much of the remainder of Missouri and Arkansas, reaching the St. Louis area and northeast Arkansas around midday (Fig. 4i). Wind gusts in excess of 20 m s^{-1} (40 kt) and sharply reduced visibility due to blowing dust followed

[3] Miller and Sanders (1980) identify nine other perturbations in the wake of the first. The latter features did not, however, bear any consistent relationship with mesoalpha-scale convective development later in the day.

[4] To simplify the presentation, and because convective outflow boundaries became less discernable after 1200 UTC, the convective bands are denoted schematically by solid lines in Figs. 4h–o.

passage of the discontinuity across north Texas and much of Arkansas. The dust is visible as light hazy areas in the satellite images in Figs. 4i–k.

At the surface, the cold front–dryline gradually assumed characteristics more typical of a classic dryline (i.e., a marked east-to-west reduction in dewpoint and a nominal change in temperature) as the feature moved east of the Mississippi River later on Wednesday, and continued eastward Wednesday night and into early Thursday. Part of this behavior undoubtedly reflects the influences of differential insolation and radiational cooling rates across the boundary. Yet the position of the 700-hPa thermal gradients and the wind shift axes at both 0000 and 1200 UTC Thursday, 4 April (Figs. 3d and 3e), relative to the surface discontinuity suggest that the feature still retained some aspects of a cold front, at least at 700 hPa. ''Hybrid'' features of this type have been observed by operational meteorologists in association with other Colorado cyclogenesis events, and they can lead to confusion or misplacement of frontal features in subjective analyses [e.g., the 1200 UTC Thursday surface analysis in Hoxit and Chappell (1975), taken from the official NWS *Daily Weather Map*]. Remarkably, this particular drylinelike boundary remained identifiable through 1200 UTC Thursday as far northeast as central Ohio (Fig. 4o), distinct from the main synoptic cold front in Indiana.

More will be said about the Missouri–Arkansas cold front–dryline in association with the discussion on the development of convective band two in section 3d(2).

d. Late morning/early afternoon, Wednesday, 3 April

Diurnal heating, occurring nearly simultaneously with the arrival of substantial low-level moisture, resulted in continued destabilization across much of the east-central and southeastern United States late Wednesday morning. By midday and primarily through vertical mixing, the Tennessee Valley warm front—largely a moisture discontinuity—had re-formed north into northern Illinois and central Indiana, not very far south of the synoptic-scale stationary front in southern Michigan (Fig. 4i). Part of the old boundary, however, remained stalled along the eastern slopes of the southern Appalachians, where overnight storms retarded its northward movement. As Fig. 7c shows, by 1800 UTC surface-based CAPE in excess of 2500 J kg^{-1} was present from the lower Ohio and Mississippi River Valleys, south and east to the Gulf coast and Georgia, while values were greater than 3500 J kg^{-1} over parts of Alabama, Mississippi, Tennessee, and Kentucky. In addition, because of the well-mixed nature of the boundary layer, and the ''quality'' of the moist inflow [surface dewpoints of 18°–20°C (mid- to upper 60s °F), well above seasonal norms; precipitable water ≥32 mm (1.25 in.)], values of the mean mixed layer CAPE were nearly as great (not shown).

1) FRACTURE OF CONVECTIVE BAND ONE

The northern part of convective band one continued to race east-northeast across the Ohio Valley through midafternoon, reaching western Pennsylvania by 1930 UTC. The convective system produced the first tornado of the Super Outbreak, a brief touchdown northwest of Indianapolis, Indiana, at around 1430 UTC.[5] The southern part, meanwhile, reached eastern Tennessee around 1630 UTC (Fig. 5a), and produced the first F3 tornado of the event near Cleveland, Tennessee (east of Chattanooga), around 1905 UTC (track 113 in Fig. 1). The southern part of band two became more difficult to discern around this time as additional storms formed in its vicinity, possibly along outflow boundaries left by the overnight storms (Fig. 4i). In summary, convective band one appeared to break into two main parts between 1500 and 1800 UTC, with the split centered over eastern Kentucky.

Hoxit and Chappell (1975) attribute the fracture of band one to its movement into a zone of large-scale subsidence centered over eastern Kentucky at 0000 UTC 4 April, based on their kinematic analysis of rawinsonde data. However, it is also worth noting that strengthening and backing of the 850-hPa winds over the southern and central Appalachians during the day likely contributed to localized enhancement of the downslope flow over eastern Kentucky and western West Virginia (Figs. 3c and 3d).

Although downslope flow and the background vertical motion field may have had some influence on the evolution of convective band one, other factors likely were important as well. For example, the surface and upper-air environments (Figs. 3c and 4h) varied considerably along the system's latitudinal extent. Thus, one might expect a concomitant along-line variation in the intensity, character, and longevity of the convection (e.g., Houze et al. 1990) in band one. Furthermore, if some of the convection occurred in conjunction with an undular bore (as previously discussed), the persistence of a shallow but strong low-level inversion over the Ohio Valley would have provided an efficient ducting layer to allow for rapid forward motion of the bore, and for the continued regeneration of elevated storms along its path east-northeastward into Pennsylvania (Figs. 4h–j). Farther south, meanwhile, rapid warming and moistening of

[5] This brief event is not shown in Fig. 1 (from Fujita 1975), but does appear in the Storm Prediction Center's severe event database and, therefore, is shown in Fig. 4g.

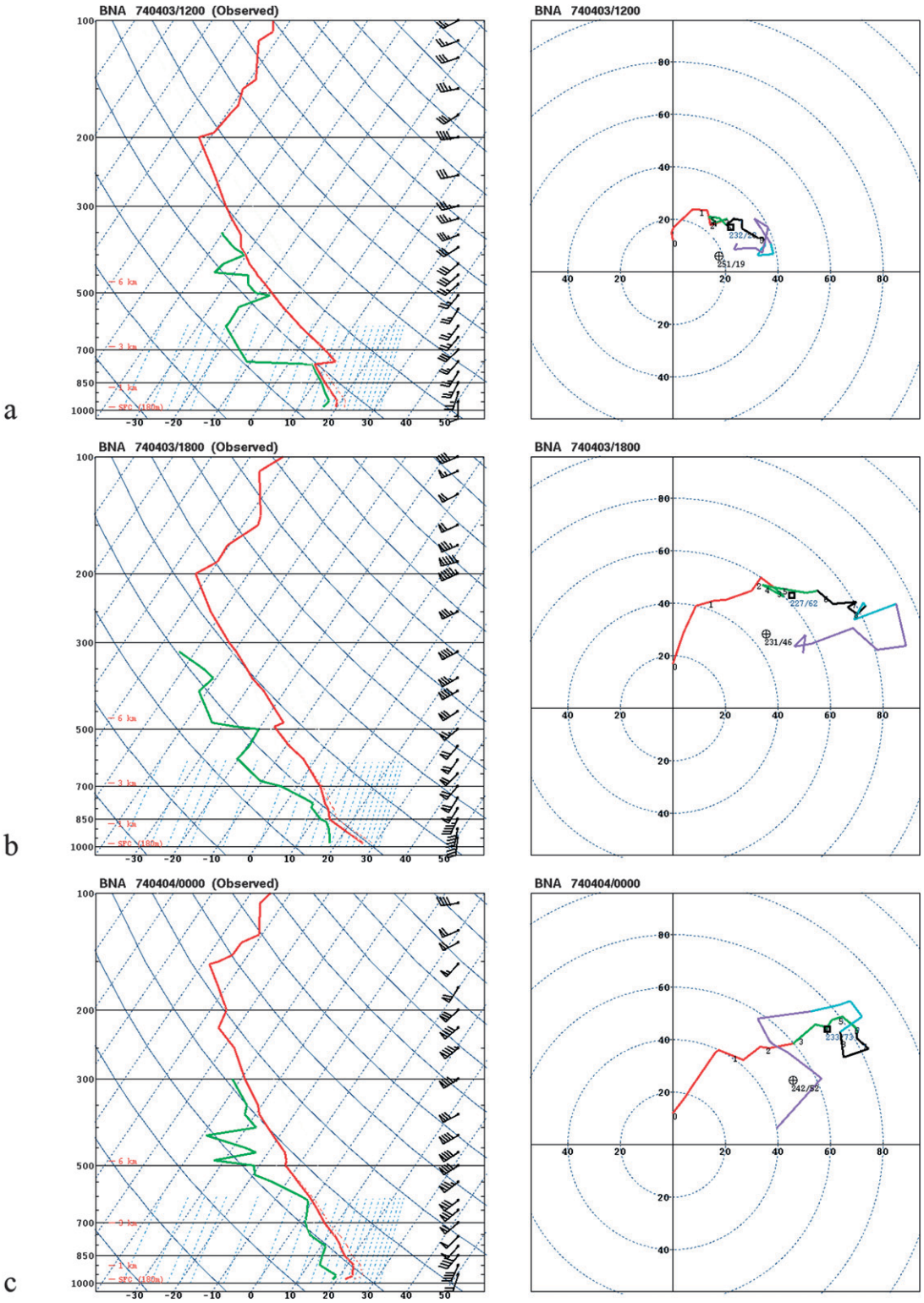

FIG. 8. (left) Rawinsonde and (right) hodograph plots for Nashville at (a) 1200 UTC 3 Apr, (b) 1800 UTC 3 Apr, and (c) 0000 UTC 4 Apr 1974. Sounding depicts temperature in red and dewpoints in green. Hodographs color coded for height (0–3 km, red; 3–5 km, green; 6–9 km, black; 9–12 km, blue; greater than 12 km, purple); black numerals denote height in km. Wind speeds on soundings and on range rings of hodographs are in kt. Black squares denote mean wind; open circles with crosses indicate Bunkers et al. (2000) estimated right-mover storm motion.

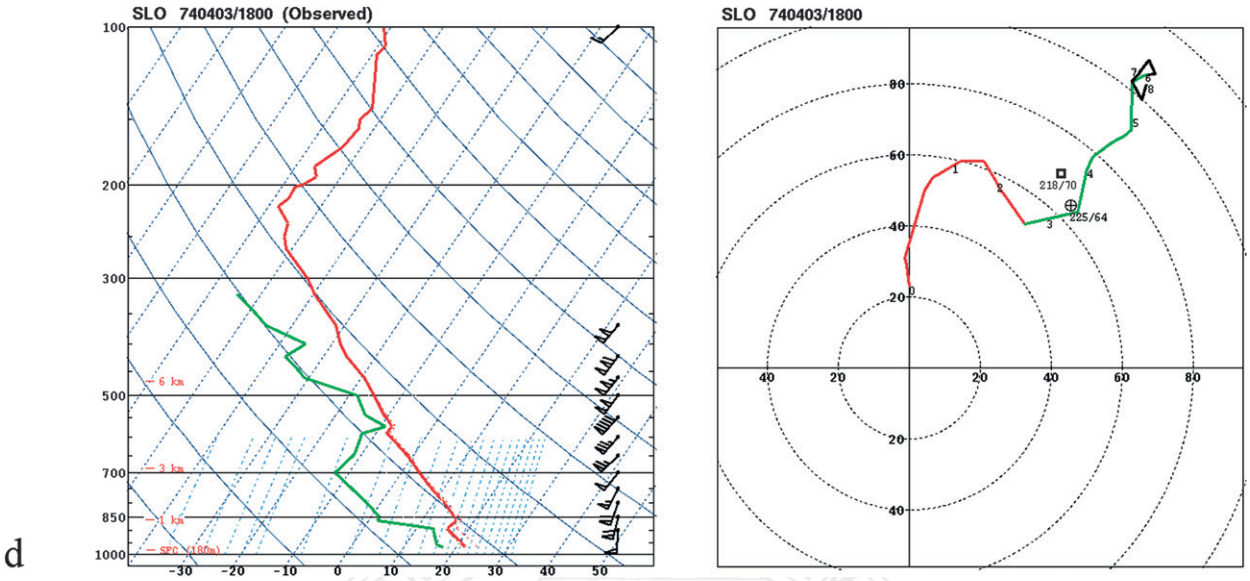

d

FIG. 8. (*Continued*)

the boundary layer may have disrupted the stability profile that favored propagation of the bore and fostered a transition toward surface-based convection over that region by midday. This transition appears to have occurred both in the wake of the bore over the Cumberland Plateau and ahead of it over the southern Appalachians.

The northern part of convective band one produced scattered damaging wind gusts and marginally severe hail in Ohio before weakening over Lake Erie and northwest Pennsylvania late in the afternoon. The southern half, meanwhile, remained active as it became indistinguishable from the additional storms that formed over Mississippi, Alabama, northern Georgia, and eastern Tennessee. In addition to the Cleveland, Tennessee, F3 tornado, an F2 tornado with a 24-km (15 mi) pathlength occurred in extreme northern Georgia around 1915 UTC (track 123 in Fig. 1). Animated satellite data suggest that band one (and/or the undular bore associated with it) served to enhance an area of existing thunderstorms as it moved east along the stalled frontal segment and outflow boundaries over the southern Appalachians. However, given the arrival of the convective band/bore at the time of maximum diurnal heating, and the contemporaneous increase in boundary layer moisture that was occurring, a causal relationship cannot be made with certainty.

2) DEVELOPMENT OF CONVECTIVE BAND TWO

In the wake of the first band of convection, a second area of thunderstorms, hereafter referred to as convective band two, formed around 1500 UTC in northeast Arkansas and extreme southeast Missouri (Fig. 5b). These storms appear to have been initiated as clearing skies (note the fast eastward movement of dense clouds associated with convective band one in satellite images shown in Figs. 4g and 4h) and strong boundary layer moisture transport very rapidly destabilized the region of confluent low-level flow some distance ahead of the cold front–dryline. Ascent associated with the southern part of the lead midlevel short-wave trough also may have played a role in fostering development (note the 12-h movement of the lead 700-hPa short-wave trough in Figs. 3c and 3d; the location of the trough is based on the leading edge of the associated thermal gradient and the wind shift axis). It is also possible that channeling of the low-level flow over northeast Arkansas (the "Delta" region of the Mississippi River Valley) may have assisted in the storm development by locally enhancing moisture transport and convergence.

The degree of destabilization that occurred in the wake of convective band one and just ahead of band two is apparent in the sequence of soundings made at Nashville, Tennessee, shown in Fig. 8. Comparison of Figs. 8a and 8b F8 suggests that a combination of surface heating, moisture inflow, sustained large-scale ascent, and perhaps cold advection weakened the convective inhibition layer; by early afternoon the sharp nose at the base of the EML had been completely eroded. This trend was accompanied by an increase in CAPE over the region (cf. Figs. 7b and 7c). Meanwhile hodographs revealed wind profiles that became increasingly favorable for tornadic supercells (e.g., Doswell 1991; Miller 2006; Esterheld and Giuliano 2008) in the strengthening flow downstream from the approaching upper-level jet streak (e.g., cf. Figs. 8a and 8b, and note the "sickle shape" hodograph

in Fig. 8b). Using an average observed storm motion of 230° at 22 m s^{-1} (45 kt), the 0–1-km storm relative helicity at 1800 UTC in middle Tennessee was more than 230 m^2 s^{-2}.

Given the environment of very strong [35 m s^{-1} (70 kt)] 0–6-km shear with nearly unidirectional southwesterly flow and moderate instability (surface-based CAPE of 2000–3000 J kg^{-1}), the storms in convective band two quickly became supercells. By 1800 UTC (roughly noon local time), cloud tops within band two had attained heights of more than 15.2 km (50 000 ft) in western Kentucky, well above the regional morning tropopause level of 11.6 km (38 000 ft). Reflecting the orientation of the axis of strongest flow aloft (from northeast Arkansas to northern Indiana at 1800 UTC, given interpolation between the 1200 UTC 3 April and 0000 UTC 4 April upper-air analyses), storms in the northern part of the band moved rapidly northeastward, while those at the trailing southern end edged only slowly eastward across western Tennessee. Band two spawned the first F5 tornado of the Super Outbreak, one that subsequently struck the town of Depauw, in southern Indiana, around 1920 UTC (track 40 in Fig. 1). As the convective band moved generally east-northeastward, it also expanded preferentially to the north, so that by early afternoon it extended from central Indiana to western Tennessee (Fig. 5b). Examination of Eta Model height and vertical motion fields (not shown), and the 1800 UTC rawinsonde data, suggests that the presence of slightly stronger synoptic-scale forcing for ascent (30–40 m, 12-h 500-hPa geopotential height falls) and weaker capping likely were responsible for the northward bias in the development. Throughout this period, the storms remained well east [by about 300 km (200 mi)] of the cold front–dryline.

3) Convective band two associated with a cold front aloft?

Locatelli et al. (2002) call attention to a thermal gradient at 700 hPa that extends from eastern Illinois and western Indiana southsouthwestward into the lower Tennessee Valley at 0000 UTC 4 April (Fig. 3d). They note that the gradient is strongest just west of convective band two, with the thermal contours oriented parallel to the band. These observations, and output from a mesoscale model simulation showing the presence of 700-hPa cold advection over the Tennessee and lower Ohio Valleys, prompt the authors to conclude that convective band two marked the leading edge of a ''cold front aloft,'' (CFA) as described by Locatelli et al. (1989) and Hobbs et al. (1990). CFAs are believed to provide both ascent and destabilization that can focus convective release in regions of potential instability, and are akin to the ''split cold fronts'' discussed by Browning and Monk (1982). CFAs differ, therefore, from the upper-level fronts that occur in association with jet streaks near the tropopause (e.g., Keyser and Shapiro 1986).

The idea that convective band two may reflect the presence of an upper-level boundary is to some extent supported by the temporal and spatial continuity of the 700-hPa thermal gradient and wind shift axis as revealed by the observed rawinsonde data in Figs. 3c and 3d. Interpolating between the 1200 UTC 3 April and 0000 UTC 4 April analyses, it seems probable that, for a period of time around midday, weak 700-hPa cooling and, presumably, ascent associated with the trough overspread western parts of the destabilizing warm sector some distance ahead of the cold front–dryline. An 18-h forecast of surface pressure and 1000–500-hPa thickness from the 29-km Eta Model (not shown) shows the axis of maximum thickness to be located about 250 km (160 mi) from the surface front in eastern Missouri and Arkansas. Lumb (1950), among others, has suggested the use of the thickness field to locate upper fronts ahead of surface boundaries.

However, the observed data are not entirely consistent with the behavior of a CFA as presented in the literature (e.g., Hobbs et al. 1990 and references therein). For example, temperatures in the 700–500-hPa layer warmed 2°–4°C during the day over much of the Ohio and Tennessee Valleys (cf. Figs. 3c and 3d). And, while modest geopotential height falls did occur during the period at 700 mb, similar *rises* occurred at 500 hPa. A vertical section taken from Omaha, Nebraska, and Waycross, Georgia, valid at 0000 UTC 4 April and shown in Hoxit and Chappell (1975, their Fig. 49) shows, at best, only a subtle hint of an elevated front near Nashville. This is in contrast to the marked and deep upper-level discontinuities depicted in the vertical sections shown in Hobbs et al. (1990). Further, particularly along its northern extent, convective band two at some points was located up to 200 km east of the eastern-most ''nose'' of the 700-hPa thermal gradient. Although the presence of weak 700-hPa cold advection atop the western parts of the warm sector during the early afternoon likely served as a destabilizing influence, this cooling could more simply be attributed to the existence of stronger westerly momentum in the southeastern quadrant of the vast Kansas upper low (Fig. 3c) relative to points farther north, rather than to the existence of a CFA. The cooling at 700 hPa also may have reflected the glancing influence of the lead short-wave impulse. Given the sparse nature of the rawinsonde network and the sizable effects of latent heating that necessarily occurred in association with convective band two (e.g., Hoxit and Chappell 1975, p. 34), our analysis cannot provide independent confirmation that band two was indeed associated with

JOBNAME: WAF 0#00 PAGE: 39 SESS: 8 OUTPUT: Tue Feb 16 00:20:51 2010 Total No. of Pages: 45
/ams/waf/0/waf2222297

a CFA. Even if a CFA were present, it is not apparent how vertical motions favorable for the initiation of deep moist convection would evolve along it. Thus, while there remains some doubt that a CFA was the dominant agent of initiation for convective band two, it does appear that the band formed in a region that experienced weak cooling at 700 hPa, and that the storms were not directly related to the nearest long-lived surface feature, the eastern Missouri–Arkansas cold front–dryline.

4) DEVELOPMENT OF CONVECTIVE BAND THREE

Shortly after convective band two arose in Arkansas and southeast Missouri, a third broken line of thunderstorms, convective band three, developed around 1600 UTC along an arc extending north from near St. Louis into west-central Illinois (Fig. 5c). Satellite- and model-derived data suggest that band three formed in a zone of strong differential positive vorticity advection associated with the lead short-wave trough moving east-northeast into the mid–Mississippi Valley, and in the immediate vicinity of the eastern Missouri cold front–dryline. The convection formed in the left exit region of a 65 m s^{-1} (130 kt) 250-hPa jet streak crossing the southern plains (Figs. 3c and 3d). As convective inhibition was quite weak (per 1800 UTC Salem, Illinois, rawinsonde data; Fig. 8d) and convergence was pronounced near the intersection of the cold front–dryline and the Illinois warm front (Fig. 4i), storms formed as soon as the convective temperature was attained [about 23°C (74°F)]. Coupled with the extreme 0–6-km shear across the region [more than 45 m s^{-1} (90 kt) at Salem], it is not surprising that these storms became supercells very quickly. By 1800 UTC, tops had reached 15.2 km (50 000 ft). Baseball-sized hail fell in central Illinois around 1720 UTC, and, shortly afterward, wind-driven baseball-sized hail produced the costliest storm damage ever up to that time in St. Louis (NOAA 1974). About an hour later, the northern part of band three dropped golf ball–sized hail in Chicago. The first tornado with band three, an F0, lasted only a minute and touched down near Morris, Illinois [about 70 km (45 mi) southwest of Chicago] around 1810 UTC. However, by 1950 UTC, band three had produced two F3s: one near Decatur and the other near Normal in east-central Illinois (tracks 4 and 5 in Fig. 1).

5) DEVELOPMENT OF CONVECTIVE BAND FOUR

Approximately 1 h after convective band three formed in eastern Missouri and central Illinois, a fourth area of storms developed in northeast Missouri and eastern Iowa. These storms appeared to mark the northern end of the Missouri cold front–dryline, and formed south of the stationary front extending northeastward from the Kansas surface low. The convection organized into a broken south-southwest–north-northeast-oriented line that moved slowly eastward across the Mississippi River into northern Illinois during the afternoon. Although the band weakened upon reaching the western suburbs of Chicago (and rain-cooled air from band three) around 0000 UTC 4 April, it remained clearly visible in the grazing illumination of the setting sun at 2324 UTC (Fig. 4k). AU3

Forming as they did close to the upper low center (Fig. 3d), and remaining well-removed from the surge of rich boundary layer moisture that moved northward ahead of convective band three, the storms in band four were comparatively low topped; maximum tops were uniform around 9–10 km (30 000–35 000 ft). This altitude nonetheless represented a substantial relative penetration of the local tropopause that, according to the 0000 UTC rawinsonde at Peoria, Illinois (not shown), was around 7 km (22 000 ft). The storms produced marginally severe hail in eastern Iowa and northwest Illinois, but no observed tornadoes. The latter fact may reflect the limited moisture (surface dewpoints around 12°C) and relatively weak low-level wind field that existed in the region relative to points south and east.

Convective band four formed immediately ahead of the deep synoptic-scale low moving slowly northeast from Kansas into Iowa. Surface thermal, moisture, and wind fields in the vicinity of the low and the convective band display a structure and evolution more representative of the frontal fracture (“T bone”) model of oceanic cyclones described by Shapiro and Keyser (1990), than of the more conventional warm front–cold front “triple point” pattern depicted in Hoxit and Chappell (1975, 25–33). The visible satellite data (i.e., Figs. 4j and 4k) support this idea, with low overcast present north and west of the southern Iowa–southern Wisconsin stationary front, and a break between those clouds and the bands of convective towers extending south along the Illinois cold front. The T-bone structure had become apparent as early as sunrise on Wednesday (1200 UTC; Fig. 4g). The absence of an identifiable triple point is a common aspect of Colorado lee cyclogenesis, although T-bone structures are not frequently observed. In this case, the T-bone configuration may have been accentuated by the fact that true warm sector air was not able to reach the cyclone center because of the expanding bands of deep convection that formed farther south and east.

e. Midafternoon, Wednesday, 3 April, through early morning, Thursday, 4 April

The Super Outbreak began in earnest around 1900 UTC (1400 CDT) as the three strongest convective bands began producing damaging tornadoes more or less continuously, and the number of severe weather warnings increased accordingly (Fig. 9). During the next 2 h, devastating tornadoes struck Depauw, Indiana; Brandenburg, Kentucky; F9

JOBNAME: WAF 0#00 PAGE: 40 SESS: 8 OUTPUT: Tue Feb 16 00:20:51 2010 Total No. of Pages: 45
/ams/waf/0/waf2222297

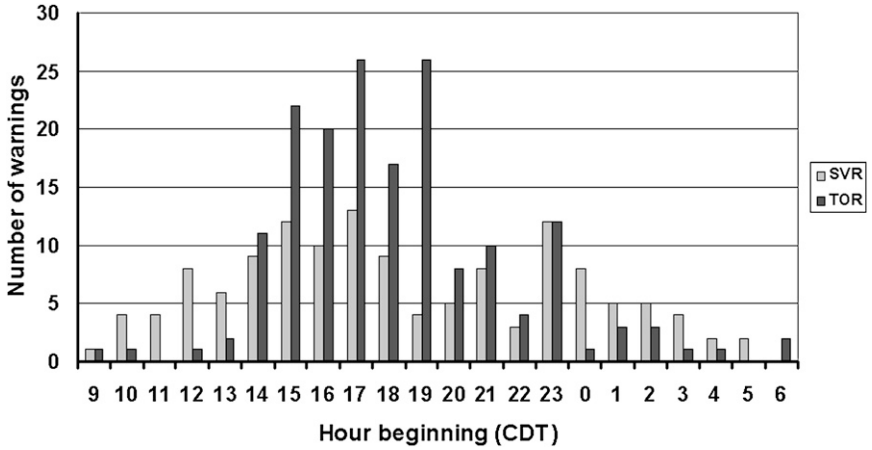

FIG. 9. Number of severe thunderstorm (light gray) and tornado (dark gray) warnings issued per hour by local NWS offices during the Super Outbreak. Time in hours central daylight time (CDT; add 0500 for UTC), with the last two digits removed. Data are from Department of Commerce (1974).

and Xenia, Ohio (tracks 40, 47, and 37, respectively, in Fig. 1); all of which were associated with band two. The violence increased after 2100 UTC (Fig. 4j), as tornadoes associated with all three convective bands occurred simultaneously in numerous communities from Alabama and Tennessee northward into Illinois, Indiana, Ohio, and Michigan. The metropolitan areas of Birmingham, Alabama; Cincinnati, Ohio; Louisville, Kentucky; and Windsor, Ontario, Canada, also were hit. In northern Indiana, band three spawned a half-mile-wide F4 that struck the town of Monticello around 2215 UTC (track 13 in Fig. 1). The tornadic storm occurred in association with a subsynoptic low that evolved near the intersection of band three with the Ohio Valley warm front (note the south-southeasterly surface winds in west-central Indiana in Fig. 4j). The tornado had a pathlength of nearly 175 km (109 mi), the longest of any in the Super Outbreak.[6] Farther south, hail up to the size of softballs accompanied band two in northern Kentucky, where radar cloud tops reached 19.8 km (65 000 ft).

The Kansas surface low began to fill slightly as it tracked slowly northeastward to near Burlington, Iowa, by 0000 UTC Thursday, 4 April (Fig. 4k). The low was situated in the left-exit region of a 70 m s^{-1} (140 kt) 250-hPa jet streak in northwest Arkansas. At 500 hPa, a band of 50 m s^{-1} (100 kt) southwesterly flow extended from northeast Texas to southern Illinois. Midlevel temperatures south and east of the jet streak, in the general area of convective band two, warmed by 3°–5°C during the day. Hoxit and Chappell (1975) attribute this warming to a combination of diabatic processes (latent heat release), warm advection, and subsidence on the equatorward side of the upper jet.

By 0000 UTC 4 April the northern part of convective band one had long since dissipated over New York and Pennsylvania. The southern part, meanwhile, became indistinguishable late in the day after interacting with supercell storms that formed along the stalled front over the western Carolinas (Fig. 5a). Farther west, band three continued eastward across Illinois, Indiana, and western Kentucky, where individual radar-observed cell motions reached 30 m s^{-1} (60 kt). The convective system also developed northward into southern Michigan and extreme southern Ontario, where several tornadoes occurred between 0030 and 0130 UTC in a region of confluent southeasterly surface flow immediately north of the warm front and remnant subsynoptic low associated with the Monticello storm (Figs. 4k and 5c). Band three did not show appreciable weakening until it encountered rain-cooled air over parts of Ohio and central Kentucky around 0300 UTC on Thursday.

While severe weather continued in conjunction with band three into Wednesday night, after 2300 UTC, the most intense activity shifted to areas south of the Ohio River in association with band two (Fig. 5b). The west–east breadth of the warm sector in this region was greater than farther north, and the air was more moist, with precipitable water around 40 mm (1.6 in.). In addition, eastward progression of the main upper trough into the Ohio Valley (Figs. 3d and 3e) allowed stronger flow aloft

[6] Subsequent to publication of the Super Outbreak Map (Fujita 1975), Fujita reclassified the original 195-km (121 mi) Monticello, Indiana, tornado as two tornadoes separated by a brief downburst near the town of Chalmers (Fujita 1978). The length figure given here is for the second tornado, which continued without interruption to near Valentine, Indiana, in the northeast part of the state.

JOBNAME: WAF 0#00 PAGE: 41 SESS: 8 OUTPUT: Tue Feb 16 00:20:54 2010 Total No. of Pages: 45
/ams/waf/0/waf2222297

to overspread the region, enhancing deep shear. The strengthening deep west-southwesterly winds, oriented nearly parallel to the low-level foci of storm initiation (*weak* elongating thunderstorm outflow boundaries; see Fig. 2 and p. 1011 in Corfidi 2003) allowed supercells to back-build and ''train'' across northern Alabama and eastern Mississippi for an extended period of time (Fig. 5b). This setup proved favorable for strong, long-track tornadoes, likely in part because it minimized the chance that storms would quickly be undercut by their own outflow. In far northern Alabama, a tornado that reached F5 intensity and had a pathlength of 82 km (51 mi) moved through Lawrence, Morgan, Limestone, and Madison Counties between 0000 and 0030 UTC (track 96 in Fig. 1). A second tornado that followed a nearly identical path barely 0.5 h later was rated F4 (track 98 in Fig. 1). The storms that produced these tornadoes remained intense as they moved into Tennessee.

Rich moisture inflow persisted along the southern end of band two through the evening, within an environment of intense [40 m s^{-1} (80 kt)] deep shear. Around 0200 UTC, a supercell that had formed in east-central Mississippi spawned a devastating long-track [164 km (102 mi)] F5 tornado that destroyed the town of Guin, Alabama (northwest of Birmingham), and continued northeast to near Huntsville (track 101 in Fig. 1). Farther north in middle Tennessee, a separate cluster of violent band two tornadoes swept rapidly northeastward into southern Kentucky between 0100 and 0200 UTC. The tornadoes diminished in Kentucky after around 0300 UTC, but severe weather continued in Tennessee beyond midnight central time (0500 UTC), as the storms encountered rising terrain and residual outflow boundaries in the far eastern part of the state (Fig. 4m). Embedded supercells continued to produce damaging winds and additional strong tornadoes until nearly dawn (1000 UTC) on Thursday northward into southern West Virginia and western Virginia (Figs. 4n, 4o, and 5b). The events in the latter two states were extremely unusual considering not only the time of day and their intensity, but also the relatively low incidence of severe weather of any kind in that region at that time of the year.

The last tornado of the outbreak, an F2, overturned trailers and unroofed homes near Baton, North Carolina [100 km (65 mi) east-northeast of Asheville] around 1345 UTC (track 148 in Fig. 1).

4. Discussion

This paper has presented an updated synoptic- and mesoscale overview of the 3–4 April 1974 Super Outbreak of tornadoes. The outbreak was clearly singular in terms of its intensity, longevity, and scope. It might be expected that an event of such magnitude would be associated with a correspondingly rare, but readily recognized, synoptic-scale signature. This, however, is not the case. For example, although the Colorado–Kansas lee cyclone that formed prior to the Super Outbreak was intense, its strength was not unprecedented; two or three cyclones of similar magnitude might be expected each decade. Further, the low weakened rather than intensified during the course of the event. Aloft, a midtropospheric jet streak had speeds in excess of 60 m s^{-1} (120 kt), but similar features occur fairly regularly over the United States during winter and spring. Likewise, the thermodynamic instability, while substantial, was not extreme; surface-based CAPE frequently exceeds 2000 J kg^{-1} in the warm sectors of migratory spring cyclones over the Ohio and Tennessee Valleys in spring. What factors, then, likely contributed to the outstanding nature of the Super Outbreak?

Instead of a single ''smoking gun,'' it appears that several contributing factors, acting together more or less synergistically, ultimately were responsible for the event. First, and not to be discounted, the unusually strong upper-level jet streak associated with the progressive Great Basin trough set the stage for a severe weather outbreak by creating large-scale conditions favorable for expansive lee cyclogenesis east of the Rockies. The jet maximum not only provided the necessary shear for intense, sustained supercells, but also helped create mesoscale areas of ascent that assisted in the initiation of convection. In addition, the strength of the background wind field increased the chance that any tornadoes that did form would be strong and long tracked.

The relatively low-amplitude nature of the upper-level flow over the central United States prior to 3 April 1974 appears to have been influential for several reasons. The pattern enabled a broad, largely undiluted EML plume to spread rapidly east from the southern and central plateau across a broad swath of the lower Mississippi, Ohio, and Tennessee Valleys. The presence of the EML led to the development of an expansive area of potential instability as the boundary layer warmed and moistened beneath it. In addition, because the mid- to upper-tropospheric flow was not strongly meridional, mid- and upper-level clouds associated with the warm conveyor belt (Carlson 1980) remained comparatively sparse (e.g., satellite images in Figs. 4i and 4j). Thick warm conveyor belt clouds often accompany cyclogenesis in highly amplified regimes wherein the strongly backed mid- and upper tropospheric flow taps moisture from the subtropics. Such cloud cover can substantially diminish warm sector diabatic heating and destabilization.

The jet pattern also minimized midtropospheric height falls in the warm sector. The leading edge of an area of

falling heights often is accompanied by a cold front or wind shift line at the surface that serves as a source of low-level linear forcing for ascent. The relative weakness of such features in this event (except near the main surface low with convective band four) helped ensure that many of the thunderstorms that formed would remain discrete or semidiscrete for extended periods of time.

For some time now it has been recognized that long-track tornadoes occur predominantly with discrete or semidiscrete supercells, rather than with solid lines or clusters of storms. The importance of nonlinear storm modes in fostering tornado development and longevity has become especially apparent in more recent years as the advent of composite radar data facilitated the examination of storm development and interaction on expanded spatial and temporal scales. Model simulations (e.g., Roebber et al. 2002) also have demonstrated the role played by weak linear forcing in maintaining discrete supercellular storms. The absence of strong linear forcing, coupled with the strength and the low-amplitude nature of the background wind field, likely discouraged rapid evolution toward linear convective modes and enhanced the potential for both tornado development and longevity throughout the afternoon and evening of 3 April 1974.

In particular, over the Tennessee Valley on the evening of 3 April, the juxtaposition of fast, nearly unidirectional low- to midtropospheric flow with a deep, moisture-rich environment fostered thunderstorm cold pools that not only became elongated parallel to the mean flow, but also remained weak (i.e., with minimal temperature differential between the cold pools and the unaffected warm sector). As the cold pools became elongated, those portions of their outflow boundaries that became oriented parallel to the flow remained nearly stationary and served as corridors of ''echo training'' for supercells (Corfidi 2003). With the production of cold, evaporatively driven downdrafts minimized by the deeply moist environment, undercutting of the storms by their own outflow also was limited. This increased their longevity and likely was a factor in the destructive, long-track tornadoes that struck northern Alabama and eastern Tennessee after sunset on 3 April.

An indirect but no less important consequence of the low-amplitude flow regime prior to 3 April 1974 was its contribution toward the development of an unusually broad, warm, and moist warm sector for early April. The warm sector was established, in part, when the trailing frontal system associated with the previous low-amplitude upper disturbance failed to effect a significant airmass change over the Southeast as Colorado cyclogenesis occurred on 2 April (Figs. 4a–c). The expansive warm sector that subsequently evolved enabled the *simultaneous* occurrence of both dryline-related thunderstorms (convective band two) and jet exit region–cold frontal storms (convective band three) as the Great Basin trough moved into the plains on the afternoon of 3 April. Because of the typically more limited areal extent of surface-based warm sectors with Colorado cyclones, severe weather episodes associated with such lows in the central United States frequently are confined to 1) dryline/lee trough storms on the initial day of the low's movement away from the Rockies and 2) jet-exit region/cold frontal activity on the succeeding one. Such was not the case on 3 April.

Climatological data suggest another factor that may have fostered the development of an unusually warm and moisture-rich boundary layer over parts of the southern and eastern United States on 3 April 1974. Mean constant pressure charts for the previous 30 days using the NCEP–NCAR reanalysis data (Kalnay et al. 1996) depict strong, largely zonal flow over the continental United States, with a persistent low-amplitude trough over the Rockies and the Great Basin (Fig. 10a). Heights and 1000–500-hPa thicknesses were above normal over the southeastern states and northern Gulf of Mexico, and below normal over the northern tier of states and Canada (Figs. 10b–d). A review of the NWS's *Daily Weather Maps (Weekly Series)* for March 1974 reveals that the anomalous pattern minimized deep cold frontal penetrations into the Gulf of Mexico through most of the month. This likely yielded a broader, warmer, and perhaps deeper moist boundary layer than is normally accessible to migrating synoptic-scale systems at this time of year. This air mass moved very rapidly northward, with minimal modification, as southerly flow in the warm sector strengthened over the southern and eastern United States early on 3 April.

The preceding observations are consistent with the spectral analysis of atmospheric energetics for the 1 March–1 May 1974 period shown in Fig. 11. The curves depict the relative amount of energy in wavenumbers 1–3 at 500 hPa averaged over the Northern Hemisphere. During the last half of March, a disproportionate amount of the energy was contained in wavenumbers 1 and 2; that is, the hemispheric flow was strongly zonal. An abrupt transition to a more highly amplified pattern is apparent in early April, with a sharp reduction in the level of energy in wavenumbers 1 and 2, and a slight increase in wavenumber 3. This pattern change was brought about, in part, by the significant lee cyclogenesis event that occurred in conjunction with the Super Outbreak.

Another factor behind the enormity of the Super Outbreak was the presence of relatively uncommon mesoscale forcing mechanisms. For example, our analysis substantiates previous studies (Miller and Sanders 1980; Locatelli et al. 2002) indicating the possible role of an

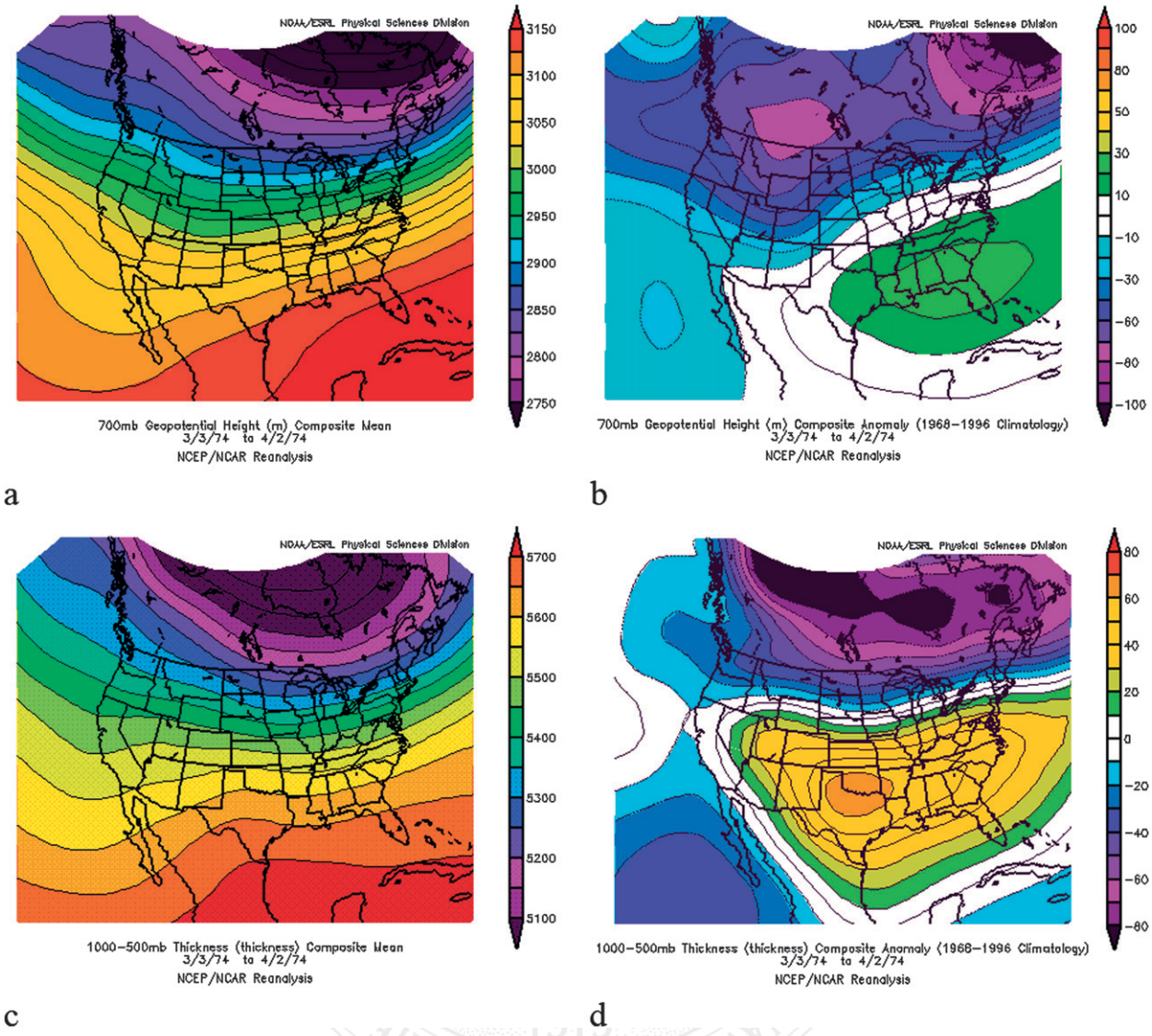

FIG. 10. (a) Mean 700-hPa geopotential height, 3 Mar–2 Apr 1974 (m, scale at right). (b) Mean 700-hPa geopotential height anomaly, 3 Mar–2 Apr 1974 (m, scale at right); anomaly based on years 1968–96. (c) Mean 1000–500-hPa thickness, 3 Mar–2 Apr 1974 (m, scale at right). (d) Mean 1000–500-hPa thickness anomaly, 3 Mar–2 Apr 1974 (m, scale at right); anomaly based on years 1968–96. Data from the NCEP–NCAR reanalysis, courtesy of NOAA/Earth Systems Research Laboratory.

undular bore in the initiation and/or maintenance of convective band one. The bore appeared to emanate from the overnight MCS in Arkansas on 3 April and provided an additional source of organized uplift through the early afternoon. It likely helped initiate thunderstorms deep within the warm sector in areas that may otherwise have remained capped to such development. In conjunction with daytime heating, the bore appeared to help rejuvenate existing warm advection storms in Georgia and the Carolinas. At the same time, a long-lived subsynoptic low enhanced the potential for low-level storm rotation and tornadoes as it tracked northeastward from northern Indiana into southeast Michigan.

Finally, circulations associated with a distinctly different mesoscale feature appeared to be responsible for focusing the development of convective band two. Although Locatelli et al. (2002) argue that these circulations were associated with a CFA, our analysis was inconclusive in that regard. Nonetheless, it remains clear that some mesoscale process, or combination of different processes, provided a quasi-linear corridor of reduced convective inhibition that allowed the formation of this second convective band. Due in part to these mesoscale forcing mechanisms, for several hours during the afternoon of 3 April, *four* bands of severe storms simultaneously were present over the east-central United States.

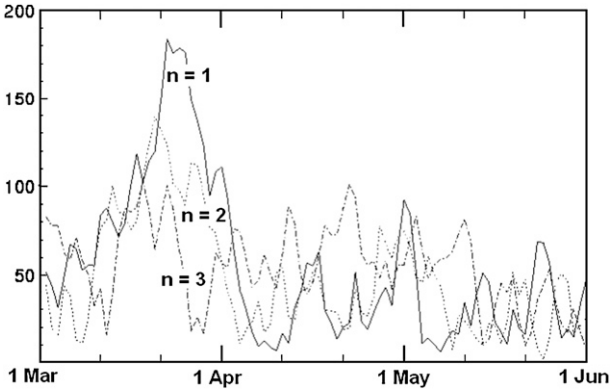

FIG. 11. The 500-hPa hemispheric spectral analysis of wavenumbers 1–3 for the period 1 Mar–1 Jun 1974.

A final, but most significant factor contributing to the singular nature of the Super Outbreak was that the diurnal cycle was favorably timed with respect to the arrival of rich boundary layer moisture and the intensification of deep shear over the Ohio and Tennessee Valleys. The combination of increasing moisture, strengthening large-scale forcing for ascent, and perhaps mesoscale forcing mechanisms likely would have led to the eventual development of severe thunderstorms along the system cold front, and possibly along parts of the dryline and warm front, even in the absence of diurnal heating on 3 April 1974. However, it is probably safe to speculate that the intensity, longevity, and organization of the convection would not have been as favorable for long-lived tornadoes had the onset of heating not so directly corresponded with the return of low-level moisture and shear.

In conclusion, this study does not provide the criteria to "raise the red flag" that an extraordinary severe weather outbreak is about to occur. Rather, it highlights the fact that forecasting specific aspects of such an event (e.g., convective initiation, evolution, and mode) remains exceptionally challenging. Further, our review suggests that a combination of well-known ingredients occasionally can synergistically interact to yield an exceedingly rare event.

Acknowledgments. The lead author would like to thank Chris Broyles, Greg Carbin, Jonathan Garner, Jared Guyer, Jack Hales, John Hart, Bob Johns, Brynn Kerr, Dan McCarthy, Joan O'Bannon, Russ Schneider, and Brian Smith for thoughtful discussion and/or assistance with this project. The lead author also would like to thank Nick Metz for the invitation to speak at Valparaiso State University's Great Lakes Meteorology Conference on the 30th anniversary of the Super Outbreak; that presentation served as the basis for this work. Harold Brooks and Russ Schneider provided Fig. 2, and Mike Ekster is acknowledged for providing valuable input regarding the Nashville hodographs. Appreciation also is extended to three anonymous reviewers whose helpful comments improved the manuscript. The NOAA Climate Database Modernization Program, National Climatic Data Center, Asheville, North Carolina, and the NOAA Central Library Data Imaging Project, Silver Spring, Maryland, are acknowledged for the online availability of *Daily Weather Maps (Weekly Series)* (http://docs.lib.noaa.gov/rescue/dwm/data_rescue_daily_weather_maps.html).

REFERENCES

Betts, A. K., 1986: A new convective adjustment scheme. Part 1: Observational and theoretical basis. *Quart. J. Roy. Meteor. Soc.,* **112,** 1306–1335.

Black, T. L., 1994: The new NMC mesoscale Eta Model: Description and forecast examples. *Wea. Forecasting,* **9,** 265–278.

Browning, K. A., and G. A. Monk, 1982: A simple model for synoptic analysis of cold fronts. *Quart. J. Roy. Meteor. Soc.,* **108,** 435–452.

Broyles, J. C., and K. C. Crosbie, 2004: Evidence of smaller tornado alleys across the United States based on a long track F3–F5 tornado climatology study from 1880–2003. Preprints, *22nd Conf. on Severe Local Storms,* Hyannis, MA, Amer. Meteor. Soc., P5.6. [Available online at http://ams.confex.com/ams/pdfpapers/81872.pdf.]

Bunkers, M. J., B. A. Klimowski, J. W. Zeitler, R. L. Thompson, and M. L. Weisman, 2000: Predicting supercell motion using a new hodograph technique. *Wea. Forecasting,* **15,** 61–79.

Carlson, T., 1980: Airflow through midlatitude cyclones and the comma cloud pattern. *Mon. Wea. Rev.,* **108,** 1498–1509.

Corfidi, S. F., 2003: Cold pools and MCS propagation: Forecasting the motion of downwind-developing MCSs. *Wea. Forecasting,* **18,** 997–1017.

Department of Commerce, 1974: The widespread tornado outbreak of April 3–4, 1974. National Disaster Survey Rep. 74-1, Rockville, MD, 42 pp.

Doswell, C. A., III, 1991: A review for forecasters on the application of hodographs to forecasting severe thunderstorms. *Natl. Wea. Dig.,* **16** (No. 1), 2–16.

Esterheld, J. M., and D. J. Giuliano, 2008: Discriminating between tornadic and non-tornadic supercells: A new hodograph technique. *E-J. Severe Storms Meteor.,* **3** (2). [Available online at http://www.ejssm.org/ojs/index.php/ejssm/article/viewArticle/33/37.]

Forbes, G. S., 1975: Relationship between tornadoes and hook echoes on April 3, 1974. Preprints, *Ninth Conf. on Severe Local Storms,* Norman, OK, Amer. Meteor. Soc., 280–285.

Fujita, T., 1975: Super Outbreak of tornadoes of April 3–4, 1974. Map printed by University of Chicago Press. AU5

——, 1978: Manual of downburst identification for project NIMROD. Satellite and Mesometeorology Research Paper 156, Dept. of Geophysical Sciences, University of Chicago, 104 pp.

Grazulis, T. P., 1993: *Significant Tornadoes, 1680–1991.* Environmental Films, 1326 pp.

Hobbs, P. V., J. D. Locatelli, and J. E. Martin, 1990: Cold fronts aloft and the forecasting of precipitation and severe weather east of the Rocky Mountains. *Wea. Forecasting,* **5,** 613–626.

Houze, R. A., Jr., B. F. Smull, and P. Dodge, 1990: Mesoscale organization of springtime rainstorms in Oklahoma. *Mon. Wea. Rev.,* **118,** 613–654.

Hoxit, L. R., and C. F. Chappell, 1975: Tornado outbreak of 3–4 April 1974: Synoptic analysis. NOAA Tech. Rep. ERL 338-APCL 37, 48 pp.

Janjić, Z. I., 1994: The step-mountain eta coordinate model: Further developments of the convection, viscous sublayer, and turbulence closure schemes. *Mon. Wea. Rev.,* **122,** 927–945.

Kalnay, E., and Coauthors, 1996: The NCEP/NCAR 40-Year Reanalysis Project. *Bull. Amer. Meteor. Soc.,* **77,** 437–471.

Keyser, D., and M. A. Shapiro, 1986: A review of the structure and dynamics of upper-level frontal zones. *Mon. Wea. Rev.,* **114,** 452–499.

Locatelli, J. D., J. M. Sienkiewicz, and P. V. Hobbs, 1989: Organization and structure of clouds and precipitation on the mid-Atlantic coast of the United States. Part I: Synoptic evolution of a frontal system from the Rockies to the Atlantic coast. *J. Atmos. Sci.,* **46,** 1327–1348.

——, M. Stoelinga, P. V. Hobbs, and J. Johnson, 1998: Structure and evolution of an undular bore on the high plains and its effects on migrating birds. *Bull. Amer. Meteor. Soc.,* **79,** 1043–1060.

——, ——, and ——, 2002: A new look at the Super Outbreak of tornadoes on 3–4 April 1974. *Mon. Wea. Rev.,* **130,** 1633–1651.

Lumb, F. E., 1950: Upper frontal analysis in the Mediterranean. *Meteor. Mag.,* **79,** 191–198.

Miller, D. A., and F. Sanders, 1980: Mesoscale conditions for the severe convection of 3 April 1974 in the east-central United States. *J. Atmos. Sci.,* **37,** 1041–1055.

Miller, D. J., 2006: Observations of low level thermodynamic and wind shear profiles on significant tornado days. Preprints, *23rd Conf. on Severe Local Storms,* St. Louis, MO, Amer. Meteor. Soc., 3.1. [Available online at http://ams.confex.com/ams/pdfpapers/115403.pdf.]

NOAA, 1974: *Storm Data*. Vol. ~~14~~ 1. AU6

Roebber, P. J., D. M. Schultz, and R. Romero, 2002: Synoptic regulation of the 3 May 1999 tornado outbreak. *Wea. Forecasting,* **17,** 399–429.

Shapiro, M. A., and D. Keyser, 1990: Fronts, jet streams, and the tropopause. *Extratropical Cyclones, The Erik Palmén Memorial Volume,* C. W. Newton and E. O. Halopainen, Eds., Amer. Meteor. Soc., 167–191.

Simpson, J. E., 1997: *Gravity Currents in the Environment and the Laboratory*. Cambridge University Press, 244 pp.

Uccellini, L. W., and D. R. Johnson, 1979: The coupling of upper and lower tropospheric jet streaks and implications for the development of severe convective storms. *Mon. Wea. Rev.,* **107,** 682–703.